Coupled mode reductions and rotating wave approximations in nonlinear equations

Yuslenita Muda

A thesis presented for degree of

Doctor of Philosophy

Department of Mathematical Sciences

University of Essex

March 2019

 would like to dedicate this thesis to my beloved parents, my dearest husband, Ahmad Jamaan for his never ending support and my lovely children, Thoriq, Rifa, Dzakir and my little prince Daniel for their togetherness in this PhD journey...

Declaration

The work in this thesis is based on research carried out with my supervisor Dr. Hadi Susanto at the Department of Mathematical Sciences, University of Essex, United Kingdom. No part of this thesis has been submitted elsewhere for any other degree or qualification, and it is all my own work, unless referenced, to the contrary, in the text.

Yuslenita Muda
March 2019

Acknowledgements

In the name of Allah, the most Gracious and the Most Merciful, and prayers and peace be upon Mohamed His servant and messenger. *Alhamdulillah*, all praises to Allah the Almighty for the strengths and His blessing for me to accomplish my thesis. I am totally sure that this work would have never become truth, without His guidance.

I am very grateful to some people who helped me during my PhD studies. Firstly, and certainly, I would like to convey my profound gratitude from the bottom of my heart to my supervisor Dr. Hadi Susanto who helped me hard from the beginning till the completion. Thank you for your support, useful suggestions and corrections on the manuscripts of this thesis, patience, motivation, passion, and your huge knowledge. You are truly an outstanding person and an able educator, I will be forever thankful to you.

Next, I am also grateful to my Supervisory Board Chair and internal examiner Dr. Georgi Grahovski, for his kindness, encouragement, supports, and constructive questions. I also address my sincere thanks to my external examiner Prof. Vassilis Rothos, for his advice, kindness and his constructive comments during the VIVA.

I owe profound gratitude to my beloved husband and truly friend, Ahmad Jamaan, whose gave me encouragement constantly, limitless giving and great sacrifice, never ending support and helped me much. I also would like to express my wholehearted thanks to my children, Thoriq, Rifa, and Dzakir for their patience, kindness, prayers and motivations. Also for my little prince, Daniel who arrived in the last period of my studies. Furthermore, I want to take an opportunity to say thanks to all my fellow friends in the department, Rudy, Rahmi, Amal, Sheila, Lana, Junaid, Omar, Tahani, Awatf, Ruwayda, Hammed, and Pascal for our useful discussion and togetherness. The most precious discussion I got from Pak Fiki, for his kindness, I would like to express my gratitude for him. I also address my fully

thanks to my lovely friends in KIBAR, Pengajian Annisa, Indonesian families in Colchester, and Rumaisa Sabiila for their prayers, kindness and togetherness.

I also would like to offer my wholehearted thanks to my mother, my late father (may Allah bless him with jannah), my brothers, my late mother in law (may Allah bless her with jannah), my father in law, and all of my and my husband's big family for their unconditional love and prayers.

Finally, I am thankful to the MoRA Scholarship from Ministry of Religious Affairs, Republic of Indonesia for providing me financial support.

Abstract

In this thesis, we investigate the applicability of coupled mode theory in the cubic-quintic nonlinear Schrödinger/Gross Pitaevskii (NLS/GP) equation with a linear double-well potential and study justifications of the rotating wave approximations in lattice systems.

First, we study the long-time dynamics near a symmetry breaking bifurcation point of the cubic-quintic NLS/GP with symmetric double-well potentials. We investigate the stability of the solutions of NLS/GP and analyze the error for the finite dimensional ansatz.

Next, we consider a class of discrete nonlinear Klein-Gordon equations with damping and parametric drive. Using small amplitude ansatzs, one usually approximates the equations using a damped, driven discrete nonlinear Schrödinger type equation. Here, we show for the first time the justification of this approximation by finding the error bound using energy estimates. Additionally, we prove the local and global existence of the solutions of Schrödinger equation. Numerical comparisons of discrete breathers obtained from the original nonlinear equation and the discrete nonlinear Schrödinger equation are presented describing the analytical results.

Finally, we consider a damped, externally driven nonlinear Klein-Gordon equation and justify the small amplitude ansatz yields a discrete nonlinear Schrödinger equation with damping and external drive. The same problems as the Klein-Gordon equation with damping and parametric drive are addressed.

Publications

Most of the work of this thesis is going to appear for publication.

- Chapter 3 will be submitted as:
  Y. Muda, R. Marangell, J.L. Marzuola, H. Susanto. Coupled mode reductions in the Cubic-Quintic NLS with a double-well potential, in preparation (2018).
- Chapter 4 has been published on online version in:
  Y. Muda, F.T. Akbar, R. Kusdiantara, B.E. Gunara, and H. Susanto. Justification of the discrete nonlinear Schrödinger equation from a parametrically driven damped nonlinear Klein-Gordon equation and numerical comparisons, https://doi.org/10.1016/j.physleta.2019.01.047, Physics Letters A (2019).
- Chapter 5 has been submitted in:
  Y. Muda, F.T. Akbar, R. Kusdiantara, B.E. Gunara, and H. Susanto. Reduction of damped, driven Klein-Gordon equations into a discrete nonlinear Schrödinger equation: justification and numerical comparisons, submitted to Asymptotic Analysis (2018).

Contents

List of Figures

Chapter 1

Introduction

1.1 What is the thesis about?

The main purpose of this thesis is to study the long-time dynamics near a symmetry breaking bifurcation point in the cubic-quintic nonlinear Schrödinger/Gross-Pitaevskii (NLS/GP) equation and to get approximate solutions of discrete Klein-Gordon equations (dKG) by means of equations of discrete nonlinear Schrödinger (dNLS) model through the justification of its solutions. For the cubic-quintic NLS/GP equation, we focus on a class of symmetric double-well potentials, while for the lattice system, we introduce an external or parametric driving with damping for dKG and dNLS.

In Chapter 2, we present Sturm-Liouville theory and its properties which are related to the calculation of an eigenvalue problem used in Chapter 3.

Our works are commenced in Chapter 3. We consider a cubic-quintic NLS/GP equation with an external linear potential. We study the applicability of the coupled mode theory in the cubic-quintic NLS/GP with a linear double-well potential. We also analyze bifurcations of equilibria for the system and their stability as well as symmetry breaking in NLS/GP.

In Chapter 4, we introduce a lattice system by considering a dKG equation with damping and parametric drive terms. We determine approximate solutions of the dKG equation from dNLS using rotating wave method. In addition, a justification is provided through an energy method approach. This method allows us to have an error bound that is proven to be small. Moreover, a numerical comparison is provided to illustrate analytical results and confirm the stability of our solutions.

Next, in Chapter 5 the model is still a lattice system by considering a dKG equation with damping and external drive terms. Applying a similar method into the model, we determine approximate solutions of the dKG, through a dNLS equation. We observe the effect of external drive terms to the solutions. Furthermore, we illustrate the error bound obtained using numerics. The main difference between Chapter 4 and Chapter 5 is lied in space of the solutions. We find that with external drive and damping, the solutions do not lie in ℓ^2-space of $\mathbb{Z}$, while with parametric drive and damping, the initial value problem for the discrete nonlinear Schrödinger equation with power nonlinearity is in weighted ℓ^2-space.

Finally, a summary of our work and interesting problems related to our methods, which are suggested for future investigation, is delivered in Chapter 6.

In the following, we will provide basic introductions to some keywords used in this thesis.

1.2 Coupled mode reduction

The term of coupled mode reduction is actually derived from the coupled mode theory. Why? Because coupled mode theory allows partial differential equations (PDEs) to be expressed as ordinary differential equations (ODEs).

In many cases, we are dealing with PDEs because most of the mathematical models are described by such equations. For example, Maxwell's equations, Navier-

Stokes equations, Gross-Pitaevskii equations describe more complex physical system and therefore, this condition usually makes the PDEs much harder to solve than ODEs.

A PDEs can be reduced to a system of ODEs by the method of separation variables. Another way to convert PDEs into ODEs is by using transform method such as Fourier transform. Assuming a solution of nonlinear PDEs as a linear combination of its linear solution, and then substituting the solution into PDEs to get ODEs can be used as well to solve a problem.

In Chapter 3, we will deal with a complicated PDEs which is cubic-quintic nonlinear Schrödinger equation. We use an assumption that a solution of cubic-quintic nonlinear Schrödinger equation is a linear combination of its linear solution. The procedure or process to get ODEs is called as coupled mode reduction.

1.3 What is a symmetry breaking?

In term of physics, symmetry properties may be attributed to physical laws (equations) or to physical objects/phenomena (solutions) [19]. In addition, a symmetry of physical laws can be broken in two ways, i.e., explicitly or spontaneously.

The simple way to know what a symmetry breaking is, let us consider a symmetrical upward dome with a trough circling the bottom. If we put a ball at the peak of the dome, the system is symmetrical with respect to a rotation around the centre axis. But the ball will break this symmetry spontaneously by rolling down the dome into the trough, which is a point of lowest energy. Thereafter, the ball has come to a rest at some fixed point on the perimeter. The dome and the ball maintain their individual symmetry, but the system does not.

Symmetry breaking indicates a situation where the dynamical equations are not manifestly invariant under the symmetry group treated. This means, in the Lagrangian (Hamiltonian) formulation the Lagrangian of the system contains

one or more terms explicitly break the symmetry. While according to [70, 97], spontaneous symmetry breaking (SSB) happens in a system when its Hamiltonian possesses a particular symmetry, whereas the ground-state wave functions do not maintain it. This yields a bifurcation, which breaks the symmetry when some control parameters cross its critical value.

In addition, it is generally known that the ground state in quantum mechanics exactly follows the symmetry of the underlying potential, while excited states may realize other representations of the same symmetry [1]. In particular, the wave function of the ground state of a particle trapped in the one-dimensional double-well potential is even, with respect to the double-well structure, while the first excited state has the opposite parity, being odd. Similarly, the wave function corresponding to the state at the bottom of the lowest Bloch band induced by the periodic potential features the same periodicity. In a simple explanation, we can see the symmetry breaking phenomena in the solution of our mathematical model.

In this thesis, we will study the long-time dynamics near a SSB, particularly we focus on symmetric double-well potentials.

1.4 Rotating wave approximation

Rotating wave approximation is the main method used in Chapters 4 and 5. We use this method to approximate solutions of discrete Klein-Gordon (dKG) equations through discrete nonlinear Schrödinger equations. In quantum optics, in order to achieve an analytic approximate solution of some Schrödinger equations, rotating wave approximation plays a very essential role [40].

To understand how rotating wave approximation works, we can find it through multiple scale analysis as follows.

1.4.1 Multiple scale analysis

A concept of expanding the solution into a perturbation series and including multiple temporal and spatial scale is called multiple scale analysis methods. Effect of this method could be meaningless on short time scales but become essential on long time-scales. In general, classical perturbation methods will fail due to resonances that lead to what is called a secular term.

Resonance and secular term

The influence of resonance in oscillatory problems are very fundamental and cannot be ignored. For example, when a driving force is presented in our system, then the influence of resonance may appear. A familiar example about resonance is when we are pushing a child on a swing. Its amplitude will become larger and larger when we are pushing at the same frequency as the child swings. We have to avoid this effect.

Now, let us discuss the following example of a harmonic oscillator of natural frequency ω_0, adopted from [10, 60].

The movement of a harmonic oscillator can be illustrated by the homogeneous ordinary differential equation

$$\ddot{y}(t) + \omega_0^2 y(t) = 0, \tag{1.1}$$

where the natural frequency of the system is ω_0 and $y(t)$ is the displacement of the oscillator at time t.

Its general solution is given by

$$y_h(t) = A\cos(\omega_0 t) + B\sin(\omega_0 t), \tag{1.2}$$

$A, B \in \mathbb{R}$ arbitrary constants. Since $|\cos(\omega_0 t)| \leq 1$ and $|\sin(\omega_0 t)| \leq 1$ for all $t \in \mathbb{R}$, we obtain

$$|y_h(t)| \leq A + B. \tag{1.3}$$

Now if we add a driving force, that periodically puts energy into the system at frequency ω, Equation (1.1) becomes nonhomogeneous and the oscillation can be described by

$$\ddot{y}(t) + \omega_0^2 y(t) = \cos(\omega t). \tag{1.4}$$

Its general solution depends on the relation between the driving frequency ω and natural frequency ω_0. If $|\omega| \neq |\omega_0|$ we obtain the general solution of (1.4):

$$y(t) = A\cos(\omega_0 t) + B\sin(\omega_0 t) + \frac{\cos(\omega t)}{\omega_0^2 - \omega^2}. \tag{1.5}$$

How about if the driving frequency gets close to the natural frequency of the system? From Equation (1.5) we can see that the denominator of the last term gets close to 0 as $|\omega| \neq |\omega_0|$. Since $\cos(\omega t)$ is bounded, the amplitude of the oscillation thus increases more and more. This can be explained in physical terms by the system absorbing more and more energy from the external force when the driving frequency ω gets close to the natural frequency ω_0 of the system. Nevertheless, we observe that for all fixed $|\omega| \neq |\omega_0|$ the solution remains bounded for all times t, since the oscillation is out of phase with the driving force.

However, in case the $|\omega| = |\omega_0|$ the solution is given by

$$y_s(t) = A\cos(\omega_0 t) + B\sin(\omega_0 t) + \frac{1}{2} t \sin(\omega t), \tag{1.6}$$

and therefore grows with t. Hence y_s is unbounded as $t \to \infty$. In this case the system can continually absorb energy from the periodic external force, so the

amplitude of the oscillation of (1.4) increases without any bound. We say that the system is in resonance with the external force.

The term $\frac{1}{2}t\sin(\omega t)$, which appears in (1.6), is called a secular term or just secularity, i.e., its amplitude grows algebraically with t. This secularity appear because the right hand side of (1.4), i.e., $\cos(\omega t)$ with $|\omega| = |\omega_0|$ itself is a solution of the homogeneous Eq. (1.1).

Let us see another example on the appearance of the secular term, which will make a problem as we are interested in bounded solutions of differential equations. The following two examples are also taken from [10].

Example 1.4.1. *The solution of differential equation*

$$\ddot{y} - y = e^{-t} \tag{1.7}$$

has a secular term, because e^{-t} satisfies the associated homogeneous equation. The general solution of (1.7) *is*

$$y(t) = Ae^{t} + Be^{-t} - \frac{1}{2}te^{-t}. \tag{1.8}$$

The particular solution $-\frac{1}{2}te^{-t}$ is secular relative to the homogeneous solution Be^{-t}. We must regard the term $-\frac{1}{2}te^{-t}$ as secular even though it is negligible compared with the homogeneous solution Ae^{t} as $t \to \infty$.

Example 1.4.2. *The solution of differential equation*

$$\ddot{y} - 2\dot{y} + y = e^{t} \tag{1.9}$$

has a secular term, because e^{t} satisfies the associated homogeneous equation. The general solution of (1.9) *is*

$$y(t) = Ae^{t} + Bte^{t} + \frac{1}{2}t^{2}e^{t}. \tag{1.10}$$

In this case, the particular solution $\frac{1}{2}t^2e^t$ is secular with respect to all solutions of the associated homogeneous equation.

How multiple scales can eliminate a secular term

Again, the following explanation is generally adopted from [10, 54, 60]. Consider the weak nonlinear oscillator equation (Duffing's equation)

$$\ddot{y} + y + \epsilon y^3 = 0, \qquad y(0) = 1, \qquad \dot{y}(0) = 0, \tag{1.11}$$

where the weak nonlinearity is given by ϵy^3 with small $|\epsilon| \ll 1$. A perturbative solution of this equation is obtained by expanding $y(t)$ as a power series in ϵ

$$y(t) = \sum_{n=0}^{\infty} \epsilon^n y_n(t), \tag{1.12}$$

where $y_0(0) = 1$, $\dot{y}_0(0) = 0$, $y_n(0) = \dot{y}_n(0) = 0$, $n \geq 1$. Substituting (1.12) into the differential equation (1.11) and equating coefficients of like powers of ϵ gives a sequence of linear differential equations

$$\begin{aligned} 0 &= \textstyle\sum_{n=0}^{\infty} \epsilon^n \ddot{y}_n + \sum_{n=0}^{\infty} \epsilon^n y_n + \epsilon \left(\sum_{n=0}^{\infty} \epsilon^n y_n \right)^3 \\ &= (\ddot{y}_0 + y_0) + \epsilon \left(\ddot{y}_1 + y_1 + y_0^3 \right) + O(\epsilon^2). \end{aligned} \tag{1.13}$$

This yields the first two differential equations

$$\ddot{y}_0 + y_0 = 0, \tag{1.14}$$

$$\ddot{y}_1 + y_1 = -y_0^3, \tag{1.15}$$

where the second equation (and also all further equations in the sequence) is inhomogeneous. The solution to (1.14), which satisfy $y_0(0) = 1$, $\dot{y}_0(0) = 0$ is

$$y_0(t) = \cos(t). \tag{1.16}$$

To solve (1.15) we appeal the trigonometric identity and obtain

$$y_0^3(t) = \cos^3(t) = \frac{1}{4}\cos(3t) + \frac{3}{4}\cos(t). \tag{1.17}$$

Hence, (1.15) becomes

$$\ddot{y}_1 + y_1 = -\left(\frac{1}{4}\cos(3t) + \frac{3}{4}\cos(t)\right), \tag{1.18}$$

and the general solution to (1.18) is

$$y_1(t) = -\frac{1}{32}\cos(t) + \frac{1}{32}\cos(3t) - \frac{3}{8}t\sin(t). \tag{1.19}$$

We can see that y_1 contains a secular term, i.e., $t\sin(t)$. Hence y_1 features linear growth in t. Then, we can write down an approximation of solution of (1.11)

$$y(t) = \cos(t) + \epsilon\left(-\frac{1}{32}\cos(t) + \frac{1}{32}\cos(3t) - \frac{3}{8}t\sin(t)\right) + O(\epsilon^2). \tag{1.20}$$

Equation (1.20) shows that the perturbation theory will break down when $t \sim \epsilon^{-1}$ since $y_1(t)$ will be of the same order as y_0. This t dependence in $y_1(t)$ is known as secular growth and arises whenever there is a resonance between y_0 and y_1. However, for all t, Bender dan Orszag [10] have proved that the exact solution $y(t)$ to (1.11) remains bounded. We can say that even though each term y_n in the series may contain secular terms, these secularities must disappear by summation.

Now, the perturbation theory in powers of ϵ is invalid when t gets larger than $O(\epsilon^{-1})$, as secular terms appear in all orders of ϵ and lead to unboundedness of a truncated perturbation series. We can omit the secular terms of a perturbation series by using the method of multiple scales, i.e., we use several further time scales $\epsilon t, \epsilon^2 t, \ldots$, such that we can deal with times t of order $O(\epsilon^{-n})$. Then it will provide a way to eliminate secular terms in the approximate solution as we will see in the following example.

Example 1.4.3. *We use the Duffing's equation as before to analyze the influence of nonlinear effects. The procedure of obtaining an ansatz can be made using a two-scale expansion i.e., t and $\tau = \epsilon t$. We introduce a new variable $\tau = \epsilon t$ and this variable is called the slow time because it does not become significant until $t \sim \epsilon^{-1}$. We consider a perturbation expansion of the solution $y(t)$ in the form*

$$y(t) = Y_0(t,\tau) + \epsilon Y_1(t,\tau) + \ldots = \sum_{n=0}^{\infty} \epsilon^n Y_n(t,\tau). \tag{1.21}$$

From (1.21) *and using the chain rule, this implies*

$$\frac{d}{dt}y(t) = \frac{\partial Y_0}{\partial t} + \epsilon\left(\frac{\partial Y_0}{\partial \tau} + \frac{\partial Y_1}{\partial t}\right) + O(\epsilon^2), \tag{1.22}$$

$$\frac{d^2}{dt^2}y(t) = \frac{\partial^2 Y_0}{\partial t^2} + \epsilon\left(2\frac{\partial^2 Y_0}{\partial \tau \partial t} + \frac{\partial^2 Y_1}{\partial t^2}\right) + O(\epsilon^2). \tag{1.23}$$

By substituting (1.21) *and Eq.* (1.22) - (1.23) *into* (1.11) *we obtain*

$$\frac{\partial^2 Y_0}{\partial t^2} + Y_0 + \epsilon\left(\frac{\partial^2 Y_1}{\partial t^2} + Y_1 + 2\frac{\partial^2 Y_0}{\partial \tau \partial t} + Y_0^3\right) + O(\epsilon^2). \tag{1.24}$$

Equating terms of powers of ϵ gives

$$\frac{\partial^2 Y_0}{\partial t^2} + Y_0 = 0, \qquad Y_0(0,0) = 1, \qquad \frac{\partial}{\partial t} Y_0(0,0), \tag{1.25}$$

$$\frac{\partial^2 Y_1}{\partial t^2} + Y_1 = -Y_0^3 - 2\frac{\partial^2 Y_0}{\partial \tau \partial t}, \qquad Y_1(0,0) = 1, \qquad \frac{\partial}{\partial t} Y_1(0,0) = -\frac{\partial}{\partial \tau} Y_0(0,0). \tag{1.26}$$

The general solution (1.25) *is*

$$Y_0(t,\tau) = A(\tau)e^{it} + \bar{A}(\tau)e^{-it}, \tag{1.27}$$

where $A(\tau)$ is an arbitrary complex function of τ and $\bar{A}(\tau)$ denotes its complex conjugate.

Substituting (1.27) *into* (1.26) *gives*

$$\frac{\partial^2 Y_1}{\partial t^2} + Y_1 = -A^3 e^{3it} - \bar{A}^3 e^{-3it} + e^{it} \underbrace{\left(-3A^2\bar{A} - 2i\frac{dA}{d\tau}\right)}_{:=p_1(\tau)} + e^{-it} \underbrace{\left(-3A\bar{A}^2 + 2i\frac{d\bar{A}}{d\tau}\right)}_{:=p_2(\tau)} \tag{1.28}$$

We can check that $e^{\pm it}$ itself is a solution of the homogeneous equation

$$\frac{\partial^2}{\partial t^2} Y_1 + Y_1 = 0,$$

corresponding to Eq. (1.26)*.*

If the terms $p_1(\tau)$, $p_2(\tau)$ in front of $e^{\pm it}$ in (1.28) *are nonzero, then $Y_1(t,\tau)$ will be secular in t. But that is exactly what we want to avoid. To ensure that there are no secular terms in $Y_1(t,\tau)$, we set $p_1(\tau)$ and $p_2(\tau)$ equal to zero*

$$-3A^2\bar{A} - 2i\frac{dA}{d\tau} = 0, \tag{1.29}$$

$$-3A\bar{A}^2 + 2i\frac{d\bar{A}}{d\tau} = 0. \tag{1.30}$$

Because (1.30) *is just the complex conjugate of* (1.29)*, we can omit it. If we have A satisfying these conditions, Y_1 will not contain secular terms and at least no secularities*

appear in the first two terms of the series representation of y in (1.21)*, but we have to be careful that we do not have any information on further terms. It means we have to restrict our time interval to* $t \in [0, T_0\epsilon^{-1}]$ *such that the error of the approximation*

$$\hat{y}(t) := Y_0(t,\tau) + \epsilon Y_1(t,\tau) \tag{1.31}$$

is of order $O(\epsilon^2)$*, i.e.* $y(t) - \hat{y}(t) = O(\epsilon^2)$*.*

From the above procedure, the approximation of Eq. (1.11) through Eq. (1.29) is what we call a rotating wave approximation.

1.5 Nonlinear lattices

Nonlinear lattices or discrete nonlinear equations are obtained when physical properties of a system are represented through an infinite set of coupled nonlinear evolution equations [47]. We know that in lattice equations, the strength of the interaction between lattices is determined by a coupling constant. This constant can be used as a perturbation parameter for the analysis of existence and stability of solutions to the lattice equations [82]. In that case, we consider the lattice equation in the limit of the small coupling constant, the so-called anti-continuum limit. MacKay and Aubry in [64] proposed this method for the first time to show the existence of discrete breathers. Furthermore, when the coupling constant approaches infinity, i.e., in the limit of the continuous approximation, one can investigate solutions to the lattice equation using perturbation analysis through the corresponding partial differential equation.

The main subjects in Chapters 4 and 5 are nonlinear lattice systems, i.e., discrete Klein-Gordon (dKG) equations and discrete nonlinear Schrödinger (dNLS) equations, which describe a lattice of coupled anharmonic oscillators [26, 59, 72]. We will see that the dNLS equations can be obtained from the dKG equations,

via a multiscale expansion in the limits of small-amplitude oscillations and weak inter-site coupling.

1.5.1 The discrete Klein-Gordon (dKG) equation

The one-dimensional discrete Klein-Gordon (dKG) equation with the hard quartic potential can be written in the form of

$$\ddot{x}_j + x_j + x_j^3 = \epsilon(x_{j+1} - 2x_j + x_{j-1}), \quad j \in \mathbb{Z}, \tag{1.32}$$

where $t \in \mathbb{R}$ is the evolution time, $x_j(t) \in \mathbb{R}$ is the horizontal displacement of the j-th particle in the one-dimensional chain, and $\epsilon > 0$ is the coupling constant of the linear interaction between neighbouring particles. Explanation about either hard or soft potential can be seen in [77]. The initial-value problem for the dKG equation (1.32) is globally well-posed in the sequence space $\ell^2(\mathbb{Z})$, see [82] for the proof.

Equation (1.32) admits a Hamiltonian

$$H = \frac{1}{2}\sum_{j\in\mathbb{Z}} \dot{x}_j^2 + x_j^2 + \epsilon(x_{j+1} - x_j)^2 + \frac{1}{4}\sum_{j\in\mathbb{Z}} x_j^4. \tag{1.33}$$

The dKG (1.32), in the case of models of weakly coupled ascillators, is a fundamental model for discrete breathers in nonlinear lattices.

1.5.2 The discrete nonlinear Schrödinger (dNLS) equation

The discrete nonlinear Schrödinger equation (dNLS) has appeared in many applications, such as those related to coupled optical wave guides [24, 32] or Bose-Einstein condensates trapped in a periodic potential [20, 91].

In one spatial dimension, the dNLS in its simplest form is

$$i\dot{A}_j + \epsilon\left(A_{j+1} - 2A_j + A_{j-1}\right) + \gamma|A_j|^2 A_j = 0, \qquad j \in \mathbb{Z}, \tag{1.34}$$

which describes a lattice of coupled anharmonic oscillators, where $i = \sqrt{-1}$. The quantity $A_j = A_j(t)$ is the complex mode amplitude of the oscillator at site j, and γ is a anharmonic parameter [23].

Note that the dNLS equation arises as the small-amplitude limit of the dKG lattice [72]. The anti-continuum limit is related to the small values of ϵ.

1.6 Bifurcation and stability analysis

In this section, we review bifurcation and stability analysis of ordinary differential equations (ODEs). The application of this theory will be directly applied in Chapter 3, 4 and 5.

In application, mathematical models are very useful to give quantitative descriptions and to derive numerical conclusions. Generally, we are dealing with an unspecified constant in a differential equation called parameter. One of the techniques that is applied to study solutions of differential equations is to allow a parameter varies and to observe the resulting changes in the behaviour of the solutions [52].

Formally, we can state the definition of bifurcation as in [35]

Definition 1.6.1. *In dynamical systems, a bifurcation occurs when a small smooth change made to the parameter values (the bifurcation parameters) of a system causes a sudden qualitative or topological change in its behaviour.*

Now, consider we have a set of ODEs, written in vector form

$$\dot{x} = f(x), \tag{1.35}$$

where x is variable.

Definition 1.6.2. *An equilibrium point x^* of the scalar differential equation* (1.35) *is a point for which $f(x^*) = 0$.*

Obviously, equilibrium points represent the simplest solutions to differential equations. Furthermore, suppose that we take a multivariate Taylor expansion of the right-hand side of our differential equation

$$\begin{aligned} \dot{x} &= f(x^*) + \left.\frac{\partial f}{\partial x}\right|_{x^*} (x - x^*) + \left.\frac{\partial^2 f}{\partial x^2}\right|_{x^*} (x - x^*)^2 + \cdots \\ &= \left.\frac{\partial f}{\partial x}\right|_{x^*} (x - x^*) + \left.\frac{\partial^2 f}{\partial x^2}\right|_{x^*} (x - x^*)^2 + \cdots \end{aligned} \tag{1.36}$$

The partial derivative in the above equation is to be interpreted as the Jacobian matrix. If the components of the state vector x are $(x_1, x_2, \cdots, x_n)$ and the components of the vector f are $(f_1, f_2, \cdots, f_n)$, then the Jacobian is

$$\mathrm{J} = \begin{bmatrix} \frac{\partial f_1}{\partial x_1} & \frac{\partial f_1}{\partial x_2} & \cdots & \frac{\partial f_1}{\partial x_n} \\ \frac{\partial f_2}{\partial x_1} & \frac{\partial f_2}{\partial x_2} & \cdots & \frac{\partial f_2}{\partial x_n} \\ \vdots & \vdots & \ddots & \vdots \\ \frac{\partial f_n}{\partial x_1} & \frac{\partial f_n}{\partial x_2} & \cdots & \frac{\partial f_n}{\partial x_n} \end{bmatrix}$$

Now, let us define $\delta x = x - x^*$. By taking a derivative of this definition, we obtain $\delta\dot{x} = \dot{x}$. If δx is small, then only the first term in Equation (1.36) is significant since the higher terms involve powers of our small displacement from equilibrium. If we want to know how trajectories behave near the equilibrium point, such as whether they move closer or away from the equilibrium point, it should be good enough to keep this term. Then we obtain

$$\delta\dot{x} = \mathrm{J}^*\delta x,$$

where J^* is the Jacobian evaluated at the equilibrium point. The matrix J^* is a constant, so this is a linear differential equation. According to the theory of linear differential equations, the solution can be written as a superposition of terms of the form $e^{\lambda_j t}$, where λ_j is the set of eigenvalues of the Jacobian.

In general, the eigenvalues of the Jacobian are complex numbers, then we can write $\lambda_j = u_j + iv_j$, where u_j and v_j are real and imaginary parts of the eigenvalue, respectively. Each of the exponential terms in the expansion can be written

$$e^{\lambda_t} = e^{(u_j+iv_j)t} = e^{u_j t}e^{iv_j t}.$$

The complex exponential can be written

$$e^{iv_j t} = \cos(v_j t) + i\sin(v_j t).$$

The complex part of the eigenvalue therefore only contributes an oscillatory component to the solution. It's the real part that matters: If $u_j > 0$ for any j, then $e^{u_j t}$ grows with time, which means that trajectories will tend to move away from the equilibrium point. Actually, what do eigenvalues tell us about stability? If the eigenvalues have real parts less than zero, then x^* is stable, and if at least one of the eigenvalues has a real part greater than zero then x^* is unstable, otherwise, there is no conclusion, it means borderline case between stability and instability require an investigation of the higher order terms. This leads us to a very important theorem as follows

Theorem 1.6.3. *(**Linear stability analysis**) An equilibrium point x^* of the differential equation* (1.35) *is stable if all the eigenvalues of J^*, the Jacobian evaluated at x^*, have negative real parts. The equilibrium point is unstable if at least one of the eigenvalues has a positive real part.*

Theorem (1.6.3) give us an information that eigenvalues allow to observe a stability analysis of linear dynamical systems. Furthermore, eigenvalues can contribute local stability analysis of nonlinear dynamical systems as well.

Example 1.6.4. *Consider the equation*

$$\dot{x} = cx - x^3.$$

To look at the stability, we need the derivative of $f(x,c)$. For $c > 0$, the equation has three equilibrium points, $x^* = 0$, and $x^* = \pm\sqrt{c}$. $Df(x,c) = c - 3x^2$, then $Df(0,c) = c > 0$, which implies that the fixed point at $x^* = 0$ is unstable. While for $Df(\pm\sqrt{c},c) = -2c < 0$, so both fixed point $x^* = \pm\sqrt{c}$ are stable.

Now, if $c < 0$, the equilibrium point is $x^* = 0$, and $Df(0,c) = c < 0$, the the equilibrium point is stable. Again, if $c = 0$, the equilibrium point is $x^* = 0$. Therefore, since $Df(0,0) = 0$, the equilibrium is nonhyperbolic and the equilibrium in this case is still stable. In this problem, the bifurcation of the system undergoes what is called a pitchfork bifurcation at the parameter value $c = 0$.

Example 1.6.5. *Given a couple of nonlinear systems*

$$\begin{aligned} \dot{x} &= -x^2 + 3x - 2xy, \\ \dot{y} &= -y^2 + 2y - xy. \end{aligned} \tag{1.37}$$

From above equation, the equilibrium point are $(0,0)$, $(0,2)$, $(3,0)$, *and* $(1,1)$ *and the Jacobian matrix is*

$$\mathrm{J} = \begin{bmatrix} \frac{\partial f_1}{\partial x} & \frac{\partial f_1}{\partial y} \\ \frac{\partial f_2}{\partial x} & \frac{\partial f_2}{\partial y} \end{bmatrix} = \begin{bmatrix} 3 - 2x - 2y & -2x \\ -y & 2 - x - 2y \end{bmatrix}. \tag{1.38}$$

Evaluating the Jacobian at $(0,0)$*, we obtain*

$$J^* = \begin{bmatrix} 3 & 0 \\ 0 & 2 \end{bmatrix}. \tag{1.39}$$

From (1.39) *we obtain the eigenvalues are* $\lambda_1 = 3$ *and* $\lambda_2 = 2$*. Because both of eigenvalues are positive, from Theorem* (1.6.3)*, we can conclude the fixed point at* $(0,0)$ *is unstable.*

Using the similar calculation, we evaluate the Jacobian at $(0,2)$*, we get*

$$J^* = \begin{bmatrix} -1 & 0 \\ -2 & -2 \end{bmatrix}. \tag{1.40}$$

From (1.40)*, the eigenvalues are* $\lambda_1 = -1$ *and* $\lambda_2 = -2$*. So, the fixed point is stable. Again, the Jacobian at* $(3,0)$ *is*

$$J^* = \begin{bmatrix} -3 & -6 \\ 0 & -1 \end{bmatrix}, \tag{1.41}$$

and obtained the eigenvalues are $\lambda_1 = -3$ *and* $\lambda_2 = -1$*. Therefore, we can say the equilibrium point is also stable. Next, at* $(1,1)$*, the Jacobian is*

$$J^* = \begin{bmatrix} -1 & -2 \\ -1 & -1 \end{bmatrix}. \tag{1.42}$$

The eigenvalues of J^* *are* $\lambda_1 = -1 + \sqrt{2}$ *and* $-1 - \sqrt{2}$*. So, the fixed point is unstable.*

1.7 Floquet theory

Floquet theory is used in Chapter 3, 4, and Chapter 5 to find linear stability numerically. To know about this material, let us see the following theory which generally adopted from [52]. In the Floquet system, we involve fundamental

matrix which is obtained from a fundamental system that is a set of n linearly independent solution of the linear system.

The fundamental matrix can be calculated by using the eigenpairs of the coefficient matrix. But for a homogeneous system of differential equations with a periodic coefficient matrix, to get the fundamental matrix, we need another approach, which is Floquet's theorem in Floquet theory.

Floquet's theorem offers a canonical form for each fundamental matrix of these periodic systems. Furthermore, Floquet's theorem affords a technique to transform a system with periodic coefficients into a system with constant coefficients. The fundamental matrix of a system of ODEs or monodromy matrix is very useful for stability analyses of periodic differential systems which are used in Chapter 4, and 5.

Because of Floquet system is closely linked to a linear system with constant coefficients, then we can apply the properties of those systems. Therefore, let us start this section by providing a theory about it.

1.7.1 Linear system

Consider linear system of the form

$$\begin{aligned}
\dot{x}_1 &= a_{11}(t)x_1 + a_{12}(t)x_2 + \cdots + a_{1n}(t)x_n + f_1(t) \\
\dot{x}_2 &= a_{21}(t)x_1 + a_{22}(t)x_2 + \cdots + a_{2n}(t)x_n + f_2(t) \\
&\vdots \\
\dot{x}_n &= a_{n1}(t)x_1 + a_{n2}(t)x_2 + \cdots + a_{nn}(t)x_n + f_n(t),
\end{aligned} \tag{1.43}$$

where we assume that the functions a_{ij}, and f_i, for $i, j = 1 \cdots n$, are continuous real-valued functions on an interval I. We say that the collection of n functions $x_1, x_2, \cdots, x_n$ is a solution on I of this linear system provided each of these n functions

is continuously differentiable on I and $t \in I$. This system can be written as an equivalent vector differential equation

$$\dot{x} = A(t)x + f(t), \tag{1.44}$$

where $x := \begin{bmatrix} x_1 \\ x_2 \\ \vdots \\ x_n \end{bmatrix}$, $\dot{x} := \begin{bmatrix} \dot{x}_1(t) \\ \dot{x}_2(t) \\ \vdots \\ \dot{x}_n(t) \end{bmatrix}$, $A(t) := \begin{bmatrix} a_{11}(t) & a_{12}(t) & \cdots & a_{1n}(t) \\ a_{21}(t) & a_{22}(t) & \cdots & a_{2n}(t) \\ \vdots & \vdots & \ddots & \vdots \\ a_{n1}(t) & a_{n2}(t) & \cdots & a_{nn}(t) \end{bmatrix}$, and $f(t) := \begin{bmatrix} f_1(t) \\ f_2(t) \\ \vdots \\ f_n(t) \end{bmatrix}$.

Note that the matrix functions A and f are continuous on I (a matrix function is continuous on I if and only if all of its entries are continuous on I). We say that an $n \times 1$ vector function x is a solution of (1.44) on I provided x is a continuously differentiable vector function on I (if and only if each component of x is continuously differentiable on I) and $x'(t) = A(t)x(t) + f(t)$, for all $t \in I$.

If we take $f = 0$ then Equation (1.44) becomes a homogeneous system of n differential equations and can be written as

$$\dot{x}(t) = A(t)x. \tag{1.45}$$

Further, first we will solve the corresponding homogeneous linear vector differential equation, $x'(t) = A(t)x$. Therefore, we need to discuss the homogeneous vector differential equation (1.45). For this purpose, we provide some theorems, definitions, and examples as studied in [52].

Theorem 1.7.1. *The linear differential equation* (1.45) *has n linearly independent solutions on I, and if* ϕ_1, ϕ_2, ..., ϕ_n *are n linearly independent solutions on I, then*

$$x = c_1\phi_1 + c_2\phi_2 + \cdots + c_n\phi_n, \tag{1.46}$$

for $t \in I$, where $c_1, c_2, \cdots, c_n$ are constants, is a general solution of (1.45).

Let us recall the definitions of eigenvalues and eigenvectors for an $n \times n$ matrix A.

Definition 1.7.2. *Let A be a given $n \times n$ constant matrix and let y be a column unknown n-vector. For any number λ the vector equation*

$$Ax = \lambda x \tag{1.47}$$

has the solution $x = 0$ called the trivial solution of the vector equation. If λ_0 is a number such that the vector equation (1.47) *with λ replaced by λ_0 has a nontrivial solution x_0, then λ_0 is called an eigenvalue of A and x_0 is called a corresponding eigenvector. We say λ_0, x_0 is an eigenpair of A.*

Assume λ is an eigenvalue of A, then Equation (1.47) has a nontrivial solution. Therefore,

$$(A - \lambda I)x = 0$$

has a nontrivial solution. From linear algebra we obtain that the characteristic equation

$$det(A - \lambda I) = 0$$

is satisfied. If λ_0 is an eigenvalue, then its corresponding eigenvector is nonzero vector x so that

$$(A - \lambda_0 I)x = 0.$$

Theorem 1.7.3. *If λ_0, x_0 is an eigenpair for the constant $n \times n$ matrix A, then*

$$x(t) = e^{\lambda_0 t} x_0, \qquad t \in \mathbb{R}, \tag{1.48}$$

defines a solution x of

$$\dot{x} = Ax, \tag{1.49}$$

on $\mathbb{R}$.

Example 1.7.4. *Solve the differential equation*

$$\dot{x} = \begin{bmatrix} 0 & 1 \\ -2 & -3 \end{bmatrix} x. \tag{1.50}$$

Define

$$A = \begin{bmatrix} 0 & 1 \\ -2 & -3 \end{bmatrix}.$$

From the characteristic equation of A, we obtain its eigenpairs are $-2, \begin{bmatrix} 1 \\ -2 \end{bmatrix}$ *and* $-1, \begin{bmatrix} 1 \\ -1 \end{bmatrix}$.
Thus by Theorem (1.7.3) *the vector functions* ϕ_1, ϕ_2 *defined by*

$$\phi_1(t) = e^{-2t} \begin{bmatrix} 1 \\ -2 \end{bmatrix}, \quad \textit{and} \quad \phi_2(t) = e^{-t} \begin{bmatrix} 1 \\ -1 \end{bmatrix}, \tag{1.51}$$

are solution on $\mathbb{R}$. *Since the vector functions* ϕ_1, ϕ_2 *are linearly independent on* $\mathbb{R}$, *a general solution x is given by*

$$x(t) = c_1 e^{-2t} \begin{bmatrix} 1 \\ -2 \end{bmatrix} + c_2 e^{-t} \begin{bmatrix} 1 \\ -1 \end{bmatrix},$$

$t \in \mathbb{R}$.

Theorem 1.7.5. *If* $y = u + iv$ *is a complex vector-valued solution of* (1.45), *where u, v are real vector-valued functions, then u, v are real vector-valued solutions of* (1.45).

Example 1.7.6. *Solve the differential equation*

$$\dot{x} = \begin{bmatrix} 3 & 1 \\ -13 & -3 \end{bmatrix} x. \tag{1.52}$$

From above we obtain the characteristic equation of the coefficient matrix

$$\lambda^2 + 4 = 0,$$

so that, and the eigenvalues are

$$\lambda_1 = 2i, \qquad \lambda_2 = -2i.$$

To find an eigenvector corresponding to $\lambda_1 = 2i$, we solve

$$\begin{bmatrix} 3-2i & 1 \\ -13 & -3-2i\lambda \end{bmatrix} \begin{bmatrix} x_1 \\ x_2 \end{bmatrix} = \begin{bmatrix} 0 \\ 0 \end{bmatrix}. \tag{1.53}$$

Therefore, the eigenpair of the coefficient matrix is

$$2i, \quad \begin{bmatrix} 1 \\ -3+2i \end{bmatrix}.$$

Hence by Theorem (1.7.3) *the solution ϕ is ϕ defined by*

$$\begin{aligned}\phi(t) &= e^{2it}\begin{bmatrix} i \\ -3+2i \end{bmatrix} \\ &= [\cos(2t)+i\sin(2t)]\begin{bmatrix} i \\ -3+2i \end{bmatrix} \\ &= \begin{bmatrix} \cos(2t) \\ -3\cos(2t)-2\sin(2t) \end{bmatrix} + i\begin{bmatrix} \sin(2t) \\ 2\cos(2t)-3\sin(2t) \end{bmatrix}.\end{aligned}$$

Using Theorem (1.7.5)*, we get that the vector functions ϕ_1, ϕ_2 defined by*

$$\phi_1(t) = \begin{bmatrix} \cos(2t) \\ -3\cos(2t)-2\sin(2t) \end{bmatrix}, \qquad \phi_2(t) = \begin{bmatrix} \sin(2t) \\ 2\cos(2t)-3\sin(2t) \end{bmatrix} \tag{1.54}$$

are real vector-valued solutions of (1.52)*. Since ϕ_1, ϕ_2 are linearly independent on $\mathbb{R}$, we have by Theorem* (1.7.1) *that a general solution x of* (1.52) *is given by*

$$x(t) = c_1\begin{bmatrix} \cos(2t) \\ -3\cos(2t)-2\sin(2t) \end{bmatrix} + c_2\begin{bmatrix} \sin(2t) \\ 2\cos(2t)-3\sin(2t) \end{bmatrix},$$

for $t \in \mathbb{R}$.

Now, let us define the matrix differential equation

$$\dot{X} = A(t)X, \tag{1.55}$$

where

$$X := \begin{bmatrix} x_{11} & x_{12} & \cdots & x_{1n} \\ x_{21} & x_{22} & \cdots & x_{2n} \\ \vdots & \vdots & \ddots & \vdots \\ x_{n1} & x_{n2} & \cdots & x_{nn} \end{bmatrix}$$

and

$$\dot{X} := \begin{bmatrix} \dot{x}_{11} & \dot{x}_{12} & \cdots & \dot{x}_{1n} \\ \dot{x}_{21} & \dot{x}_{22} & \cdots & \dot{x}_{2n} \\ \vdots & \vdots & \ddots & \vdots \\ \dot{x}_{n1} & \dot{x}_{n2} & \cdots & \dot{x}_{nn} \end{bmatrix}$$

are $n \times n$ matrix variables. A continuous matrix function $n \times n$ on an interval I is given by A and to be the matrix differential equation corresponding to the vector differential equation in (1.45). Matrix function Φ is a solution of (1.55) on I afforded Φ is a continuously differentiable $n \times n$ matrix function on I and

$$\dot{\Phi}(t) = A(t)\Phi(t),$$

for $t \in I$. A relationship between the vector differential equation (1.45) and the matrix differential equation (1.55) is given in the following theorem.

Theorem 1.7.7. *Assume A is a continuous $n \times n$ matrix function on an interval I and assume that Φ defined by*

$$\Phi(t) = [\phi_1(t), \phi_2(t), \cdots, \phi_n(t)], \qquad t \in I,$$

is the $n \times n$ matrix function with columns $\phi_1(t), \phi_2(t), \cdots, \phi_n(t)$. Then Φ is a solution of the matrix differential equation (1.55) *on I if and only if each column ϕ_i is a solution of the vector differential equation* (1.45) *on I for $1 \leq i \leq n$. Furthermore, if Φ is a solution of the matrix differential equation* (1.55)*,then*

$$x(t) = \Phi(t)c$$

is a solution of the vector differential equation (1.45) *for any constant $n \times 1$ vector c.*

Definition 1.7.8. *An $n \times n$ matrix function Φ is said to be a **fundamental matrix** for the vector differential equation* (1.45) *provided Φ is a solution of the matrix equation* (1.55) *on I and $\det \Phi(t) \neq 0$ on I.*

Example 1.7.9. *Find a fundamental matrix Φ for*

$$\dot{x} = \begin{bmatrix} -2 & 3 \\ 2 & 3 \end{bmatrix} x. \tag{1.56}$$

The characteristic equation is

$$\lambda^2 - \lambda - 12 = 0$$

so, the eigenvalues are $\lambda_1 = -3$, and $\lambda_2 = 4$. The corresponding eigenvectors are

$$\begin{bmatrix} 3 \\ -1 \end{bmatrix} \quad \text{and} \quad \begin{bmatrix} 1 \\ 2 \end{bmatrix}.$$

Therefore, the solutions of (1.56) *are*

$$\phi_1(t) = e^{-3t} \begin{bmatrix} 3 \\ -1 \end{bmatrix}, \quad \text{and} \quad \phi_2(t) = e^{4t} \begin{bmatrix} 1 \\ 2 \end{bmatrix},$$

for $t \in \mathbb{R}$. From Theorem (1.7.7)*, we obtain the matrix function Φ defined by*

$$\Phi(t) = [\phi_1, \phi_2] = \begin{bmatrix} 3e^{-3t} & e^{4t} \\ -e^{-3t} & 2e^{4t} \end{bmatrix},$$

for $t \in \mathbb{R}$ is a matrix solution of the matrix equation corresponding to (1.55)*. Since $\det \Phi(t) \neq 0$, for all $t \in \mathbb{R}$, Φ is a fundamental matrix of* (1.56) *on $\mathbb{R}$. It follows from Theorem*

(1.7.7) *that a general solution x of* (1.56) *is given by*

$$x(t) = \Phi(t)c = \begin{bmatrix} 3e^{-3t} & e^{4t} \\ -e^{-3t} & 2e^{4t} \end{bmatrix} c,$$

for $t \in \mathbb{R}$, where c is an arbitrary 2×1 constant vector.

1.7.2 Floquet's theorem

From above explanation, we know the fundamental matrix of a homogeneous system of differential equations with a constant coefficient matrix can be calculated by using the eigenpairs. However, for a homogeneous system of differential equations with a periodic coefficient matrix, we need another approach to obtain the fundamental matrix. In this case we will use Floquet's theorem because this theorem offers a canonical form for each fundamental matrix of these periodic systems.

In this sub section, we provide some statements about the fundamental system of a periodic homogeneous system. But, we will not prove it as available in [52].

Definition 1.7.10. *A matrix A is a periodic with period $T > 0$ if $A(t+T) = A(t)$ for every t.*

Now, let us rewrite Equation (1.45) and note that $A(t)$ is always a periodic matrix with period T and consider the Floquet system as follow

$$\dot{x} = A(t)x. \tag{1.57}$$

Theorem 1.7.11. *If Φ is a fundamental matrix for* (1.57)*, then $Y = \Phi B$ where B is an arbitrary $n \times n$ nonsingular constant matrix is a general fundamental matrix of* (1.57)*.*

Theorem 1.7.12. *(**Jordan Canonical Form**) If A is an $n \times n$ constant matrix, then there is a nonsingular $n \times n$ constant matrix P so that $A = PJP^{-1}$, where J is a block diagonal*

matrix of the form

$$J = \begin{bmatrix} J_1 & 0 & \cdots & 0 \\ 0 & J_2 & \ddots & \vdots \\ \vdots & \ddots & \ddots & 0 \\ 0 & \cdots & 0 & J_k \end{bmatrix}$$

where either J_i is the 1×1 matrix $J_i = [\lambda_i]$ or

$$J_i = \begin{bmatrix} \lambda_i & 1 & 0 & \cdots & 0 \\ 0 & \lambda_i & 1 & \ddots & \vdots \\ \vdots & \ddots & \ddots & \ddots & \vdots \\ \vdots & \ddots & \ddots & \lambda_i & 1 \\ 0 & \cdots & 0 & 0 & \lambda_i \end{bmatrix} \tag{1.58}$$

$1 \leq i \leq k$, and the λ_i's are the eigenvalues of A.

Because of every nonsingular matrix can be written as the exponential of one other matrix [84], then we have the following theorem.

Theorem 1.7.13. *(**Log of matrix**) If C is an $n \times n$ nonsingular matrix, then there is a matrix B such that $e^B = C$.*

Now, let us deliver Floquet's Theorem as follows

Theorem 1.7.14. *(**Floquet's Theorem**) If Φ is a fundamental matrix for the Floquet system* (1.57)*, where the matrix function A is continuous on $\mathbb{R}$ and has minimum positive period ω, then the matrix function Ψ defined by $\Psi(t) := \Phi(t + \omega)$, $t \in \mathbb{R}$ is also a fundamental matrix. Furthermore there is a nonsingular, continuously differentiable $n \times n$ matrix function P which is periodic with period ω and an $n \times n$ constant matrix B (possibly complex) so that*

$$\Phi(t) = P(t)e^{Bt},$$

for all $t \in \mathbb{R}$.

Definition 1.7.15. *Let Φ be a fundamental matrix for the Floquet system* (1.57)*. Then the eigenvalues μ of*

$$C := \Phi^{-1}(0)\Phi(\omega) \tag{1.59}$$

*are called the **Floquet multipliers** of the Floquet system* (1.57)*.*

The application above theory will be found in Chapter 3, 4 and 5.

1.8 Preliminary definitions

In here, we provide and adopt the following definitions, which will be used in this thesis as well.

1. A Hilbert space is a complete inner product space (equipped with the natural norm) and any Hilbert space is a Banach space.

   Example 1.8.1. *$\ell^2(\mathbb{Z})$ is a Hilbert space with the inner product*

   $$\langle x, y\rangle = \sum_{k=1}^{\infty} x_k \bar{y}_k, \qquad ||x|| = \left(\sum_{k=1}^{\infty} |x_k|^2\right)^{1/2}. \tag{1.60}$$

2. From [3], a linear operator T is bounded in its domain $\mathcal{D}$ if

   $$\sup_{f\in\mathcal{D}, ||f||=1} ||Tf|| \leq \infty. \tag{1.61}$$

   The left member of this inequality is called the norm of the operator T in $\mathcal{D}$ and is denoted by the symbol $||T||$ or, sometimes, by $||T||_{\mathcal{D}}$, then we have the norm of a bounded linear operator T can be defined equivalently by

   $$||T|| = \sup_{f\in\mathcal{D}, ||f||=1} ||Tf|| = \sup_{f\in\mathcal{D}} \frac{||Tf||}{||f||}. \tag{1.62}$$

3. A Banach algebra is an algebra $\mathcal{A}$ with a norm $\|\cdot\|$ such that $(\mathcal{A}, \|\cdot\|)$ is a Banach space and

$$\|xy\| \leq \|x\|\|y\|, \quad (x, y \in \mathcal{A}). \tag{1.63}$$

Chapter 2

Sturm-Liouville equations and eigenvalue problems

In this chapter, we provide basic theory, general information, and an introductory calculations of eigenvalue problems which are relevant and useful for Chapter 3.

2.1 Sturm-Liouville theory

In mathematics and its applications, many problems emerge in the form of boundary value problems that involve second-order differential equations. One of them is the classical Sturm-Liouville equation, which is a second-order linear differential equation of the form

$$-\frac{d}{dx}\left[p(x)\frac{dy}{dx}\right]+q(x)y=\lambda w(x)y, \qquad x\in[a,b], \tag{2.1}$$

where $p(x)$, $q(x)$, and $w(x)$ are given continuous functions defined on the finite closed interval $[a,b]$ with $p(x)$ and $w(x)$ both positive-valued on (a,b), and λ is an unknown constant called the eigenvalue parameter. The function $w(x)$ is called the weight function for the Sturm-Liouville equation.

We can define the Sturm-Liouville operator as

$$\mathcal{L} = \frac{1}{w(x)}\left[-\frac{d}{dx}p(x)\frac{d}{dx} + q(x)\right], \qquad w(x) > 0, \tag{2.2}$$

So, the Sturm-Liouville eigenvalue problem is given by the differential equation $\mathcal{L}y = \lambda y$, or the equation (2.1).

In addition, the Sturm-Liouville equation is defined together with the boundary condition at a and b to find the solution y. The value of λ in the equation (2.1) is not given and finding the value of λ for which there exists a nontrivial (nonzero) solution y of (2.1) satisfying the boundary condition is part of the problem called the Sturm-Liouville problem. A nonzero function y that solves the Sturm-Liouville problem (2.1) with boundary conditions is called an *eigenfunction*, and the corresponding value of λ is called its *eigenvalue*. Note that, the eigenvalues of a Sturm-Liouville problem are the values of λ for which nonzero solution exists.

There are some types of Sturm-Liouville problem, and we provide it as the following definition:

Definition 2.1.1. *The Sturm-Liouville differential equation on a finite interval* $[a,b]$ *with homogeneous mixed boundary conditions, that is*

$$-\frac{d}{dx}\left[p(x)\frac{dy}{dx}\right] + q(x)y = \lambda w(x)y, \qquad x \in [a,b]$$
$$\alpha_1 y(a) + \beta_1 y'(a) = 0$$
$$\alpha_2 y(b) + \beta_2 y'(b) = 0$$

with $p(x) > 0$ *and* $w(x) > 0$ *for* $x \in [a,b]$ *is called as regular Sturm-Liouville system or problem. The homogeneous mixed boundary conditions are also called symmetric boundary conditions.*

The main aim is to find all values λ for which a nontrivial solution y exists. It is implicitly assumed that y and its derivative are continuous on $[a,b]$, which also means that they are bounded. We are not interested in the trivial solution $y = 0$ since every Sturm-Liouville system has a trivial solution.

Boundary conditions for a solution y of a differential equation on interval $[a,b]$ are classified as

1. Boundary conditions of the form

$$\begin{aligned} \alpha_1 y(a) + \beta_1 y'(a) &= \alpha, \\ \alpha_2 y(b) + \beta_2 y'(b) &= \beta, \end{aligned} \tag{2.3}$$

   where $\alpha_j, \beta_j, \alpha$ and β are constants, are called *mixed Diriclet Neumann* boundary conditions. When both $\alpha = \beta = 0$, then the boundary conditions are said to be homogeneous. Special cases are *Dirichlet* boundary conditions when $\beta_1 = \beta_2 = 0$ and *Neumann* boundary conditions when $\alpha_1 = \alpha_2 = 0$.

2. Boundary conditions of the form

$$\begin{aligned} y(a) &= y(b), \\ y'(a) &= y'(b). \end{aligned} \tag{2.4}$$

   are called *periodic* boundary conditions.

Now, consider the second-order differential equations of the form

$$a_2(x)y'' + a_1(x)y' + a_0(x)y = f(x) \tag{2.5}$$

We want to show that equation (2.5) can be turned into a differential equation of Sturm-Liouville (2.1). Particularly, Equation (2.5) can be put into the form:

$$-\frac{d}{dx}\left(p(x)\frac{dy}{dx}\right)+q(x)y=F(x), \tag{2.6}$$

and we can provide that condition in the following theorem as mentioned in [61].

Theorem 2.1.2. *Any second order linear operator can be put into the form of the Sturm-Liouville operator (2.2).*

Proof. To proof the theorem, first we can consider the Equation (2.5). If $a_1(x)=a_2'(x)$ then we can write the equation in the form

$$\begin{aligned} f(x) &= a_2(x)y''+a_1(x)y'+a_0(x)y \\ &= (a_2(x)y')'+a_0(x)y. \end{aligned} \tag{2.7}$$

The resulting equation above has been changed in the Sturm–Liouville form. We just introduce $p(x)=a_2(x)$ and $q(x)=a_0(x)$. ■

However, not all second-order differential equations are modest to transform. Consider the differential equation

$$x^2y''+xy'+2y=0.$$

In this case, $a_2(x)=x^2$ and $a_2'(x)=2x\neq a_1(x)$. The linear differential operator in this equation is not of Sturm-Liouville type. But, we can change it to a Sturm-Liouville operator.

In the Sturm-Liouville operator, the derivative terms are gathered together into one exact derivative. We seek a multiplicative function $\mu(x)$ that we can multiply through (2.5) so that it can be written in Sturm-Liouville form. We first divide out

$a_2(x)$, giving

$$y'' + \frac{a_1(x)}{a_2(x)}y' + \frac{a_0(x)}{a_2(x)}y = \frac{f(x)}{a_2(x)}.$$

Now, we multiply the differential equation by μ:

$$\mu(x)y'' + \mu(x)\frac{a_1(x)}{a_2(x)}y' + \mu(x)\frac{a_0(x)}{a_2(x)}y = \mu(x)\frac{f(x)}{a_2(x)}.$$

The first two terms can now be combined into an exact derivative $(\mu y')'$ if $\mu(x)$ satisfies

$$\frac{d\mu}{dx} = \mu(x)\frac{a_1(x)}{a_2(x)}.$$

This is formally solved to give

$$\mu(x) = e^{\int \frac{a_1(x)}{a_2(x)}dx}.$$

Thus, the original equation can be multiplied by factor

$$\frac{\mu(x)}{a_2(x)} = \frac{1}{a_2(x)}e^{\int \frac{a_1(x)}{a_2(x)}dx}$$

to turn it into Sturm-Liouville form. In other words, we say that the Equation (2.5) can be put into Sturm-Liouville form (2.6), where $p(x) = e^{\int \frac{a_1(x)}{a_2(x)}dx}$, $q(x) = p(x)\frac{a_0(x)}{a_2(x)}$, and $F(x) = p(x)\frac{f(x)}{a_2(x)}$.

Example 2.1.3. *For the example above,*

$$x^2y'' + xy' + (x^2 - v^2) = 0,$$

can be written in Sturm-Liouville form as

$$(xy')' + \left(\frac{x - v^2}{x}\right)y = 0.$$

2.2 Properties of the Sturm-Liouville problems

In this section we will discuss an interesting explanation about eigenvalues and eigenfunction. These things will be delivered by giving some properties of them. Some of the properties for the regular Sturm-Liouville problem are that the eigenvalues are always real and bounded [42]. If the interval $[a,b]$ is finite, then the eigenvalues are discrete and the eigenfunctions corresponding to each eigenvalue are oscillatory in nature.

Let us start by considering a regular Sturm-Liouville problem as definition (2.1.1) as follow:

$$\begin{aligned} -\frac{d}{dx}\left[p(x)\frac{dy}{dx}\right] + q(x)y &= \lambda w(x)y, \qquad x \in [a,b], \\ \alpha_1 y(a) + \beta_1 y'(a) &= 0, \\ \alpha_2 y(b) + \beta_2 y'(b) &= 0. \end{aligned}$$

Let $L^2[a,b]$ be the Hilbert space of square integrable functions with an inner product

$$\langle f,g\rangle = \int_a^b \overline{f(x)}g(x)w(x)dx$$

where $w(x)$ is a nonnegative function on $[a,b]$ and called weight function. When $w(x) \equiv 1$, these definitions become to the "ordinary" ones. We will see that Sturm-Liouville operator is self-adjoint, but first we define the domain of an operator and introduce concept of adjoint operators.

Definition 2.2.1. *The domain of a differential operator L is the set of all $u \in L^2[a,b]$ satisfying a given set of homogeneous boundary conditions.*

Definition 2.2.2. *The adjoint, $L^\dagger$, of operator L satisfies*

$$\langle u, Lv\rangle = \langle L^\dagger u, v\rangle$$

for all v in the domain of L and u in the domain of $L^\dagger$.

We can see an example in [61], as follow.

Example 2.2.3. *We will find the adjoint of second order linear differential operator of* $L = a_2(x)\frac{d^2}{dx^2} + a_1(x)\frac{d}{dx} + a_0(x)$.

In order to find the adjoint, we place the operator under an integral. So, we consider the inner product

$$\langle u, Lv\rangle = \int_a^b u\,(a_2 v'' + a_1 v' + a_0 v)\,dx.$$

We have to move the operator L from v and determine what operator is acting on u in order to formally preserve the inner product. For a simple operator like $L = \frac{d}{dx}$, this is easily done using integration by parts. For the given operator, we will need to apply several integrations by parts to the individual terms. We will consider the individual terms.

First, we consider the $a_1 v'$ term. Integration by parts yields

$$\int_a^b u(x)a_1(x)v'(x)dx = a_1(x)u(x)v(x)\Big|_a^b - \int_a^b (u(x)a_1(x))'\,v(x)dx. \tag{2.8}$$

Now, we consider the $a_2 v''$ term. In this case it will take two integrations by parts:

$$\begin{aligned}\int_a^b u(x)a_2(x)v''(x)dx =& a_2(x)u(x)v'(x)\Big|_a^b - \int_a^b (u(x)a_2(x))' v(x)'dx \\ =& \left[a_2(x)u(x)v'(x) - (a_2(x)u(x))' v(x)\right]\Big|_a^b \\ &+ \int_a^b (u(x)a_2(x))'' v(x)dx.\end{aligned} \tag{2.9}$$

Combining these results, we obtain

$$\begin{aligned}\langle u, Lv\rangle =& \int_a^b u\left(a_2 v'' + a_1 v' + a_0 v\right) dx \\ =& \left[a_1(x)u(x)v(x) + a_2(x)u(x)v'(x) - (a_2(x)u(x))' v(x)\right]\Big|_a^b \\ &+ \int_a^b \left[(a_2 u)'' - (a_1 u)' + a_0 u\right] v dx.\end{aligned} \tag{2.10}$$

By applying the homogeneous boundary conditions for v, we have to find boundary condition for u such that

$$\left[a_1(x)u(x)v(x) + a_2(x)u(x)v'(x) - (a_2(x)u(x))' v(x)\right]\Big|_a^b = 0.$$

Now we just have

$$\langle u, Lv\rangle = \int_a^b \left[(a_2 u)'' - (a_1 u)' + a_0 u\right] v dx \equiv \langle L^\dagger u, v\rangle.$$

Hence, we obtain the adjoint operator of L

$$L^\dagger = \frac{d^2}{dx^2}a_2(x) - \frac{d}{dx}a_1(x) + a_0(x). \tag{2.11}$$

If $L^\dagger = L$ and the domain of both operators are the same, then the operator is called *self-adjoint*.

Example 2.2.4. *Determine $L^\dagger$ for the operator $Lu = \frac{du}{dx}$, where u satisfies the boundary conditions.*

We have to find the adjoint operator such that $\langle v, Lu\rangle = \langle L^\dagger v, u\rangle$. Hence, we can write it as

$$\langle v, Lu\rangle = \int_0^1 v\frac{du}{dx}dx = uv\Big|_0^1 - \int_0^1 u\frac{dv}{dx}dx = \langle L^\dagger v, u\rangle.$$

From above we obtain that $L^\dagger = -\frac{d}{dx}$.

Now, let us prove that Sturm-Liouville operator is self adjoint.

Theorem 2.2.5. *Let $\mathcal{H}$ be the subspace of functions that satisfy the boundary conditions of Sturm-Liouville problem. Sturm-Liouville operator* (2.2) *is self-adjoint operator on $\mathcal{H}$.*

Proof. Since we want to prove that Sturm-Liouville operator is self adjoint, so we have to show that $\langle f, Lg\rangle = \langle Lf, g\rangle$. First, let us define

$$\begin{aligned}\langle f, Lg\rangle &= \int_a^b \overline{f(x)}(Lg)(x)w(x)dx \\ &= \int_a^b \overline{f(x)}\left[-\frac{d}{dx}[p(x)g'(x)] + q(x)g(x)\right]dx\end{aligned}$$

and

$$\begin{aligned}\langle Lf, g\rangle &= \int_a^b L\overline{f(x)}g(x)w(x)dx \\ &= \int_a^b \left[-\frac{d}{dx}[p(x)\overline{f'(x)} + q(x)\overline{f(x)}\right]g(x)dx.\end{aligned}$$

By integrating the first and the second term by parts, we obtain

$$\begin{aligned}\langle f, Lg\rangle &= -\left[p(x)\overline{f(x)}g'(x)\right]_a^b + \int_a^b \left[\overline{f'(x)}p(x)g'(x) + \overline{f(x)}q(x)g(x)\right]dx, \\ \langle Lf, g\rangle &= -\left[p(x)\overline{f'(x)}g(x)\right]_a^b + \int_a^b \left[\overline{f'(x)}p(x)g'(x) + \overline{f(x)}q(x)g(x)\right]dx.\end{aligned}$$

Therefore,

$$\begin{aligned}\langle f, Lg\rangle - \langle Lf, g\rangle &= -\left[p(x)\overline{f(x)}g'(x)\right]_a^b + \left[p(x)\overline{f'(x)}g(x)\right]_a^b \\ &= p(b)\left(\overline{f'(b)}g(b) - \overline{f(b)}g'(b)\right) - p(a)\left(\overline{f'(a)}g(a) - \overline{f(a)}g'(a)\right).\end{aligned}$$

Since both f and g conform the same boundary condition, then $\alpha_1 f(a) + \beta_1 f'(a) = 0$. So, $\alpha_1\overline{f(a)} + \beta_1\overline{f'(a)} = 0$ and $\alpha_1 g(a) + \beta_1 g'(a) = 0$.

Thus, if $\alpha_1 \neq 0$ or $\beta_1 \neq 0$, it yields

$$\left(\overline{f'(a)}g(a) - \overline{f(a)}g'(a)\right) = 0.$$

Similarly,

$$\left(\overline{f'(b)}g(b) - \overline{f(b)}g'(b)\right) = 0.$$

Hence

$$\langle f, Lg\rangle = \langle Lf, g\rangle$$ ■

Example 2.2.6. *We consider the constant coefficient second order differential operator*

$$Ly = \left[\frac{\partial^2}{\partial x^2} - C\right]y, \quad C \text{ real},$$

defined on the domain $L^2[a,b]$ *with the boundary conditions*

$$\alpha_1 y(a) + \beta_1 y'(a) = 0;$$

$$\alpha_2 y(b) + \beta_2 y'(b) = 0,$$

and $\alpha_1, \beta_1, \alpha_2, \beta_2$ *are real and not zero.*

Let us claim that $L^\dagger = L$, or that operator is self-adjoint, so for $y, z \in L^2[a,b]$ we have

$$\begin{aligned}
\langle Ly, z\rangle &= \int_a^b (y''(x) - Cy(x))\overline{z(x)}dx \\
&= y'(x)\overline{z(x)}\Big|_a^b - \int_a^b \left[y'(x)\overline{z'(x)} + Cy(x)\overline{z(x)}\right]dx \\
&= \left[y'(x)\overline{z(x)} - y(x)\overline{z'(x)}\right]_a^b + \int_a^b y(x)\overline{[z''(x) - Cz(x)]}dx \\
&= \left[y'(x)\overline{z(x)} - y(x)\overline{z'(x)}\right]_a^b + \langle y, Lz\rangle.
\end{aligned}$$

Because both of y and z obey the same boundary conditions, then we have the self-adjointness property.

Hereafter, let us prove the theorem that says that eigenvalues of Sturm-Liouville problem are real and two eigenfunctions of a Sturm-Liouville system with corresponding to two different eigenvalues are orthogonal. Before we deal with that, we need to introduce two important identities for the Sturm-Liouville operator,

$$\mathcal{L} = \frac{d}{dx}\left(p\frac{d}{dx}\right) + q, \tag{2.12}$$

i.e.,

- Lagrange's identity, that is $u\mathcal{L}v - v\mathcal{L}u = [p(uv' - vu')]'$.
- Green's identity, that is $\int_a^b (u\mathcal{L}v - v\mathcal{L}u)dx = [p(uv' - vu')]_a^b$.

Now, we are able to prove the following theorem.

Theorem 2.2.7. *The eigenvalues of Sturm-Liouville problem are real*

Proof. Let $\phi_n(x)$ be a solution of the eigenvalue problem associated with λ_n:

$$\mathcal{L}\phi_n = -\lambda_n w\phi_n.$$

The conjugate of that equation is

$$\mathcal{L}\overline{\phi}_n = -\overline{\lambda}_n w\overline{\phi}_n.$$

Then, multiply both equation by $\overline{\phi}_n$ and ϕ_n respectively and subtract to yield

$$\begin{aligned}\overline{\phi}_n\mathcal{L}\phi_n - \phi_n\mathcal{L}\overline{\phi}_n &= (\overline{\lambda}_n - \lambda_n)w\phi_n\overline{\phi}_n \\ \implies \int_a^b \left(\overline{\phi}_n\mathcal{L}\phi_n - \phi_n\mathcal{L}\overline{\phi}_n\right)dx &= (\overline{\lambda}_n - \lambda_n)\int_a^b w\phi_n\overline{\phi}_n.\end{aligned}$$

By applying the Green's identity to the left hand side, we obtain

$$\begin{aligned}\left[p\left(\overline{\phi}_n\phi_n' - \phi_n\overline{\phi}_n'\right)\right]\Big|_a^b &= (\overline{\lambda}_n - \lambda_n)\int_a^b w\phi_n\overline{\phi}_n \\ \iff 0 &= (\overline{\lambda}_n - \lambda_n)\int_a^b w\|\phi_n\|^2 dx.\end{aligned}$$

Since the integral is nonzero, so we have $\overline{\lambda}_n = \lambda_n$. Hence, the eigenvalues are real. ■

Theorem 2.2.8. *The eigenfunctions corresponding to different eigenvalues of the Sturm-Liouville problem are orthogonal.*

Proof. Let $\phi_n(x)$ and $\phi_m(x)$ be solutions of an eigenvalue problem associated with λ_n and λ_m with $\lambda_n \neq \lambda_m$. Therefore, we have

$$\mathcal{L}\phi_n = -\lambda_n w\phi_n,$$

and

$$\mathcal{L}\phi_m = -\lambda_m w\phi_m.$$

Respectively, multiply the above equations by ϕ_m and ϕ_n and then subtract the results to get

$$\phi_m \mathcal{L}\phi_n - \phi_n \mathcal{L}\phi_m = (\lambda_m - \lambda_n) w \phi_n \phi_m$$

Integrate both side and apply Green's identity and the boundary condition for a self-adjoint operator to have

$$0 = (\lambda_m - \lambda_n) \int_a^b w \phi_n \phi_m dx.$$

Because the eigenvalues are different, so we have

$$\int_a^b w \phi_n \phi_m dx = 0.$$

Therefore, the eigenfunctions are orthogonal with respect to the weight function $w(x)$. ■

2.3 The spectrum of a linear operator

The spectrum of a linear operator on a finite-dimensional case precisely consists of its eigenvalues. However, a linear operator on infinite-dimensional space may have an additional element in its spectrum, and may have no eigenvalues. Let us see an example discussed in [41].

Example 2.3.1. *Consider the right shift operator T on the Hilbert space ℓ^2*

$$T : \ell^2 \to \ell^2, \quad \textbf{\textit{where}}$$

$$T(x_1, x_2, x_3, \ldots) = (0, x_1, x_2, \ldots)$$

If $x \in \ell^2$ so $x = (x_1, x_2, x_3, \ldots)$ then $Tx = (0, x_1, x_2, \ldots)$. This operator does not have an eigenvalues, because if $Tx = \lambda x$ then $(0, x_1, x_2, \ldots) = \lambda(x_1, x_2, x_3, \ldots)$ and by

expanding this expression we obtain that $x_1 = 0, x_2 = 0$, and so on. On the other hand, 0 is in the spectrum because the operator $T - \lambda I = T - 0I = T$ and $T - \lambda I$ is not invertible. The operator is also not surjective since any vector with nonzero component is not in its range, or in other words, we can say that for every $y \in \ell^2$ (in range/codomain) we could not find $x \in \ell^2$ (in domain) such that $y = Tx$.

Definition 2.3.2. *Let $\mathcal{H}$ be a Hilbert space. The resolvent set of an operator A, denoted by $\rho(A)$, is the set of complex numbers λ such that $(A - \lambda I) : \mathcal{H} \to \mathcal{H}$ is one-to-one and onto. The spectrum of A, denoted by $\sigma(A)$, is the complement of the resolvent set in $\mathbb{C}$, meaning that $\sigma(A) = \mathbb{C} \backslash \rho(A)$ [22].*

As in the finite-dimensional case, a complex number λ is called an eigenvalue of A, if there is a nonzero vector $u \in \mathcal{H}$ such that $Au = \lambda u$. In that case, $ker(A - \lambda I) \neq 0$, so $A - \lambda I$ is not injective, and $\lambda \in \sigma(A)$. However, that complex number can belong to the spectrum. We will subdivide the spectrum of linear operator as the following definition.

Definition 2.3.3. *Let A be a linear operator from Hilbert space $\mathcal{H}$ to $\mathcal{H}$.*

1. *The point spectrum $\sigma_p(A)$ of A consists of all $\lambda \in \sigma(A)$ such that $A - \lambda I$ is not injective. In this case λ is called an eigenvalue of A.*

2. *The continuous spectrum $\sigma_c(A)$ of A consists of all $\lambda \in \sigma(A)$ such that $A - \lambda I$ is injective but not surjective, and range$(A - \lambda I)$ is dense in $\mathcal{H}$*

Since $A - \lambda I$ is a linear operator, the inverse is also linear if it exists. Hence, the spectrum consists precisely of those scalars λ for which $A - \lambda I$ is not bijective.

2.3.1 Discrete or point spectrum

According to the definition, if an operator is not injective, so there is some nonzero x with $A(x) = 0$, then it is clearly not invertible. If λ is an eigenvalue of A, one

necessarily has $\lambda \in \sigma(A)$. The set of eigenvalues of A is then called the discrete or point spectrum of A, denoted by $\sigma_p(A)$.

We will give an example of discrete spectrum that related to the Sturm-Liouville problem. First, let us start from our Sturm-Liouville equation of the form:

$$\Omega\hat{\psi} = -\hat{\psi}_{xx} + V(x)\hat{\psi}, \tag{2.13}$$

where $V(x)$ is a given function and in this case it will be known as a potential. In here, we can define that our linear operator in this problem is $T = -\partial_{xx} + V(x)$.

2.3.1.1 Discrete spectrum of a one-well potential

In this part, we will solve the eigenvalue problem (2.13) with $V(x)$ representing a one-well potential. We will also determine the discrete spectrum of that problem.

Consider the linear Schrodinger equation:

$$i\psi_t = -\psi_{xx} + V(x)\psi\ , \tag{2.14}$$

with

$$\psi(x,t) = \hat{\psi}(x)e^{-i\Omega t}\ . \tag{2.15}$$

If equation (2.15) and its derivative is substituted into equation (2.14), we will obtain the Sturm-Liouville equation (2.13).

Let us consider a piece-wise constant potential defined as:

$$V(x) = \begin{cases} -d, & |x| < a \\ 0, & |x| > a\ . \end{cases} \tag{2.16}$$

Therefore, if we substitute (2.16) into equation (2.13), then we have three different regions for ψ, i.e.:

$$\hat{\psi}_{xx} + \Omega\hat{\psi} = 0, \qquad x < -a, \tag{2.17}$$

$$\hat{\psi}_{xx} + \Omega\hat{\psi} + d\hat{\psi} = 0, \qquad -a < x < a, \tag{2.18}$$

$$\hat{\psi}_{xx} + \Omega\hat{\psi} = 0, \qquad x > a. \tag{2.19}$$

The general solution for (2.17) and (2.19) is $\hat{\psi}(x) = C_1 e^{-\sqrt{-\Omega}\,x} + C_2 e^{\sqrt{-\Omega}\,x}$, while for (2.18), the general solution is $\hat{\psi}(x) = C_3 e^{-\sqrt{-\Omega-d}\,x} + C_4 e^{-\sqrt{-\Omega-d}\,x}$. Since we want to obtain a bounded solution, then the general solution for each region is:

$$\hat{\psi}_I = A_1 e^{\sqrt{-\Omega}\,x}, \qquad x < -a, \tag{2.20}$$

$$\hat{\psi}_{II} = A_2\ \cos(\sqrt{\Omega + d}\,x) + B_2\ \sin(\sqrt{\Omega + d}\,x), \qquad -a < x < a, \tag{2.21}$$

$$\hat{\psi}_{III} = B_3 e^{-\sqrt{-\Omega}\,x}, \qquad x > a. \tag{2.22}$$

Note that the potential has a symmetry under parity, i.e. $V(x) = V(-x)$. It implies that if $\hat{\psi}(x)$ a solution, then $\hat{\psi}(-x)$ is a solution as well. Therefore, we have even ($\hat{\psi}_0$) and odd ($\hat{\psi}_1$) solutions in this case.

1. Even solution

Based on the above solution for each region on the first case, we can write an even solution, i.e.:

$$\hat{\psi}_0(x) = \begin{cases} A_1\, e^{\sqrt{-\Omega_0}\,x}, & x < -a, \\ A_2\ \cos(\sqrt{\Omega_0 + d}\,x), & -a < x < a, \\ B_3\, e^{-\sqrt{-\Omega_0}\,x}, & x > a. \end{cases} \tag{2.23}$$

and its derivative

$$\frac{d}{dx}\hat{\psi}_0(x) = \begin{cases} A_1\ \sqrt{-\Omega_0}\, e^{\sqrt{-\Omega_0}\,x}, & x < -a, \\ A_2\ \sqrt{\Omega_0 + d}\ \sin(\sqrt{\Omega_0 + d}\,x), & -a < x < a, \\ -B_3\ \sqrt{-\Omega_0}\, e^{-\sqrt{-\Omega_0}\,x}, & x > a. \end{cases} \tag{2.24}$$

Since $\hat{\psi}_0(x)$ and $\frac{d}{dx}\hat{\psi}_0(x)$ must be continuous, then we have the following conditions:

$$\begin{aligned} A_1 e^{-\sqrt{-\Omega_0}\,a} &= A_2\ \cos(\sqrt{\Omega_0 + d}\,a), \\ A_1\ \sqrt{-\Omega_0}\, e^{-\sqrt{-\Omega_0}\,a} &= A_2\ \sqrt{\Omega_0 + d}\ \sin(\sqrt{\Omega_0 + d}\,a), \\ B_3 e^{-\sqrt{-\Omega_0}\,a} &= A_2\ \cos(\sqrt{\Omega_0 + d}\,a), \\ -B_3\ \sqrt{-\Omega_0}\, e^{-\sqrt{-\Omega_0}\,a} &= -A_2\ \sqrt{\Omega_0 + d}\ \sin(\sqrt{\Omega_0 + d}\,a). \end{aligned} \tag{2.25}$$

With a simple calculation, we can simplify equations (2.25) and obtain the coefficient $A_1 = B_3$. By choosing $A_1 = 1 = B_3$, we will obtain the transcendental equation

$$\tan(\sqrt{\Omega_0 + d}\,a) = \frac{\sqrt{-\Omega_0}}{\sqrt{\Omega_0 + d}}\,. \tag{2.26}$$

The above equation cannot be solved analytically, we thus search for a solution graphically. By taking $d = 1$ and $a = 4$, then we get the solutions for the transcendental equation as the intersection in Figure 2.1. Furthermore, we can plot the eigenfunctions for each Ω_0 as shown in Figure 2.2.

2. Odd solution

The following is an odd solution for $\hat{\psi}_1(x)$ for the first case:

$$\hat{\psi}_1(x) = \begin{cases} A_1\, e^{\sqrt{-\Omega_1}\,x}, & x < -a, \\ B_2\ \sin(\sqrt{\Omega_1 + d}\,x), & -a < x < a, \\ B_3\, e^{-\sqrt{-\Omega_1}\,x}, & x > a, \end{cases} \tag{2.27}$$

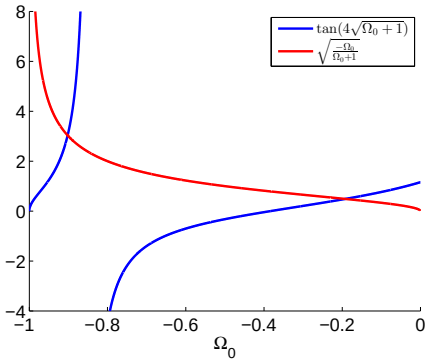

Figure 2.1. Graphic solution of the eigenvalue Equation (2.26). The solutions are the intersections between the red and blue curves, i.e., $\Omega_{0_1} = -0.9019757111$ and $\Omega_{0_2} = -0.1921114320$.

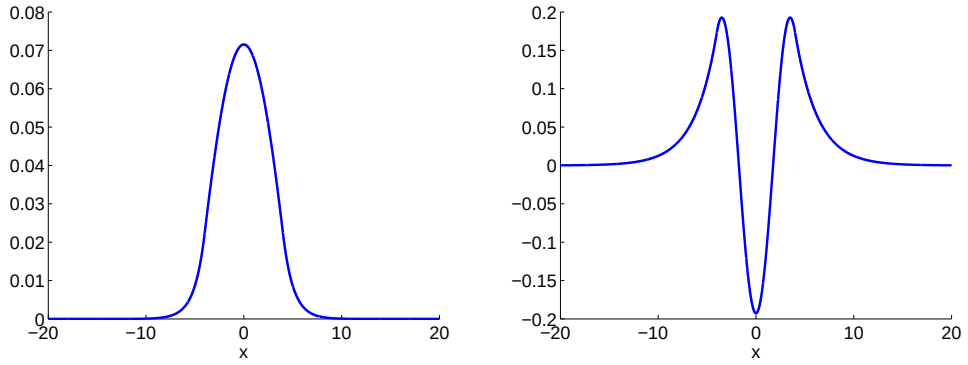

(a) $\Omega_{0_1} = -0.9019757111$ (b) $\Omega_{0_2} = -0.1921114320$

Figure 2.2. The graphs of eigenfunction corresponding to the eigenvalue Ω_0 presented in Figure 2.1.

and its derivative

$$\hat{\psi}_1(x) = \begin{cases} A_1 \sqrt{-\Omega_1}\, e^{\sqrt{-\Omega_1}\, x}, & x < -a, \\ -B_2 \sqrt{\Omega_1 + d}\, \cos(\sqrt{\Omega_1 + d}\, x), & -a < x < a, \\ -B_3 \sqrt{-\Omega_1}\, e^{-\sqrt{-\Omega_1}\, x}, & x > a, \end{cases} \tag{2.28}$$

Since $\hat{\psi}_1(x)$ and $\frac{d}{dx}\hat{\psi}_1(x)$ must be also continuous, then we have the following conditions:

$$\begin{aligned} A_1\, e^{-\sqrt{-\Omega_1}\,a} &= B_2\, \sin(-\sqrt{\Omega_1+d}\,a), \\ A_1\, \sqrt{-\Omega_1}\, e^{-\sqrt{-\Omega_1}\,a} &= B_2\, \sqrt{\Omega_1+d}\, \cos(\sqrt{\Omega_1+d}\,a), \\ B_3 e^{-\sqrt{-\Omega_1}\,a} &= B_2\, \sin(\sqrt{\Omega_1+d}\,a), \\ -B_3\, \sqrt{-\Omega_1}\, e^{-\sqrt{-\Omega_1}\,a} &= B_2\, \sqrt{\Omega_1+d}\, \cos(\sqrt{\Omega_1+d}\,a). \end{aligned} \tag{2.29}$$

If we solve equations (2.29), we obtain the coefficient $A_1 = -B_3$. By doing the similar ways with the even solutions, we can choose $A_1 = 1$ which implies $B_3 = -1$ and obtain a transcendental equation for Ω as:

$$\cot(\sqrt{\Omega_1+d}\,a) = \frac{-\sqrt{-\Omega_1}}{\sqrt{\Omega_1+d}}. \tag{2.30}$$

By plotting $\cot(\sqrt{\Omega_1+d}\,a)$ and $\frac{-\sqrt{-\Omega_1}}{\sqrt{\Omega_1+d}}$ separately, and taking $d = 1$ and $a = 4$, we get the graphs in Figure 2.3. Next, we can plot the eigenfunction for the odd solution as shown in Figure 2.4.

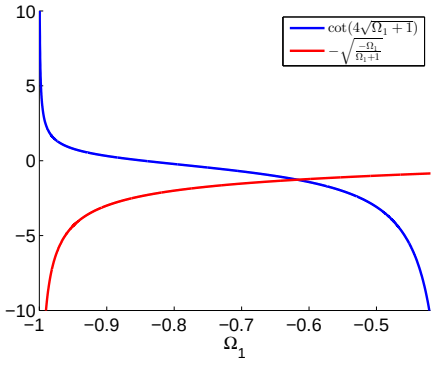

Figure 2.3. Graphic solution of the eigenvalue Equation (2.30). The solutions are the intersections between the red and blue curves, i.e., $\Omega_1 = -0.6172793577$.

From the graphs in Figures 2.2 and 2.4, we can see that eigenfunction decays to zero when x tend to $\pm\infty$ or we can write it down as $\int_{-\infty}^{\infty} \left|\hat{\psi}_1(x)\right|^2 dx < \infty$.

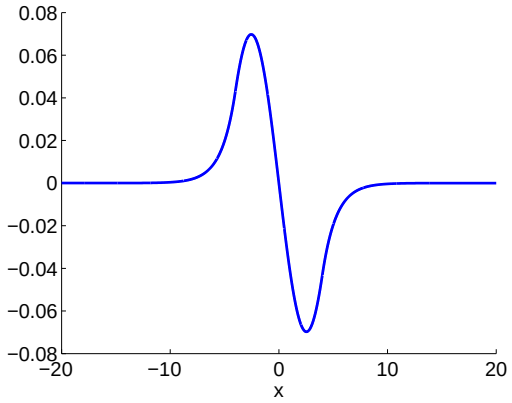

Figure 2.4. Graphs of eigenfunctions corresponding to the eigenvalue Ω_1 in Figure (2.3)

2.3.1.2 Discrete spectrum of a double-well potential

In this part, we will determine the discrete spectrum of a double-well potential that will be used in our next chapter. Let us consider a double-well potential for the same Sturm-Liouville Equation (2.13):

$$V(x) = \begin{cases} -d, & a < |x| < a+b \\ 0, & \text{elsewhere} \end{cases} \tag{2.31}$$

If the above potential is substituted into Equation (2.13), then we have five different regions for ψ, and the solution for each region is:

$$\hat{\psi}_I = A_1 e^{\sqrt{-\Omega}\,x}, \qquad x < -a-b, \tag{2.32}$$

$$\hat{\psi}_{II} = A_2 \cos(\sqrt{d+\Omega}\,x) + B_2 \sin(\sqrt{d+\Omega}\,x), \qquad -a-b < x < -a, \tag{2.33}$$

$$\hat{\psi}_{III} = A_3 \cosh(\sqrt{-\Omega}\,x) \text{ or } B_3 \sinh(\sqrt{-\Omega}\,x), \qquad -a < x < a, \tag{2.34}$$

$$\hat{\psi}_{IV} = A_4 \cos(\sqrt{d+\Omega}\,x) + B_4 \sin(\sqrt{d+\Omega}\,x), \qquad a < x < a+b, \tag{2.35}$$

$$\hat{\psi}_V = A_5 e^{-\sqrt{-\Omega}\,x}, \qquad x > a+b. \tag{2.36}$$

Following the similar calculations with the one-well potential, we also have even and odd solutions.

1. Even solution

Based on the above solutions for each region, we can write an even solution for double-well potential case as follow:

$$\hat{\psi}_0(x) = \begin{cases} A_1 e^{\sqrt{-\Omega_0}\,x}, & x < -a-b, \\ A_2 \sin(\sqrt{d+\Omega_0}\,x) + B_2 \cos(\sqrt{d+\Omega_0}\,x), & -a-b < x < -a, \\ A_3 \cosh(\sqrt{-\Omega_0}\,x)), & x > -a. \end{cases} \tag{2.37}$$

Since $\hat{\psi}_0(x)$ and $\frac{d}{dx}\hat{\psi}_0(x)$ must be continuous, again we have parity solutions for Equation (2.37) written as:

$$\begin{aligned} A_1 e^{\sqrt{-\Omega_0}\,(-a-b)} &= A_2 \sin(\sqrt{d+\Omega_0}\,(-a-b)) \\ &\quad + B_2 \cos(\sqrt{d+\Omega_0}\,(-a-b)), \\ A_1 \sqrt{-\Omega_0} e^{\sqrt{-\Omega_0}\,(-a-b)} &= A_2 \sqrt{d+\Omega_0} \cos(-\sqrt{d+\Omega_0}\,(-a-b)) \\ &\quad - B_2 \sqrt{d+\Omega_0} \sin(\sqrt{d+\Omega_0}\,(-a-b)), \\ A_3 \cosh(\sqrt{-\Omega_0}\,(-a)) &= A_2 \sin(\sqrt{d+\Omega_0}\,(-a)) \\ &\quad + B_2 \cos(\sqrt{d+\Omega_0}\,(-a)), \\ A_3 \sqrt{-\Omega_0} \sinh(\sqrt{-\Omega_0}\,(-a)) &= A_2 \sqrt{d+\Omega_0} \cos(-\sqrt{d+\Omega_0}\,(-a)) \\ &\quad - B_2 \sqrt{d+\Omega_0} \sin(\sqrt{d+\Omega_0}\,(-a)). \end{aligned} \tag{2.38}$$

Numerically, we get an even solution for $\Omega_0 = -0.4550947238$ with $a = 4, b = 2, d = 1$. The graph of the eigenfunction can be seen in Figure 2.5.

2. Odd solution

The following is an odd solution for $\hat{\psi}_1(x)$ for the double-well potential case:

$$\hat{\psi}_1(x) = \begin{cases} A_1 e^{\sqrt{-\Omega_1}\,x}, & x < -a-b, \\ A_2 \sin(\sqrt{d+\Omega_1}\,x) + B_2 \cos(\sqrt{d+\Omega_1}\,x), & -a-b < x < -a, \\ B_3 \sinh(\sqrt{-\Omega_1}\,x)), & x > -a. \end{cases} \tag{2.39}$$

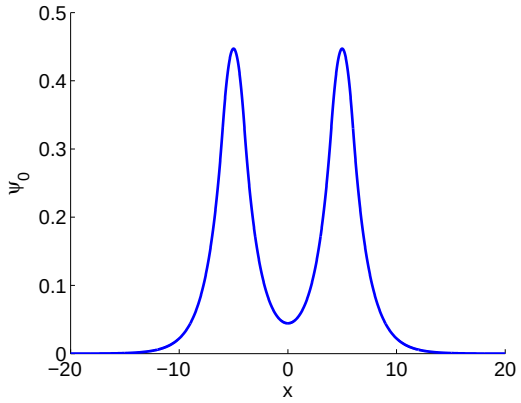

Figure 2.5. Graph of an eigenfunction corresponding to the eigenvalue Ω_0 in a double-well potential.

Again, since $\hat{\psi}_1(x)$ and $\frac{d}{dx}\hat{\psi}_1(x)$ must be continuous, we have the following condition:

$$\begin{aligned}
A_1 e^{\sqrt{-\Omega_1}(-a-b)} &= A_2 \sin(\sqrt{d+\Omega_1}(-a-b)) \\
&\quad + B_2 \cos(\sqrt{d+\Omega_1}(-a-b)), \\
A_1 \sqrt{-\Omega_1} e^{\sqrt{-\Omega_1}(-a-b)} &= A_2 \sqrt{d+\Omega_1} \cos(-\sqrt{d+\Omega_1}(-a-b)) \\
&\quad - B_2 \sqrt{d+\Omega_1} \sin(\sqrt{d+\Omega_1}(-a-b)), \\
A_3 \sinh(\sqrt{-\Omega_1}(-a)) &= A_2 \sin(\sqrt{d+\Omega_1}(-a)) \\
&\quad + B_2 \cos(\sqrt{d+\Omega_1}(-a)), \\
A_3 \sqrt{-\Omega_1} \cosh(\sqrt{-\Omega_1}(-a)) &= A_2 \sqrt{d+\Omega_1} \cos(-\sqrt{d+\Omega_1}(-a)) \\
&\quad - B_2 \sqrt{d+\Omega_1} \sin(\sqrt{d+\Omega_1}(-a)).
\end{aligned} \tag{2.40}$$

Solving equations numerically, we obtain an odd solution for $\Omega_1 = -0.4523889358$ with the same parameter as in the even solution in Figure 2.5. Plot of the eigenfunction for the odd solution is given in Figure 2.6. Figure 2.5 and 2.6 show that the eigenfunctions decay to zero when x goes to $\pm\infty$ in the same way as the one-well potential problem.

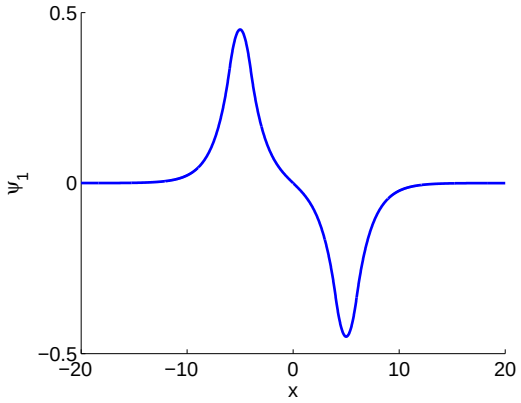

Figure 2.6. Graph of the eigenfunction corresponding to the eigenvalue Ω_1 in a double-well potential.

2.3.2 Continuous spectrum

In Section 2.3, we provide the definition of discrete or point spectrum as well as continuous spectrum. However, in general we have several definitions of continuous spectrum in [6, 11, 51] which are not equivalent. However, for self-adjoint operators, all the definitions coincide. Here, we choose to deliver the definitions in [6] as follow

Definition 2.3.4. *For bounded operator $T : H \to H$ on a Hilbert space, we define*

1. *The **resolvent** consists of $\lambda \in \mathbb{C}$ for which $T - \lambda I$ is invertible.*
2. *The **point spectrum** consists of $\lambda \in \mathbb{C}$ for which $T - \lambda I$ is not injective .*
3. *The **continuous spectrum** consists of $\lambda \in \mathbb{C}$ for which $T - \lambda I$ is one to one, is not onto but for which $Im(T - \lambda I)$ is dense.*
4. *The **residual spectrum** consists of $\lambda \in \mathbb{C}$ with $T - \lambda I$ being one to one but $Im(T - \lambda I)$ is not dense.*

Definition 2.3.5. *For an operator $T : H \to H$ (not necessarily bounded) on a Hilbert space, we define*

1. *The **resolvent** consists of $\lambda \in \mathbb{C}$ for which $T - \lambda I$ is one to one and $Im(T - \lambda I)$ is dense in H and $(T - \lambda I)^{-1}$ is bounded on the image of $D(T)$.*

2. *The **point spectrum** consists of $\lambda \in \mathbb{C}$ for which $T - \lambda I$ is not one to one on $D(T)$.*

3. *The **continuous spectrum** consists of $\lambda \in \mathbb{C}$ for which $T - \lambda I$ is one to one, $Im(T - \lambda I)$ is dense but $(T - \lambda I)^{-1}$ is not bounded on $Im(T - \lambda I)$.*

4. *The **residual spectrum** consists of $\lambda \in \mathbb{C}$ with $T - \lambda I$ is one to one but $Im(T - \lambda I)$ is not dense.*

2.3.2.1 Continuous spectrum of the one-well potential

In here, we want to find the eigenfunction of continuous spectrum of the one-well potential. Since we already dealt with the eigenfunction for discrete spectrum, now with similar calculations, we obtain the following solution for each region:

$$\hat{\psi}_I = A_1 \sin\left(\sqrt{\Omega}\, x\right) + B_1 \cos\left(\sqrt{\Omega}\, x\right), \tag{2.41}$$

$$\hat{\psi}_{II} = A_2 \sin\left(\sqrt{\Omega + d}\, x\right) \text{ or } B_2 \cos\left(\sqrt{\Omega + d}\, x\right), \tag{2.42}$$

$$\hat{\psi}_{III} = A_3 \sin\left(\sqrt{\Omega}\, x\right) + B_3 \cos\left(\sqrt{\Omega}\, x\right). \tag{2.43}$$

As we must also have the symmetry under parity as mentioned above, i.e., if $\hat{\psi}(x)$ a solution, then $\hat{\psi}(-x)$ is a solution as well, we can separate the solution into even and odd solution again.

First, let us find our continuous spectrum for our eigenvalue problem $\Omega\hat{\psi} = -\hat{\psi}_{xx} + V(x)\hat{\psi}$. This equation can be rewritten as

$$\hat{\psi}_x = q,$$

$$q_x = (V(x) - \Omega)\hat{\psi}(x).$$

A simple calculation shows that we will obtain our eigenvalue $\Omega = k^2$ for every $k \in \mathbb{R}$. So, for every positive Ω we always can find the corresponding eigenfunction.

1. Even solution

The conditions below are for even parity solutions:

$$\begin{aligned}
A_2 \cos(\sqrt{\Omega + d}(-a)) &= A_1 \sin\left(\sqrt{\Omega}(-a)\right) + B_1 \cos\left(\sqrt{\Omega}(-a)\right), \\
-A_2 \sqrt{\Omega + d} \sin(\sqrt{\Omega + d}(-a)) &= A_1 \sqrt{\Omega} \cos\left(\sqrt{\Omega}(-a)\right) - B_1 \sqrt{\Omega} \sin\left(\sqrt{\Omega}(-a)\right), \\
A_2 \cos(\sqrt{\Omega + d}(a)) &= A_3 \sin\left(\sqrt{\Omega}(a)\right) + B_3 \cos\left(\sqrt{\Omega}(a)\right), \\
-A_2 \sqrt{\Omega + d} \sin(\sqrt{\Omega + d}(a)) &= A_3 \sqrt{\Omega} \cos\left(\sqrt{\Omega}(a)\right) - B_3 \sqrt{\Omega} \sin\left(\sqrt{\Omega}(a)\right).
\end{aligned} \tag{2.44}$$

By taking $A_2 = 1$, we can solve Equation (2.44) and plot the graph with parameter $a = 4$, $d = 1$, and $\Omega = 1$ as shown in Figure 2.7.

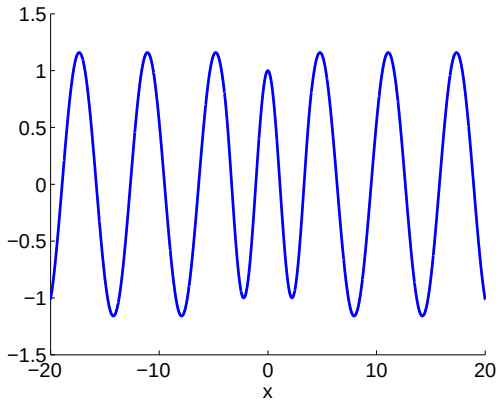

Figure 2.7. Graph of an even eigenfunction with $\Omega = 1$.

2. Odd solution

Furthermore, for the odd parity solutions, we have the conditions:

$$\begin{aligned}
A_2 \sin(\sqrt{\Omega + d}(-a)) &= A_1 \sin\left(\sqrt{\Omega}(-a)\right) + B_1 \cos\left(\sqrt{\Omega}(-a)\right), \\
A_2 \sqrt{\Omega + d} \cos(\sqrt{\Omega + d}(-a) &= A_1 \sqrt{\Omega} \cos\left(\sqrt{\Omega}(-a)\right) - B_1 \sqrt{\Omega} \sin\left(\sqrt{\Omega}(-a)\right), \\
A_2 \sin(\sqrt{\Omega + d}(a)) &= A_3 \sin\left(\sqrt{\Omega}(a)\right) + B_3 \cos\left(\sqrt{\Omega}(a)\right), \\
A_2 \sqrt{\Omega + d} \cos(\sqrt{\Omega + d}(a)) &= A_3 \sqrt{\Omega} \cos\left(\sqrt{\Omega}(a)\right) - B_3 \sqrt{\Omega} \sin\left(\sqrt{\Omega}(a)\right).
\end{aligned} \tag{2.45}$$

Again, by choosing $A_2 = 1$, Equation (2.45) can be solved. Then, if we take the same parameter as the even solution before, the graph of the eigenfunction is drawn in Figure 2.8.

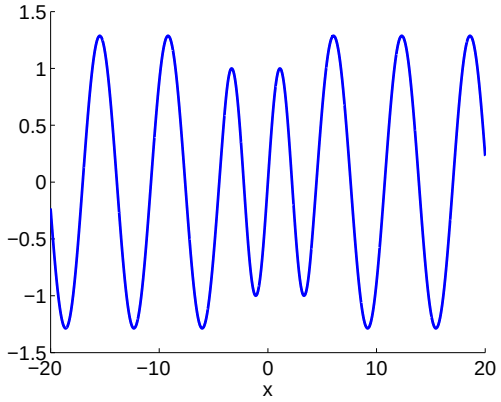

Figure 2.8. Eigenfunction of odd solution with $\Omega = 1$.

2.3.2.2 Continuous spectrum of the double-well potential

1. Even solution

Next, using the continuous spectrum on page 38, we will see the graph of continuous spectrum for the even solutions. Recall the solution for our eigenvalues problem as the following:

$$\hat{\psi}_I = A_1 \cos(\sqrt{\Omega}\, x) + B_1 \sin(\sqrt{\Omega}\, x), \tag{2.46}$$

$$\hat{\psi}_{II} = A_2 \cos(\sqrt{\Omega + d}\, x) + B_2 \sin(\sqrt{\Omega + d}\, x), \tag{2.47}$$

$$\hat{\psi}_{III} = A_3 \cos(\sqrt{\Omega}\, x) \text{ or } B_3 \sin(\sqrt{\Omega}\, x). \tag{2.48}$$

Therefore, with similar calculations as for the one-well potential, we take $A_2 = 1$ and by taking the parameter values $a = 4$, $b = 2$, $d = 1$ and $\Omega = 2.5$, we can plot our eigenfunction as shown in Figure 2.9.

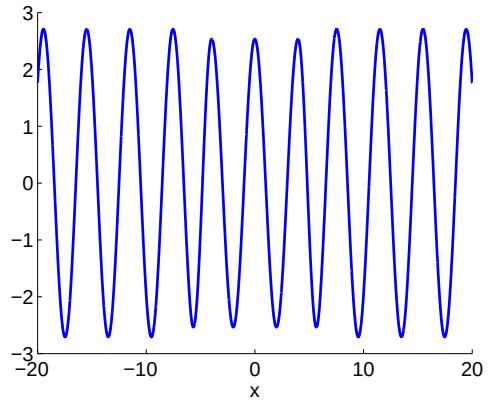

Figure 2.9. Graph of the eigenfunction with $\Omega = 2.5$ for even solution.

2. Odd solution

Similar calculations for the same parameter values will give the eigenfunction as seen in Figure 2.10.

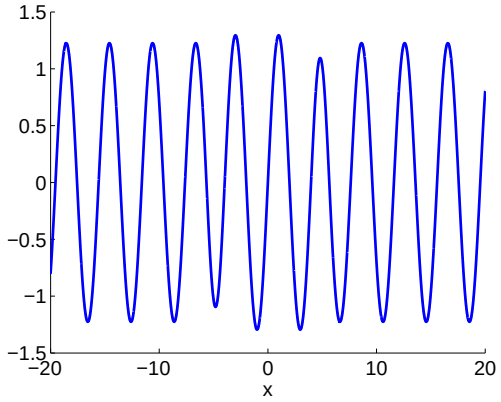

Figure 2.10. Graph of the eigenfunction with $\Omega = 2.5$ for odd solution.

Chapter 3

Coupled mode reductions in the Cubic-Quintic NLS with a double-well potential

3.1 Introduction

We consider the cubic-quintic nonlinear Schrödinger/Gross-Pitaevskii (NLS/GP) equation with a linear potential

$$i\frac{\partial\psi(x,t)}{\partial t} = -\frac{\partial^2\psi(x,t)}{\partial x^2} + V(x)\psi(x,t) + g\left|\psi(x,t)\right|^2\psi(x,t) + h\left|\psi(x,t)\right|^4\psi(x,t). \qquad (3.1)$$

Here, ψ denotes a wave function, V the external potential and g and h are the cubic and quintic nonlinearity constants, respectively. We will consider a nonlinear NLS/GP with a focusing ($g = -1$) nonlinear potential. Derivations of NLS/GP type solutions with the standard Kerr ($|u|^2u$) nonlinearity exist in the context of optics [16, 71], and Bose-Einstein condensate (BECs) confined by a magnetically-induced linear potential [34, 78]. Cubic-quintic nonlinearities arise in a variety of physical settings, such as in glasses and organic optical media whose dielectric response

features a self-defocusing quintic correction to the self-focusing cubic Kerr effect [15, 43, 96].

In this section, we study the long-time dynamics near a symmetry breaking bifurcation point for (3.1) using the shadowing theorem techniques of [69, 80]. In particular, we focus on a class of symmetric *double-well* potentials. A model to keep in mind is the two parameter family of symmetric double well potentials:

$$V(x) = \begin{cases} -d, & a < |x| < a + b \\ 0. & \text{elsewhere,} \end{cases} \tag{3.2}$$

which converges as $d \to \infty$ and $b \to 0+$ to a double-delta well at $\pm a$. For the sake of illustration, in the following we will take $d = 1$, $a = 4$, and $b = 2$. Double-well potentials in optics serve as models of coupled parallel wave guides or as a simple version quantum tunneling in Bose-Einstein condensate models. As discussed in [48], the combined effects of a confining double-well potential with focusing cubic nonlinearity lead to the phenomenon of spontaneous symmetry breaking of the ground state at sufficiently high optical power or particle number. The notion of symmetry breaking has been studied in a variety of contexts, in terms of constructing stationary solutions as in [55, 56], dynamical shadowing theorems as in [69, 76, 80], more complicated well-structure [44, 50] as well as countless numerical works as reviewed in [65]. The governing equation (3.1) with the potential (3.2) was also studied by Birnbaum and Malomed [14], where a class of symmetry breaking bifurcations appears (see also, e.g., [92] for a similar work but using nonlocal cubic-quintic nonlinearity). One important difference with the Kerr nonlinearity is the presence of various further bifurcations beyond just those observed in the standard cubic case, such as saddle-centre bifurcations of both symmetric and asymmetric solutions. The question we are interested in is: can the

shadowing theorem techniques (i.e., coupled mode theory) of [69, 80] cover the cubic-quintic nonlinearity problem as well?

The NLS/GP equation (3.1) is a Hamiltonian system and expressible in the form:

$$i\partial_t \psi = \frac{\delta \mathcal{H}}{\delta \psi^*}, \tag{3.3}$$

where $\mathcal{H}$ denotes the Hamiltonian density:

$$\mathcal{H}[\psi] \;=\; \int \left(|\partial_x \psi|^2 + V|\psi|^2 + \frac{g}{4}|\psi|^4 + \frac{h}{6}|\psi|^6 \right) dx.$$

The conserved squared L^2 norm (particle number / optical power) is:

$$N[\psi] \;=\; \int |\psi|^2 dx. \tag{3.4}$$

We are interested in the dynamics near special classes of *nonlinear bound states* of NLS/GP. Nonlinear bound states are solutions of the form

$$\psi(x,t) = \hat{\psi}(x) e^{-i\Omega t},$$

where ψ_Ω is a spatially localized solution of

$$(-\partial_{xx} + V(x))\hat{\psi} - |\hat{\psi}|^2\hat{\psi} + h|\hat{\psi}|^4\hat{\psi} = \Omega\hat{\psi}. \tag{3.5}$$

Solutions to (3.5) can be computed at low mass using a Lyapunov-Schmidt reduction off of the spectrum of the linear operator $(-\partial_{xx} + V)$ in a similar fashion to the works [55, 56] and continued to large mass. We will assume that the spectrum of our double well potential, namely the values $\Omega < 0$ such that

$$(-\partial_{xx} + V(x))\hat{\psi} = \Omega\hat{\psi}, \quad \hat{\psi} \in H^1(\mathbb{R}), \tag{3.6}$$

has a simple, special structure. The spaces $H^s(\mathbb{R})$ (as well as $L^p(\mathbb{R})$ and $W^{k,p}$ in the following) are the standardly defined Sobolev integration spaces. In this case, there is a least energy ground state eigenfunction, ψ_0 with corresponding simple eigenvalue Ω_0 [81]. If the separation between wells is sufficiently large, $L \ll 1$, then the ground state eigenfunction is a positive symmetric state with equal concentration on each potential well. In addition, for L sufficiently large there is an anti-symmetric (odd) state, ψ_1 with energy Ω_1, such that $\Omega_0 < \Omega_1 < 0$. For references on the linear spectral properties of multi-modal potential wells, see [45, 48, 85].

In the cubic-quintic case (3.1), the character of solutions and the solution set varies with the solution norm. Indeed, if we consider the set of solutions of (3.5) on the level set

$$\int |\psi_\Omega|^2 = N, \tag{3.7}$$

we find that for large enough well-separation, there is a *symmetry breaking threshold* N_{cr} [56].

1. If $N < N_{cr}$ there is a unique positive, symmetric and bimodal state.

2. For $N > N_{cr}$, (modulo phase) there are three positive localized states: a symmetric state (which exists for all $N > 0$) and two *asymmetric states*, biased respectively to the right and left wells.

3. As N increases beyond N_{cr} this symmetry broken state becomes increasingly concentrated in one of the wells [5, 56].

4. The symmetric (bimodal) state is dynamically stable for $N < N_{cr}$ and unstable for $N > N_{cr}$. For $N > N_{cr}$ the asymmetric states are stable.

We wish to show that on large but finite time scales, the dynamics are controlled by a finite dimensional dynamical system, which is significantly more rich and complex in the setting of the quintic-cubic than of that in [69, 80].

Toward a formulation of precise results, we first introduce a class of double-well potentials in one dimension. Following [45], start with a single rapidly decaying potential well centered at 0, $V_0(x)$, for which the Schrödiner operator $H_0 = -\partial_x^2 + V_0$ has exactly one (simple) eigenvalue Ω. Then, construct a double well potential

$$V_L(x) = V_0(x-L) + V_0(x+L), \;\; L > 0 \tag{3.8}$$

and define the Schrödinger operator

$$H_L = -\partial_x^2 + V_L. \tag{3.9}$$

There exists $L_0 > 0$ such that for $L > L_0$, H_L has a pair of simple eigenvalues, $\Omega_0 = \Omega_0(L)$ and $\Omega_1 = \Omega_1(L)$ and corresponding eigenfunctions ψ_0 (even) and ψ_1 (odd):

$$\begin{aligned} &H_L\psi_j = \Omega_j\psi_j, \; j = 0,1; \quad \psi_j \in L^2, \\ &\Omega_0 < \Omega_1 < 0. \end{aligned}$$

The symmetry breaking threshold, $N_{cr}(L)$ which is $N_{cr}(L) = \mathcal{O}(\omega_1(L) - \omega_0(L)) = \mathcal{O}(e^{-kL}), \quad k > 0$, is exponentially small for large well-separation. Therefore, to study the dynamics in a neighborhood of the symmetry breaking point, it is natural to use coordinates associated with the *linear* operator H_0. Throughout this result, we will assume that V is such that ψ_0 and ψ_1 are the only discrete eigenfunctions of H_0 and in addition that V is sufficiently smooth and decaying. We note that the

essential estimates are also satisfied for double piecewise-constant function wells, that we explore in our numerical computations.

The outline of this chapter is as follows. We start our work by deriving the coupled-mode approximation as the finite dimensional reduction in Sec. 3.2, using two different coordinate representations. Standing wave solutions are considered in Sec. 3.3, where the equilibria of the coupled-mode equations are derived and their stabilities are analysed. We show that there are spontaneous symmetry-breaking and turning point bifurcations. Moreover, dynamics near the symmetry breaking bifurcation point are delivered in Sec. 3.4. In Sec. 3.5, we consider small perturbation dynamics around a solution of the finite dimensional reduction. The aim is to show that for any sufficiently small amplitude periodic solution about an equilibrium state of the finite dimensional reduction (above or below the symmetry breaking bifurcation threshold), there is a solution of the NLS/GP equation whose projection into the finite dimensional phase space, shadows this finite dimension orbit on very long time scales. Finally, Sec. 3.6 presents numerical comparisons of the equilibria of the NLS/GP and those of the coupled-mode approximations.

3.2 Coupled mode equations for cubic-quintic nonlinearity

Based on a calculation of the linear eigenvalue problem (3.6) in Chapter 2, Subsection (2.3.1.2), we obtain a ground state eigenfunction ψ_0 with corresponding eigenvalue Ω_0 and excited state eigenfunction ψ_1 with the energy Ω_1 such that $\Omega_0 < \Omega_1 < 0$. For the specific parameter values mentioned above, $\Omega_0 = -0.455$ and $\Omega_1 = -0.452$.

First, define a projection onto the bound states and the continuous spectral part of H_L, respectively, as

$$P_j f = \langle \psi_j, f \rangle \psi_j = (\pi_j f)\psi_j, \quad j = 0, 1,$$
$$P_c f = (I - P_0 - P_1) f,$$

where we have the L^2-inner product: $\langle f, g \rangle = \int_{\mathbb{R}} f \bar{g}$.

Now, let us describe steady state solutions of the form

$$\psi(x,t) = c_0(t)\psi_0(x) + c_1(t)\psi_1(x) + R(x,t), \tag{3.10}$$

with $\langle \psi_j, R(\cdot, t) \rangle = 0, \quad j = 0, 1.$

Using the above ansatz, substituting it into (3.1), and applying the projection operators P_0, P_1, and P_c, we obtain

$$\begin{aligned}
i\dot{c}_0 =& \Omega_0 c_0 + gA|c_0|^2 c_0 + gC\left(2c_0|c_1|^2 + \bar{c}_0 c_1^2\right) + hU|c_0|^4 c_0 \\
&+ hW\left(6|c_0|^2 c_0|c_1|^2 + \bar{c}_1^2 c_0^3 + 3|c_0|^2 \bar{c}_0 c_1^2\right) + hY\left(3c_0|c_1|^4 + 2\bar{c}_0|c_1|^2 c_1^2\right) \\
&+ F_0(c_0, c_1, \bar{c}_0, \bar{c}_1; R, \bar{R}), \\
i\dot{c}_1 =& \Omega_1 c_1 + gE|c_1|^2 c_1 + gC\left(2c_1|c_0|^2 + \bar{c}_1 c_0^2\right) + hM|c_1|^4 c_1 \\
&+ hY\left(6|c_1|^2 c_1|c_0|^2 + \bar{c}_0^2 c_1^3 + 3|c_1|^2 \bar{c}_1 c_0^2\right) + hW\left(3c_1|c_0|^4 + 2\bar{c}_1|c_0|^2 c_0^2\right) \\
&+ F_1(c_0, c_1, \bar{c}_0, \bar{c}_1; R, \bar{R}), \\
i\dot{R} - H_L R =& P_c F_b(c_0, c_1, \bar{c}_0, \bar{c}_1) + P_c F_R(c_0, c_1, \bar{c}_0, \bar{c}_1; R, \bar{R}),
\end{aligned} \tag{3.11}$$

where $A=\int\psi_0^4dx$, $C=\int\psi_0^2\psi_1^2dx$, $E=\int\psi_1^4dx$, $U=\int\psi_0^6dx$, $M=\int\psi_1^6dx$, $W=\int\psi_0^4\psi_1^2dx$, $Y=\int\psi_0^2\psi_1^4dx$, and $F_j=\pi_jF_R$, $j=0,1$, with

$$\begin{aligned}
F_R &= \Big[2|c_0|^2\psi_0^2+2|c_1|^2\psi_1^2+2(c_0\bar{c}_1+c_1\bar{c}_0)\psi_0\psi_1-3h|c_0|^4\psi_0^4-3h|c_1|^4\psi_1^4\\
&\quad -3h(c_0^2\bar{c}_1^2+\bar{c}_0^2c_1^2)\psi_0^2\psi_1^2-6h(|c_0|^2c_0\bar{c}_1+|c_0|^2\bar{c}_0c_1)\psi_0^3\psi_1\\
&\quad -6h(\bar{c}_0|c_1|^2c_1+c_0|c_1|^2\bar{c}_1)\psi_0\psi_1^3-12h|c_0|^2|c_1|^2\psi_0^2\psi_1^2\Big]R\\
&\quad +\Big[c_0^2\psi_0^2+c_1^2\psi_1^2+2c_0c_1\psi_0\psi_1-2h|c_0|^2c_0^2\psi_0^4-2h|c_1|^2c_1^2\psi_1^4\\
&\quad -2hc_0^3\bar{c}_1\psi_0^3\psi_1-2hc_1^3\bar{c}_0\psi_1^3\psi_0-6h(c_0^2|c_1|^2+|c_0|^2c_1^2)\psi_0^2\psi_1^2\\
&\quad -6h|c_0|^2c_0c_1\psi_0^3\psi_1-6hc_0|c_1|^2c_1\psi_0\psi_1^3\Big]\bar{R}\\
&\quad +\Big[\ \bar{c}_0\psi_1+\bar{c}_1\psi_0-3hc_0\bar{c}_1^2\psi_0\psi_1^2-3h\bar{c}_0^2c_1\psi_0^2\psi^1-3h|c_0|^2\bar{c}_0\psi_0^3\\
&\quad -3h|c_1|^2\bar{c}_1\psi_1^3-6h|c_0|^2\bar{c}_1\psi_0^2\psi_1-6h|c_1|^2\bar{c}_0\psi_0\psi_1^2\Big]R^2\\
&\quad +\Big[2c_0\psi_0+2c_1\psi_1-6hc_0^2\bar{c}_1\psi_0^2\psi_1-6h\bar{c}_0c_1^2\psi_0\psi_1^2-6h|c_0|^2c_0\psi_0^3\\
&\quad -6h|c_1|^2c_1\psi_1^3-12h|c_0|^2c_1\psi_0^2\psi_1-12hc_0|c_1|^2\psi_0\psi_1^2\Big]|R|^2\\
&\quad +\Big[1-6h|c_0|^2\psi_0^2-6h|c_1|^2\psi_1^2-6h(c_0\bar{c}_1+\bar{c}_0c_1)\psi_0\psi_1\Big]|R|^2R\\
&\quad -\Big[hc_0^3\psi_0^3+3hc_0^2c_1\psi_0^2\psi_1+3hc_0c_1^2\psi_0\psi_1^2+hc_1^3\psi_1^3\Big]\bar{R}^2\\
&\quad -\Big[h\bar{c}_0^2\psi_0^2+h\bar{c}_1^2\psi_1^2+2h\bar{c}_0\bar{c}_1\psi_0\psi_1\Big]R^3\\
&\quad -\Big[3hc_0^2\psi_0^2+3hc_1^2\psi_1^2+6hc_0c_1\psi_0\psi_1\Big]|R|^2\bar{R}\\
&\quad -[3hc_0\psi_0+3hc_1\psi_1]|R|^4-h|R|^4R,
\end{aligned}\tag{3.12}$$

and

$$\begin{aligned}
F_b &= |c_0|^2c_0\psi_0^3+(c_0^2\bar{c}_1+2|c_0|^2c_0)\psi_0^2\psi_1+(c_1^2\bar{c}_0+2c_0|c_1|^2)\psi_0\psi_1^2+|c_1|^2c_1\psi_1^3\\
&\quad -h|c_0|^4c_0\psi_0^5-h|c_1|^4c_1\psi_1^5-hc_0^3\bar{c}_1^2\psi_0^3\psi_1^2-h\bar{c}_0^2c_1^3\psi_0^2\psi_1^3-2h|c_0|^2c_0^2\bar{c}_1\psi_0^4\psi_1\\
&\quad -2h\bar{c}_0|c_1|^2c_1^2\psi_0\psi_1^4-3h|c_0|^4c_1\psi_0^4\psi_1-3hc_0|c_1|^4\psi_0\psi_1^4-3h|c_0|^2\bar{c}_0c_1^2\psi_0^3\psi_1^2\\
&\quad -3hc_0^2|c_1|^2\bar{c}_1\psi_0^2\psi_1^3-6h|c_0|^2|c_1|^2\psi_0^2\psi_1^3-6h|c_0|^2c_0|c_1|^2\psi_0^3\psi_1^2.
\end{aligned}\tag{3.13}$$

By taking $g = -1$, $c_0 = \frac{\hat{c}_0}{\sqrt{A}}$ and $c_1 = \frac{\hat{c}_1}{\sqrt{E}}$, we have:

$$\begin{aligned}
i\dot{\hat{c}}_0 =&\Omega_0\hat{c}_0 - |\hat{c}_0|^2\hat{c}_0 - \frac{C}{E}\left(2\hat{c}_0|\hat{c}_1|^2 + \bar{\hat{c}}_0\hat{c}_1^2\right)\\
&+ h\frac{U}{A^2}|\hat{c_0}|^4\hat{c}_0 + h\frac{W}{AE}\left(6|\hat{c}_0|^2\hat{c}_0|\hat{c}_1|^2 + \bar{\hat{c}}_1^2\hat{c}_0^3 + 3|\hat{c}_0|^2\bar{\hat{c}}_0\hat{c}_1^2\right)\\
&+ h\frac{Y}{E^2}\left(3\hat{c}_0|\hat{c}_1|^4 + 2\bar{\hat{c}}_0|\hat{c}_1|^2\hat{c}_1^2\right) + F_0(c_0, c_1, \bar{c}_0, \bar{c}_1; R, \bar{R}),\\
i\dot{\hat{c}}_1 =&\Omega_1\hat{c}_1 - |\hat{c}_1|^2\hat{c}_1 - \frac{C}{A}\left(2\hat{c}_1|\hat{c}_0|^2 + \bar{\hat{c}}_1\hat{c}_0^2\right)\\
&+ h\frac{M}{E^2}|\hat{c}_1|^4\hat{c}_1 + h\frac{Y}{AE}\left(6|\hat{c}_1|^2\hat{c}_1|\hat{c}_0|^2 + \bar{\hat{c}}_0^2\hat{c}_1^3 + 3|\hat{c}_1|^2\bar{\hat{c}}_1\hat{c}_0^2\right)\\
&+ h\frac{W}{A^2}\left(3\hat{c}_1|\hat{c}_0|^4 + 2\bar{\hat{c}}_1|\hat{c}_0|^2\hat{c}_0^2\right) + F_1(c_0, c_1, \bar{c}_0, \bar{c}_1; R, \bar{R}),\\
i\dot{R} - H_L R =&P_c F_b(c_0, c_1, \bar{c}_0, \bar{c}_1) + P_c F_R(c_0, c_1, \bar{c}_0, \bar{c}_1; R, \bar{R}).
\end{aligned} \tag{3.14}$$

For the specific parameter values above, $\frac{C}{E} \approx \frac{C}{A} \approx \frac{U}{A^2} \approx \frac{M}{E^2} \approx \frac{W}{AE} \approx \frac{Y}{AE} \approx \frac{Y}{E^2} \approx \frac{W}{A^2} \approx 1$. Writing c_j's without 'hat' to make it easier, equation (3.14) becomes:

$$\begin{aligned}
i\dot{c}_0 =&\Omega_0 c_0 - |c_0|^2 c_0 - 2c_0|c_1|^2 - \bar{c}_0 c_1^2 + h|c_0|^4 c_0\\
&+ h\left(6|c_0|^2 c_0|c_1|^2 + \bar{c}_1^2 c_0^3 + 3|c_0|^2\bar{c}_0 c_1^2\right) + h\left(3c_0|c_1|^4 + 2\bar{c}_0|c_1|^2 c_1^2\right)\\
&+ F_0(c_0, c_1, \bar{c}_0, \bar{c}_1; R, \bar{R}),
\end{aligned} \tag{3.15a}$$

$$\begin{aligned}
i\dot{c}_1 =&\Omega_1 c_1 - |c_1|^2 c_1 - 2c_1|c_0|^2 - \bar{c}_1 c_0^2 + h|c_1|^4 c_1\\
&+ h\left(6|c_1|^2 c_1|c_0|^2 + \bar{c}_0^2 c_1^3 + 3|c_1|^2\bar{c}_1 c_0^2\right) + h\left(3c_1|c_0|^4 + 2\bar{c}_1|c_0|^2 c_0^2\right)\\
&+ F_1(c_0, c_1, \bar{c}_0, \bar{c}_1; R, \bar{R}),
\end{aligned} \tag{3.15b}$$

$$i\dot{R} - H_L R = P_c F_b(c_0, c_1, \bar{c}_0, \bar{c}_1) + P_c F_R(c_0, c_1, \bar{c}_0, \bar{c}_1; R, \bar{R}). \tag{3.15c}$$

3.2.1 Alternative coordinate

In the following, we introduce the change of coordinates:

$$(c_0(t), c_1(t), \bar{c}_0(t), \bar{c}_1(t), R(.,t)) \longmapsto (\Gamma(t), \alpha(t), \beta(t), \theta(t), R(.,t)),$$

defined by

$$c_0(t) = \Gamma(t)e^{i\theta(t)}, \tag{3.16}$$

$$c_1(t) = (\alpha(t) + i\beta(t))e^{i\theta(t)}, \tag{3.17}$$

such that

$$\psi(x,t) = (\Gamma(t)\psi_0 + (\alpha(t) + i\beta(t))\psi_1)e^{i\theta(t)}. \tag{3.18}$$

Substituting ansatz (3.18) into (3.15) yields:

$$\begin{aligned}&(i\dot{\Gamma} - \dot{\theta}\Gamma - \Omega_0\Gamma)\psi_0 + (i\dot{\alpha} - \dot{\beta} - \dot{\theta}(\alpha + i\beta) - (\alpha + i\beta)\Omega_1)\psi_1\\ &+i\dot{R} - H_L R - \dot{\theta}R = F_b(\Gamma,\alpha,\beta) + F_R(\Gamma,\alpha,\beta;R,\bar{R}),\end{aligned}$$

where F_b, F_R is determined similarly to (3.12) and (3.13) (see Appendix A for further details). This leads to the system

$$\dot{\Gamma} = \left[-2\alpha\beta + 4h\alpha\beta^3 + 4h\alpha^3\beta + 4h\alpha\beta\Gamma^2\right]\Gamma + \text{Error}(R,\bar{R};\Gamma,\alpha,\beta), \tag{3.19a}$$

$$\begin{aligned}\dot{\alpha} =& \left[\Omega_1 - (\alpha^2 + \beta^2) - \Gamma^2 + \dot{\theta} + h(\alpha^4 + \beta^4) + 2h\beta^2(\alpha^2 + \Gamma^2) + h\Gamma^2(6\alpha^2 + \Gamma^2)\right]\beta\\ &+ \text{Error}(R,\bar{R};\Gamma,\alpha,\beta),\end{aligned} \tag{3.19b}$$

$$\begin{aligned}\dot{\beta} =& -\left[\Omega_1 - (\alpha^2 + \beta^2 + \Gamma^2) - 2\Gamma^2 + \dot{\theta} + h(\alpha^4 + \beta^4) + 2h(\alpha^2\beta^2 + 3\beta^2\Gamma^2 + 5\alpha^2\Gamma^2)\right.\\ &\left.+5h\Gamma^4\right]\alpha + \text{Error}(R,\bar{R};\Gamma,\alpha,\beta),\end{aligned} \tag{3.19c}$$

$$\begin{aligned}\dot{\theta} =& -\Omega_0 + \Gamma^2 + (3\alpha^2 + \beta^2) - h(\beta^4 + \Gamma^4 + 5\alpha^4) - 2h(\beta^2\Gamma^2 + 3\alpha^2\beta^2 + 5\alpha^2\Gamma^2)\\ &+ \Gamma^{-1}\text{Error}(R,\bar{R};\Gamma,\alpha,\beta),\end{aligned} \tag{3.19d}$$

$$iR_t = (H_L - \Omega_0)R - \Gamma^{-1}\Re(\pi_0(F))R + P_cF_b(\Gamma,\alpha,\beta) + P_cF_R(\Gamma,\alpha,\beta;R,\bar{R}). \tag{3.19e}$$

The terms containing $\dot{\theta}$ in (3.19b) and (3.19c) can be replaced using (3.19d) to yield

$$\dot{\Gamma} = \left[-2\alpha\beta + 4h\alpha\beta^3 + 4h\alpha^3\beta + 4h\alpha\beta\Gamma^2\right]\Gamma + \mathrm{Error}_\Gamma(R,\bar{R};\Gamma,\alpha,\beta), \tag{3.20a}$$

$$\dot{\alpha} = [\Omega_1 - \Omega_0 + 2\alpha^2 - 4h\alpha^2\beta^2 - 4h\alpha^4 - 4h\alpha^2\Gamma^2]\beta + \mathrm{Error}_\alpha(R,\bar{R};\Gamma,\alpha,\beta), \tag{3.20b}$$

$$\begin{aligned}\dot{\beta} = &-[\Omega_1 - \Omega_0 - 2\Gamma^2 + 2\alpha^2 - 4h\alpha^2\beta^2 - 4h\alpha^4 + 4h\beta^2\Gamma^2 + 4h\Gamma^4]\alpha \\ &+ \mathrm{Error}_\beta(R,\bar{R};\Gamma,\alpha,\beta),\end{aligned} \tag{3.20c}$$

$$\begin{aligned}\dot{\theta} = &-\Omega_0 + \Gamma^2 + (3\alpha^2 + \beta^2) - h(\beta^4 + \Gamma^4 + 5\alpha^4) - 2h(\beta^2\Gamma^2 + 3\alpha^2\beta^2 + 5\alpha^2\Gamma^2) \\ &+ \mathrm{Error}_\theta(R,\bar{R};\Gamma,\alpha,\beta),\end{aligned} \tag{3.20d}$$

$$\begin{aligned}iR_t = &(H_L - \Omega_0)R + \Big[\Gamma^2 + 3\alpha^2 + \beta^2 - h(\beta^4 + \Gamma^4 + 5\alpha^4) \\ &-2h(\beta^2\Gamma^2 + 3\alpha^2\beta^2 + 5\alpha^2\Gamma^2)\Big]R + P_cF_b(\Gamma,\alpha,\beta) + P_cF_R(\Gamma,\alpha,\beta;R,\bar{R}),\end{aligned} \tag{3.20e}$$

with

$$\begin{aligned}P_cF_b \;= P_c\Big[&\Gamma^3\psi_0^3 + (\alpha^2+\beta^2)(\alpha+i\beta)\psi_1^3 + \Gamma(\alpha+i\beta)\psi_0\psi_1^2 + 2\Gamma(\alpha^2+\beta^2)\psi_0\psi_1^2 \\ &+\Gamma^2(\alpha-i\beta)\psi_0^2\psi_1 + 2\Gamma^2(\alpha+i\beta)\psi_0^2\psi_1 - h\Gamma^5\psi_0^5 - h(\alpha^2+\beta^2)^2(\alpha+i\beta)\psi_1^5 \\ &-h\Gamma^3(\alpha-i\beta)^2\psi_0^3\psi_1^2 - h\Gamma^2(\alpha+i\beta)^3\psi_0^2\psi_1^3 - 2h\Gamma^3(\alpha-i\beta)\psi_0^4\psi_1 \\ &-2h\Gamma(\alpha^2+\beta^2)(\alpha+i\beta)^2\psi_0\psi_1^4 - 3h\Gamma^4(\alpha+i\beta)\psi_0^4\psi_1 - 3h\Gamma(\alpha^2+\beta^2)^2\psi_0\psi_1^4 \\ &-3h\Gamma^3(\alpha+i\beta)^2\psi_0^3\psi_1^2 - 3h\Gamma^2(\alpha^2+\beta^2)(\alpha-i\beta)\psi_0^2\psi_1^3 \\ &-6h\Gamma^2(\alpha^2+\beta^2)(\alpha+i\beta)\psi_0^2\psi 1^3 - 6h\Gamma^3(\alpha^2+\beta^2)\psi_0^3\psi_1^2\Big],\end{aligned} \tag{3.21}$$

and

$$
\begin{aligned}
P_cF_R \;=\; & P_c\Big([2\Gamma^2\psi_0^2+4\Gamma\alpha\psi_0\psi_1+2(\alpha^2+\beta^2)\psi_1^2-3h\Gamma^4\psi_0^4-3h(\alpha^2+\beta^2)^2\psi_1^4\\
&-6h\Gamma^2(\alpha^2+\beta^2)\psi_0^2\psi_1^2-12h\Gamma^3\alpha\psi_0^3\psi_1-12h\Gamma(\alpha^3+\alpha\beta^2)\psi_0\psi_1^3\\
&-12h\Gamma^2(\alpha^2+\beta^2)\psi_0^2\psi_1^2]R+[\Gamma^2\psi_0^2+(\alpha+i\beta)^2\psi_1^2+2\Gamma(\alpha+i\beta)\psi_0\psi_1\\
&-2h\Gamma^4\psi_0^4-2h(\alpha^2+\beta^2)(\alpha+i\beta)^2\psi_1^4-2h\Gamma^3(\alpha-i\beta)\psi_0^3\psi_1\\
&-2h\Gamma(\alpha+i\beta)^3\psi_0\psi_1^3-12h\Gamma^2\alpha(\alpha+i\beta)\psi_0^2\psi_1^2\\
&-6h\Gamma^3(\alpha+i\beta)\psi_0^3\psi_1-6h\Gamma(\alpha^2+\beta^2)(\alpha+i\beta)\psi_0\psi_1^3]\bar{R}\\
&+[\Gamma\psi_0+(\alpha-i\beta)\psi_1-3h\Gamma(\alpha-i\beta)^2\psi_0\psi_1^2-3h\Gamma^2(\alpha+i\beta)\psi_0^2\psi_1-3h\Gamma^3\psi_0^3\\
&-3h(\alpha^2+\beta^2)(\alpha-i\beta)\psi_1^3-6h\Gamma^2(\alpha-i\beta)\psi_0\psi_1-6h\Gamma(\alpha^2+\beta^2)\psi_0\psi_1^2]R^2\\
&+[2\Gamma\psi_0+2(\alpha+i\beta)\psi_1-6h\Gamma^2(\alpha-i\beta)\psi_0^2\psi_1-6h\Gamma(\alpha+i\beta)^2\psi_0\psi_1^2\\
&-6h\Gamma^3\psi_0^3-6h(\alpha^2+\beta^2)(\alpha+i\beta)\psi_1^3-12h\Gamma^2(\alpha+i\beta)\psi_0^2\psi_1\\
&-12h\Gamma(\alpha^2+\beta^2)\psi_0\psi_1^2]|R|^2\\
&+[1-6h\Gamma^2\psi_0^2-6h(\alpha^2+\beta^2)\psi_1^2-12h\Gamma\alpha\psi_0\psi_1]|R|^2R\\
&-[h\Gamma^3\psi_0^3+3h\Gamma^2(\alpha+i\beta)\psi_0^2\psi_1+3h\Gamma(\alpha+i\beta)^2\psi_0\psi_1^2+h(\alpha+i\beta)^3\psi_1^3]\bar{R}^2\\
&-[h\Gamma^2\psi_0^2+h(\alpha-i\beta)^2\psi_1^2+2h\Gamma(\alpha-i\beta)\psi_0\psi_1]R^3\\
&-[3h\Gamma^2\psi_0^2+3h(\alpha+i\beta)^2\psi_1^2+6h\Gamma(\alpha+i\beta)\psi_0\psi_1]|R|^2\bar{R}\\
&-[3h\Gamma\psi_0+3h(\alpha+i\beta)\psi_1]|R|^4-h|R|^4R\Big).
\end{aligned}
\tag{3.22}
$$

3.3 Symmetry breaking bifurcations

Neglecting the R terms, the relevant equations from system (3.20) to study symmetry breaking bifurcations are

$$
\begin{aligned}
\dot{\alpha} &= \Big(\Omega_1-\Omega_0+2\alpha^2-4h\alpha^2\beta^2-4h\alpha^4-4h\alpha^2\Gamma^2\Big)\beta,\\
\dot{\beta} &= -\Big(\Omega_1-\Omega_0+2\alpha^2-2\Gamma^2-4h\alpha^2(\beta^2+\alpha^2)+4h\Gamma^2(\beta^2+\Gamma^2)\Big)\alpha,\\
\dot{\Gamma} &= \Big(-2\alpha\beta+4h\alpha\beta^3+4h\alpha^3\beta+4h\alpha\beta\Gamma^2\Big)\Gamma.
\end{aligned}
\tag{3.23}
$$

One can verify that

$$N = \Gamma^2 + \alpha^2 + \beta^2, \tag{3.24}$$

and system (3.23) has a Hamiltonian

$$\begin{aligned} H \quad &= \Omega_0\Gamma^2 + \Omega_1(\alpha^2+\beta^2) - \tfrac{1}{2}\Gamma^4 - \tfrac{1}{2}(\alpha^2+\beta^2)^2 - 2\Gamma^2(\alpha^2+\beta^2) - \Gamma^2(\alpha^2-\beta^2) \\ &+\tfrac{1}{3}h\left(\Gamma^6+\alpha^6+\beta^6\right) + 3h\Gamma^2(\alpha^2+\beta^2)^2 + h\alpha^2(\beta^4+5\Gamma^4) + h\beta^2(\alpha^4+\Gamma^4) \\ &+2h\Gamma^2(\alpha^4-\beta^4). \end{aligned} \tag{3.25}$$

We obtain a closed system for (α,β) using that N is conserved. Then, we may reduce the system to:

$$\begin{aligned} \dot{\alpha} &= \left(\Delta\Omega + 2\alpha^2 - 4hN\alpha^2\right)\beta, \\ \dot{\beta} &= -\left(\Delta\Omega - (2-4hN)(N-2\alpha^2-\beta^2)\right)\alpha, \end{aligned} \tag{3.26}$$

where $\Delta\Omega = \Omega_1 - \Omega_0$, and the Hamiltonian becomes

$$H \quad = \left[\tfrac{\Delta\Omega}{2}(\alpha^2+\beta^2) + \alpha^2(1-2hN)(\alpha^2+\beta^2-N)\right]. \tag{3.27}$$

In this case, we have

$$\begin{pmatrix} \dot{\alpha} \\ \dot{\beta} \end{pmatrix} = J\nabla H, \tag{3.28}$$

where

$$J = \begin{bmatrix} 0 & 1 \\ -1 & 0 \end{bmatrix}.$$

3.3.1 Bifurcation of equilibria for (3.23) and Symmetry Breaking in NLS/GP

Next, we look for standing wave solutions. Consider again (3.19). Let us transform the system to a rotating frame by setting

$$\theta(t) = \Theta(t) - \Omega t, \tag{3.29}$$

and obtain

$$\begin{aligned}
\dot{\alpha} =& \Big[\Omega_1 - \Omega + \dot{\Theta}(t) - (\alpha^2+\beta^2) - \Gamma^2 + h(\alpha^4+\beta^4+\Gamma^4) + 2h\beta^2(\Gamma^2+\alpha^2) \\
&+6h\Gamma^2\alpha^2\Big]\beta, && \text{(3.30a)}\\
\dot{\beta} =& -\Big[\Omega_1 - \Omega + \dot{\Theta}(t) - (\alpha^2+\beta^2) - 3\Gamma^2 + h(\alpha^4+\beta^4+5\Gamma^4)\,\alpha \\
&+2h(\alpha^2\beta^2+3\Gamma^2\beta^2+5\Gamma^2\alpha^2)\Big]\alpha, && \text{(3.30b)}\\
\dot{\Gamma} =& -\Big[2\alpha\beta - 4h\alpha\beta(\beta^2+\alpha^2+\Gamma^2)\Big]\Gamma, && \text{(3.30c)}\\
\dot{\Theta} =& \Omega - \Omega_0 + \Gamma^2 + 3\alpha^2 + \beta^2 - h(\beta^4+\Gamma^4+5\alpha^4) - 2h(\beta^2\Gamma^2+3\alpha^2\beta^2+5\alpha^2\Gamma^2). && \text{(3.30d)}
\end{aligned}$$

The states we seek are equilibria in this rotating frame. Thus, we obtain

$$\begin{aligned}
&\Big[\,\Omega_1 - \Omega - (\alpha^2+\beta^2) - \Gamma^2 + h(\alpha^4+\beta^4+\Gamma^4) + 2h\beta^2(\Gamma^2+\alpha^2) + 6h\Gamma^2\alpha^2\,\Big]\,\beta = 0, && \text{(3.31a)}\\
&\Big[\,\Omega_1 - \Omega - (\alpha^2+\beta^2) - 3\Gamma^2 + h(\alpha^4+\beta^4+5\Gamma^4) + 2h(\alpha^2\beta^2+3\Gamma^2\beta^2+5\Gamma^2\alpha^2)\,\Big]\alpha = 0, && \text{(3.31b)}\\
&\Big[2\alpha\beta - 4h\alpha\beta(\beta^2+\alpha^2+\Gamma^2)\Big]\Gamma = 0, && \text{(3.31c)}\\
&\Omega - \Omega_0 + \Gamma^2 + 3\alpha^2 + \beta^2 - h(\beta^4+\Gamma^4+5\alpha^4) - 2h(\beta^2\Gamma^2+3\alpha^2\beta^2+5\alpha^2\Gamma^2) = 0, && \text{(3.31d)}
\end{aligned}$$

whose solutions we consider on the level set

$$\Gamma^2 + \alpha^2 + \beta^2 = N. \tag{3.32}$$

Set $\beta = 0$. Then, Eq. (3.31c) is satisfied and (3.31b)-(3.31d) become:

$$\Big[\ \Omega_1 - \Omega_0 + 2(\alpha^2 - \Gamma^2) + 4h(\Gamma^4 - \alpha^4)\ \Big]\alpha = 0, \tag{3.33}$$

$$\Omega - \Omega_0 + \Gamma^2 + 3\alpha^2 - h(\Gamma^4 + 5\alpha^4) - 10h\alpha^2\Gamma^2) = 0. \tag{3.34}$$

3.3.1.1 Symmetric states

Taking $\alpha = 0$, we obtain from (3.34)

$$\Gamma^2 = \frac{1}{2h}\Big(1 \pm \sqrt{4\Omega h - 4\Omega_0 h + 1}\Big). \tag{3.35}$$

The symmetric solution existing for $h = 0$ corresponds to the minus sign, from which we can say that for $N \geq 0$:

$$\Gamma_* = N^{\frac{1}{2}} = \sqrt{1 - \sqrt{1 + 4h(\Omega - \Omega_0)}/\sqrt{2h}},\ \alpha_* = \beta_* = 0,\ \Omega_* = \Omega_0 - N(1 - hN). \tag{3.36}$$

Solution (3.35) with the plus sign becomes singular in the limit $h \to 0$. We will study the latter one here only numerically. Clearly the two types of solutions merge at a turning point

$$\Omega = \Omega_0 - \frac{1}{4h}. \tag{3.37}$$

3.3.1.2 Symmetry broken states

Symmetry breaking occurs in the system when some control parameter crosses its critical value. A second bifurcating family can be found as follows.

Consider $\alpha \neq 0$. Then one will obtain a polynomial of order 4 for either α or Γ, which leads to long expressions. Therefore, instead we will solve it asymptotically. The asymptotic solution existing for $h = 0$ is

$$\alpha = \frac{1}{4}\sqrt{2(3\Omega_0 - \Omega_1 - 2\Omega)} + \frac{2\Omega^2 - 4\Omega\Omega_0 + \Omega_0^2 + 2\Omega_0\Omega_1 - \Omega_1^2}{4\sqrt{2(3\Omega_0 - \Omega_1 - 2\Omega)}}h + \ldots, \tag{3.38a}$$

$$\Gamma = \frac{1}{4}\sqrt{2(3\Omega_1 - \Omega_0 - 2\Omega)} + \frac{2\Omega^2 - 4\Omega\Omega_1 - \Omega_0^2 + 2\Omega_0\Omega_1 + \Omega_1^2}{4\sqrt{2(3\Omega_1 - \Omega_0 - 2\Omega)}}h + \ldots. \tag{3.38b}$$

From α and Γ above we can obtain N as

$$N = \frac{1}{4}(\Omega_0 + \Omega_1 - 2\Omega) + \frac{1}{2}(\Omega - \Omega_1)(\Omega - \Omega_0)h + \ldots.$$

We also obtain a (singular when $h \to 0$) asymmetric state as

$$\alpha = \frac{1}{2\sqrt{h}} + (-2\Gamma^2 - \Omega_0 + \Omega))\sqrt{h} + O(h), \tag{3.39a}$$

$$\Gamma = \frac{1}{4}\sqrt{2(3\Omega_1 - \Omega_0 - 2\Omega)} + \frac{2\Omega^2 - 4\Omega\Omega_1 - \Omega_0^2 + 2\Omega_0\Omega_1 + \Omega_1^2}{4\sqrt{2(3\Omega_1 - \Omega_0 - 2\Omega)}}h + O(h^{3/2}). \tag{3.39b}$$

As we will see from the computational results later that in total there are generally three asymmetric solutions, including the regular and the singular states (3.38) and (3.39), that are connected to each other through turning point bifurcations.

3.3.2 Stability of equilibria; finite dimensional analysis

We consider the stability of the regular solution branches existing for $h = 0$ obtained in the previous section. We rewrite the system (3.30), using the last equation to

eliminate $-\Omega+\dot{\Theta}$ from the equations for α and β. Thus we have

$$\begin{cases} \dot{\alpha} = \Big[\ \Omega_1 - \Omega_0 + 2\alpha^2 - 4h\alpha^2(\beta^2+\alpha^2+\Gamma^2)\ \Big]\ \beta, \\ \dot{\beta} = -\Big[\ \Omega_1 - \Omega_0 + 2\alpha^2 - 2\Gamma^2 - 4h\alpha^2(\beta^2+\alpha^2) + 4h\Gamma^2(\beta^2+\Gamma^2)\ \Big]\alpha, \\ \dot{\Gamma} = -\Big[\ 2\alpha\beta - 4h\alpha\beta(\alpha^2+\beta^2+\Gamma^2)\ \Big]\Gamma, \\ \dot{\Theta} = \Omega - \Omega_0 + \Gamma^2 + 3\alpha^2 + \beta^2 - h(\beta^4+\Gamma^4+5\alpha^4) - 2h(\beta^2\Gamma^2+3\alpha^2\beta^2+5\alpha^2\Gamma^2). \end{cases} \tag{3.40}$$

Note that in these coordinates the equations for α, β and Γ decouple from the equation for Θ.

We now start on detailed linear stability analysis of these states.

Linearization about an arbitrary equilibrium solution

$$(\alpha(t),\beta(t),\Gamma(t),\theta(t))$$

gives the linearized perturbation equation

$$\begin{aligned} \partial_t \begin{bmatrix} \delta\alpha \\ \delta\beta \\ \delta A \\ \delta\theta \end{bmatrix} &= \begin{bmatrix} B_{11} & B_{12} & B_{13} & 0 \\ B_{21} & B_{22} & B_{23} & 0 \\ B_{31} & B_{32} & B_{33} & 0 \\ B_{41} & B_{42} & B_{43} & 0 \end{bmatrix} \begin{bmatrix} \delta\alpha \\ \delta\beta \\ \delta A \\ \delta\theta \end{bmatrix} \\ &= B(t) \begin{bmatrix} \delta\alpha \\ \delta\beta \\ \delta A \\ \delta\theta \end{bmatrix}, \end{aligned} \tag{3.41}$$

where

$B_{11} = 4\alpha\beta - 8h\alpha\beta(\beta^2+2\alpha^2+\Gamma^2)$,

$B_{12} = \Omega_1 - \Omega_0 + 2\alpha^2 - 4h\alpha^2(3\beta^2+\alpha^2+\Gamma^2)$, $B_{13} = -8h\alpha^2\beta\Gamma$,

$B_{21} = \Omega_0 - \Omega_1 - 6\alpha^2 + 2\Gamma^2 + 12h\alpha^2(\beta^2+\frac{5}{3}\alpha^2) - 4h\Gamma^2(\beta^2+\Gamma^2)$, $B_{22} = 8h\alpha\beta(\alpha^2-\Gamma^2)$,

$B_{23} = 4\alpha\Gamma - 8h\alpha\Gamma(\beta^2 + 2\Gamma^2)$, $B_{31} = -2\beta\Gamma + 4h\beta\Gamma(3\alpha^2 + \beta^2 + \Gamma^2)$,

$B_{32} = -2\alpha\Gamma + 4h\alpha\Gamma(\alpha^2 + 3\beta^2 + \Gamma^2)$, $B_{33} = -2\alpha\beta + 4h\alpha\beta(\alpha^2 + \beta^2 + 3\Gamma^2)$,

$B_{41} = 6\alpha - 12h\alpha(\beta^2 + \frac{5}{3}\alpha^2 + \frac{5}{3}\Gamma^2)$,$B_{42} = 2\beta - 4h\beta(\beta^2 + \Gamma^2 + 3\alpha^2)$,

$B_{43} = 2\Gamma - 4h\Gamma(\Gamma^2 + \beta^2 + 3\alpha^2)$.

Since the evolution of α, β and A decouple from that for Θ, we consider the behavior of the reduced system

$$\partial_t \begin{bmatrix} \delta\alpha \\ \delta\beta \\ \delta A \end{bmatrix} = \tilde{B}(t) \begin{bmatrix} \delta\alpha \\ \delta\beta \\ \delta A \end{bmatrix} = \begin{bmatrix} B_{11} & B_{12} & B_{13} \\ B_{21} & B_{22} & B_{23} \\ B_{31} & B_{32} & B_{33} \end{bmatrix} \begin{bmatrix} \delta\alpha \\ \delta\beta \\ \delta A \end{bmatrix}. \tag{3.42}$$

3.3.2.1 Linearized dynamics about the symmetric equilibrium state

For the symmetric equilibrium, as displayed in (3.36), we have

$$(\alpha_-^{eq}, \beta_-^{eq}, A_-^{eq}, \theta_-^{eq}(t)) = (0, 0, N^{\frac{1}{2}}, (N - \Omega_0 - hN^2)t). \tag{3.43}$$

Note that $N = \Gamma^2 = \frac{1}{2h}(1 - \sqrt{1 + 4h(\Omega - \Omega_0)})$.

Hence,

$$B = B_- = \begin{bmatrix} 0 & \Omega_1 - \Omega_0 & 0 & 0 \\ \Omega_0 - \Omega_1 + 2N - 4hN^2 & 0 & 0 & 0 \\ 0 & 0 & 0 & 0 \\ 0 & 0 & 2N^{\frac{1}{2}} - 4hN^{\frac{1}{3}} & 0 \end{bmatrix}.$$

For the reduced system, we have

$$\tilde{B}_- = \begin{bmatrix} 0 & \Omega_1 - \Omega_0 & 0 \\ 3\Omega_0 - \Omega_1 - 2\Omega - 2h(\Omega - \Omega_0)^2 + 32h^2(\Omega - \Omega_0)^3 & 0 & 0 \\ 0 & 0 & 0 \end{bmatrix}, \tag{3.44}$$

whose eigenvalues are as follows:

$$\lambda_0 = 0,\ \ \lambda_+ = \sqrt{(\Omega_1 - 3\Omega_0 + 2\Omega)(\Omega_0 - \Omega_1)} + \frac{(\Omega - \Omega_0)^2(\Omega_0 - \Omega_1)}{\sqrt{(\Omega_1 - 3\Omega_0 + 2\Omega)(\Omega_0 - \Omega_1)}}h,$$
$$\lambda_- = -\sqrt{(\Omega_1 - 3\Omega_0 + 2\Omega)(\Omega_0 - \Omega_1)} - \frac{(\Omega - \Omega_0)^2(\Omega_0 - \Omega_1)}{\sqrt{(\Omega_1 - 3\Omega_0 + 2\Omega)(\Omega_0 - \Omega_1)}}h.$$

As $(\Omega_0 - \Omega_1) < 0$, then if $(\Omega_1 - 3\Omega_0 + 2\Omega) < 0$, our point is unstable and conversely if $(\Omega_1 - 3\Omega_0 + 2\Omega) > 0$ then our system is stable elliptic point.

3.3.2.2 Linearized dynamics about asymmetric equilibrium states

For the (regular, existing when $h = 0$) asymmetric equilibrium, we have up to order $O(h^{3/2})$

$$\begin{aligned}(\alpha_+^{eq}, \beta_+^{eq}, A_+^{eq}, \theta_+^{eq}(t)) \ = \Bigg(& \tfrac{1}{4}\sqrt{2(3\Omega_0 - \Omega_1 - 2\Omega)} + \tfrac{2\Omega^2 - 4\Omega\Omega_1 - \Omega_0^2 + 2\Omega_0\Omega_1 - \Omega_1^2}{4\sqrt{2(3\Omega_0 - \Omega_1 - 2\Omega)}}h, \\ & 0, \tfrac{1}{4}\sqrt{2(3\Omega_0 - \Omega_1 - 2\Omega)} + \tfrac{2\Omega^2 - 4\Omega\Omega_1 - \Omega_0^2 + 2\Omega_0\Omega_1 - \Omega_1^2}{4\sqrt{2(3\Omega_0 - \Omega_1 - 2\Omega)}}h, \\ & \tfrac{1}{16h}(h\Omega_0 + h\Omega_1 + \sqrt{8h^2(\Omega_0 - \Omega_1)^2 + 1} + 1)\Bigg).\end{aligned}$$

Hence,

$$B_+ = \begin{bmatrix} 0 & B_+(12) & 0 & 0 \\ B_+(21) & 0 & B_+(23) & 0 \\ 0 & B_+(32) & 0 & 0 \\ B_+(41) & 0 & B_+(43) & 0 \end{bmatrix}.$$

where

$$\begin{aligned}
B_+(12) &= \Omega_1 - \Omega_0 + 2\alpha^2 - 4h\alpha^2(\alpha^2+\Gamma^2)\\
B_+(21) &= \Omega_0 - \Omega_1 + 2\Gamma^2 - 6\alpha^2 + 4h(5\alpha^4 - \Gamma^4)\\
B_+(23) &= 4\alpha\Gamma - 16h\alpha\Gamma^3\\
B_+(32) &= -2\alpha\Gamma + 4h\alpha\Gamma(\alpha^2+\Gamma^2)\\
B_+(41) &= 6\alpha - 20h\alpha(\alpha^2+\Gamma^2)\\
B_+(43) &= 2\Gamma - 4h\Gamma(\Gamma^2+5\alpha^2)
\end{aligned}$$

In this case, we substitute (3.45) into the expression for $\tilde{B}$ in (3.42) and obtain:

$$\tilde{B}_+ = \begin{bmatrix} 0 & \tilde{B}_{12} & 0 \\ \tilde{B}_{21} & 0 & \tilde{B}_{23} \\ 0 & \tilde{B}_{32} & 0 \end{bmatrix}. \tag{3.45}$$

where

$$\begin{aligned}
\tilde{B}_{12} &= \tfrac{3}{4}\Omega_1 - \tfrac{1}{4}\Omega_0 - \tfrac{1}{2}\Omega - (\Omega_0-\Omega_1)^2 h,\\
\tilde{B}_{21} &= \tfrac{1}{2}\Omega_1 - \tfrac{3}{2}\Omega_0 + \Omega - \tfrac{1}{8}(\Omega_0-\Omega_1)^2 h,\\
\tilde{B}_{23} &= \tfrac{1}{2}\sqrt{(\Omega_1+2\Omega-3\Omega_0)(\Omega_0-3\Omega_1+2\Omega)} + O(h),\\
\tilde{B}_{32} &= -\tfrac{1}{4}\sqrt{(\Omega_1+2\Omega-3\Omega_0)(\Omega_0-3\Omega_1+2\Omega)} + O(h).
\end{aligned}$$

The eigenvalues of $\tilde{B}$ are:

$$\begin{aligned}
\lambda_0 &= 0,\\
\lambda_+ &= \tfrac{1}{2}\sqrt{-(2\Omega-3\Omega_0+\Omega_1)(2\Omega-3\Omega_1+\Omega_0)}\\
&\quad + \frac{(\Omega_0-\Omega_1)(2\Omega^2-3\Omega\Omega_0-\Omega\Omega_1-\Omega_0^2+5\Omega_0\Omega_1-2\Omega_1^2)}{4\sqrt{-(2\Omega-3\Omega_0+\Omega_1)(2\Omega-3\Omega_1+\Omega_0)}}h,\\
\lambda_- &= -\tfrac{1}{2}\sqrt{-(2\Omega-3\Omega_0+\Omega_1)(2\Omega-3\Omega_1+\Omega_0)}\\
&\quad - \frac{(\Omega_0-\Omega_1)(2\Omega^2-3\Omega\Omega_0-\Omega\Omega_1-\Omega_0^2+5\Omega_0\Omega_1-2\Omega_1^2)}{4\sqrt{-(2\Omega-3\Omega_0+\Omega_1)(2\Omega-3\Omega_1+\Omega_0)}}h.
\end{aligned}$$

Therefore, the bifurcating asymmetric states are stable elliptic points.

3.4 Dynamics near the symmetry breaking bifurcation point

In this section, we are shifting to polar coordinate, to see dynamics near the bifurcation point. Let us set $c_0 = r_0 e^{i\theta_0}$ and $c_1 = r_1 e^{i\theta_1}$ and substituted into (3.15) this leads to the following system of ODE's are (but we neglect R):

$$\begin{aligned}
\dot{r}_0 &= r_0 r_1^2 \sin(2\Delta\theta) + h r_0^3 r_1^2 \sin(2\Delta\theta) - 2h r_0 r_1^4 \sin(2\Delta\theta) + 3h r_0^3 r_1^2 \sin(2\theta_1) \\
\dot{r}_1 &= -r_0^2 r_1 \sin(2\Delta\theta) - h r_0^2 r_1^3 \sin(2\Delta\theta) + 2h r_0^4 r_1 \sin(2\Delta\theta) + 3h r_0^2 r_1^3 \sin(2\theta_0)
\end{aligned}$$

and

$$\begin{aligned}
(\dot{\Delta\theta}) &= \Omega_1 - \Omega_0 + (r_0^2 - r_1^2)(1 + \cos(2\Delta\theta)) - (4h r_1^4 - 4h r_0^4)(4 + 4\cos(2\Delta\theta)) \\
&\quad + 3h r_0^2 r_1^2 (\cos(2\theta_0) - \cos(2\theta_1)),
\end{aligned} \tag{3.46}$$

where $\Delta\theta = \theta_0 - \theta_1$. Given the system above, we can say that the bifurcation of stability occurs at

$$N_{crit} = \frac{1}{32h}\left(1 - \sqrt{32h(\Omega_0 - \Omega_1) + 1}\right). \tag{3.47}$$

Since we are interested in the behavior quite near the bifurcation point, let we define

$$\begin{aligned}
r_0 &= \sqrt{N_{cr}} + \epsilon_0, \\
r_1 &= \epsilon_1, \\
N &= N_{crit} + n,
\end{aligned}$$

where

$$n = \epsilon_0^2 + \epsilon_1^2 + 2\sqrt{N_{cr}}\epsilon_0.$$

Then, we have

$$\begin{aligned}\dot{\epsilon_0} &= 2h\epsilon_1^4\left(\sqrt{N_{cr}}+\epsilon_0\right)\sin(2\Delta\theta)+h\epsilon_1^2\left(\sqrt{N_{cr}}+\epsilon_0\right)^3(3\sin(2\theta_1)-\sin(2\Delta\theta))\\ &\quad +\epsilon_1^2\left(\sqrt{N_{cr}}+\epsilon_0\right)\sin(2\Delta\theta),\end{aligned}$$

$$\begin{aligned}\dot{\epsilon_1} &= -2h\epsilon_1\left(\sqrt{N_{cr}}+\epsilon_0\right)^4\sin(2\Delta\theta)+h\epsilon_1^3\left(\sqrt{N_{cr}}+\epsilon_0\right)^2(3\sin(2\theta_0)+\sin(2\Delta\theta))\\ &\quad -\epsilon_1\left(\sqrt{N_{cr}}+\epsilon_0\right)^2\sin(2\Delta\theta),\end{aligned}$$

and

$$\begin{aligned}(\dot{\Delta\theta}) &= \Omega_0-\Omega_1+\left(\epsilon_1^2-\left(\sqrt{N_{cr}}+\epsilon_0\right)^2\right)(1+\cos(2\Delta\theta))\\ &\quad +2h\left(\epsilon_1^4-\left(\sqrt{N_{cr}}+\epsilon_0\right)^4\right)\\ &\quad +2h\left(\epsilon_1^4-\left(\sqrt{N_{cr}}+\epsilon_0\right)^4\right)\cos(2\Delta\theta)\\ &\quad +3h\epsilon_1^2\left(\sqrt{N_{cr}}+\epsilon_0\right)^2(\cos(2\Delta\theta)).\end{aligned}$$

Looking at the phase equation, we have

$$\begin{aligned}(\dot{\Delta\theta}) &= \Omega_0-\Omega_1-n+2\epsilon_1^2-N_{cr}+2h\epsilon_1^4-2hN_{cr}^2\\ &\quad -8h\sqrt{N_{cr}^3}\epsilon_0-12hN_{cr}\epsilon_0^2-8h\sqrt{N_{cr}}\epsilon_0^3-2h\epsilon_0^4\\ &\quad +\left(3h\epsilon_1^2N_{cr}+6h\epsilon_1^2\sqrt{N_{cr}}\epsilon_0+3h\epsilon_1^2\epsilon_0^2\right)(\cos(2\Delta\theta))\\ &\quad -\left(8h\sqrt{N_{cr}^3}\epsilon_0+8h\sqrt{N_{cr}}\epsilon_0^3+2h\epsilon_0^4-2h\epsilon_1^4+12hN_{cr}\epsilon_0^2+2hN_{cr}^2\right.\\ &\quad \left.+n-2\epsilon_1^2-N_{cr}\right)\cos(2\Delta\theta).\end{aligned}$$

However, we would also like to see analytically that such things exist for long times. As a first approximation of this, let us take the ansatz

$$\psi(x,t)=e^{i\theta_0(t)}\left(\sqrt{N_{cr}}+\epsilon_0(t)\right)\psi_0+e^{i\theta_1(t)}\epsilon_0(t)\psi_1+R(x,t), \tag{3.48}$$

and plug it into equation 3.1 and let $-\Delta + V = H$, so we have

$$
\begin{aligned}
(i\partial_t - H)R \;=\; & \Big[e^{i\theta_0}(\sqrt{N_{cr}}+\epsilon_0)\psi_0(\dot\theta_0+\omega_0) - ie^{i\theta_0}\dot\epsilon_0\psi_0 + e^{i\theta_1}\epsilon_1\psi_1(\dot\theta_1+\omega_1) \\
& -ie^{i\theta_1}\dot\epsilon_1\psi_1 - e^{i\theta_0}(\sqrt{N_{cr}}+\epsilon_0)^3\psi_0^3 - e^{i\theta_1}\epsilon_1^3\psi_1^3 \\
& -e^{i\theta_0}(\sqrt{N_{cr}}+\epsilon_0)\epsilon_1^2\psi_0\psi_1^2(2+e^{2i(\Delta\theta)} \\
& -e^{i\theta_1}(\sqrt{N_{cr}}+\epsilon_0)^2\epsilon_1\psi_0^2\psi_1(2+e^{-2i(\Delta\theta)}) + he^{i\theta_0}(\sqrt{N_{cr}}+\epsilon_0)^5\psi_0^5 \\
& +he^{i\theta_1}\epsilon_1^5\psi_1^5 + he^{i\theta_0}(\sqrt{N_{cr}}+\epsilon_0)^3\epsilon_1^2\psi_0^3\psi_1^2(6+e^{-2i(\Delta\theta)}) \\
& +he^{i\theta_1}(\sqrt{N_{cr}}+\epsilon_0)^2\epsilon_1^3\psi_0^2\psi_1^3(6+e^{2i(\Delta\theta)}) \\
& +3he^{i\theta_1}(\sqrt{N_{cr}}+\epsilon_0)^4\psi_0^4\epsilon_1\psi 1 + 2he^{i\theta_0}(\sqrt{N_{cr}}+\epsilon_0)\epsilon_1^4\psi_0\psi_1^4(\tfrac{3}{2}+e^{2i(\Delta\theta)}) \\
& +3he^{i\theta_1}(\sqrt{N_{cr}}+\epsilon_0)^2\epsilon_1^3\psi_0^2\psi_1^3e^{-2i(\Delta\theta)} \\
& +3he^{i\theta_0}(\sqrt{N_{cr}}+\epsilon_0)^3\epsilon_1^2\psi_0^3\psi_1^2e^{-2i(\Delta\theta)} \\
& +2he^{i\theta_1}(\sqrt{N_{cr}}+\epsilon_0)^4\epsilon_1\psi_0^4\psi_1e^{2i(\Delta\theta)}\Big] \\
& -2\Big[(\sqrt{N_{cr}}+\epsilon_0)^2\psi_0^2 + 2(\sqrt{N_{cr}}+\epsilon_0)\epsilon_1\psi_0\psi_1\cos(\theta_0-\theta_1) + \psi_1^2\epsilon_1^2 \\
& -\tfrac{3}{2}h\Big((\sqrt{N_{cr}}+\epsilon_0)^4\psi_0^4 + \epsilon_1^4\psi_1^4\Big) - 6h(\sqrt{N_{cr}}+\epsilon_0)^2\psi_0^2\epsilon_1^2\psi_1^2 \\
& -3h\,e^{i(\Delta\theta)}(\sqrt{N_{cr}}+\epsilon_0)^3\epsilon_1\psi_0^3\psi_1(1+e^{-2i(\Delta\theta)}) \\
& -3h\,e^{i(\Delta\theta)}(\sqrt{N_{cr}}+\epsilon_0)\epsilon_1^3\psi_0\psi_1^3(1+e^{-2i(\Delta\theta)}) \\
& -\tfrac{3}{2}h\,e^{2i(\Delta\theta)}(\sqrt{N_{cr}}+\epsilon_0)^2\epsilon_1^2\psi_0^2\psi_1^2(1+e^{-4i(\Delta\theta)})\Big]R \\
& -e^{i(\theta_1+\theta_0)}\Big[(\sqrt{N_{cr}}+\epsilon_0)^2\psi_0^2e^{-i(\Delta\theta)} + \epsilon_1^2\psi_1^2e^{i\Delta\theta} + 2(\sqrt{N_{cr}}+\epsilon_0)\epsilon_1\psi_0\psi_1 \\
& -6h(\sqrt{N_{cr}}+\epsilon_0)^2\epsilon_1^2\psi_1^2\psi_0^2e^{i(\Delta\theta)} - 6h(\sqrt{N_{cr}}+\epsilon_0)^3\epsilon_1\psi_0^3\psi_1 \\
& -6h(\sqrt{N_{cr}}+\epsilon_0)^2\epsilon_1^2\psi_1^2\psi_0^2e^{-i(\Delta\theta)} - 2h\Big((\sqrt{N_{cr}}+\epsilon_0)^4\psi_0^4 + \epsilon_1^4\psi_1^4\Big)e^{-i(\Delta\theta)} \\
& -2h(\sqrt{N_{cr}}+\epsilon_0)\epsilon_1^3\psi_0\psi_1^3(3+e^{-2i(\Delta\theta)}) \\
& -2h(\sqrt{N_{cr}}+\epsilon_0)^3\epsilon_1\psi_0^3\psi_1e^{-2i(\Delta\theta)}\Big]\bar R \\
& -\Big[e^{-i\theta_0}(\sqrt{N_{cr}}+\epsilon_0)\psi_0 + e^{-i\theta_1}\epsilon_1\psi_1 - 3he^{-i\theta_0}(\sqrt{N_{cr}}+\epsilon_0)^3\psi_0^3 \\
& -3he^{-i\theta_1}\epsilon_1^3\psi_1^3 - 3he^{-i\theta_0}(\sqrt{N_{cr}}+\epsilon_0)\epsilon_1^2\psi_0\psi_1^2(2+e^{-2i(\Delta\theta)}) \\
& -3he^{-i\theta_1}(\sqrt{N_{cr}}+\epsilon_0)^2\epsilon_1\psi_0^2\psi_1(2+e^{2i(\Delta\theta)})\Big]R^2 \\
& +\Big[he^{3i\theta_0}(\sqrt{N_{cr}}+\epsilon_0)^3\psi_0^3 + he^{3i\theta_1}\epsilon_1^3\psi_1^3
\end{aligned}
\tag{3.49}
$$

$$
\begin{aligned}
&+3he^{-i\theta_0}(\sqrt{N_{cr}}+\epsilon_0)\epsilon_1^2\psi_0\psi_1^2e^{2i(\theta_1+\theta_0)}\\
&+3he^{-i\theta_1}(\sqrt{N_{cr}}+\epsilon_0)^2\epsilon_1\psi_0^2\psi_1e^{2i(\theta_1+\theta_0)}\Big]\bar{R}^2\\
&+\Big[he^{-2i\theta_0}(\sqrt{N_{cr}}+\epsilon_0)^2\psi_0^2+2he^{-i(\theta_1+\theta_0)}(\sqrt{N_{cr}}+\epsilon_0)\epsilon_1\psi_1\psi_0+e^{-2i\theta_1}h\epsilon_1^2\psi_1^2\Big]R^3\\
&-\Big[2e^{i\theta_0}(\sqrt{N_{cr}}+\epsilon_0)\psi_0+2e^{i\theta_1}\epsilon_1\psi_1\\
&-6he^{i\theta_1}(\sqrt{N_{cr}}+\epsilon_0)^2\epsilon_1\psi_0^2\psi_1(2+e^{2i(\theta_0-\theta_1)})\\
&-6he^{i\theta_0}(\sqrt{N_{cr}}+\epsilon_0)\epsilon_1^2\psi_0\psi_1^2(2+e^{2i(\Delta\theta)})-6he^{i\theta_0}(\sqrt{N_{cr}}+\epsilon_0)^3\psi_0^3-6he^{i\theta_1}\epsilon_1^3\psi_1^3\Big]|R|^2\\
&-\Big[1-6h\Big((\sqrt{N_{cr}}+\epsilon_0)^2\psi_0^2+\epsilon_1^2\psi_1^2\Big)\\
&-6he^{i(\theta_0-\theta_1)}(\sqrt{N_{cr}}+\epsilon_0)\psi_1\epsilon_1\psi_0(1+e^{2i(\Delta\theta)})\Big]|R|^2R\\
&+\Big[3he^{2i\theta_0}(\sqrt{N_{cr}}+\epsilon_0)^2\psi_0^2+3he^{2i\theta_1}\epsilon_1^2\psi_1^2\\
&+6he^{i(\theta_0+\theta_1)}(\sqrt{N_{cr}}+\epsilon_0)\psi_0\epsilon_1\psi_1\Big]|R|^2\bar{R}\\
&+\Big[3h\Big(e^{i\theta_0}(\sqrt{N_{cr}}+\epsilon_0)\psi_0+e^{i\theta_1}\epsilon_1\psi_1\Big)\Big]|R|^4\\
&+h|R|^4R.
\end{aligned}
$$

Then, using the ODE's, we have

$$
\begin{aligned}
(i\partial_t-H)R \;=\;& Pc\Big[-ie^{i\theta_1}\dot{\epsilon}_1\psi_1-e^{i\theta_0}(\sqrt{N_{cr}}+\epsilon_0)^3\psi_0^3-e^{i\theta_1}\epsilon_1^3\psi_1^3\\
&-e^{i\theta_0}(\sqrt{N_{cr}}+\epsilon_0)\epsilon_1^2\psi_0\psi_1^2(2+e^{2i(\Delta\theta)}\\
&-e^{i\theta_1}(\sqrt{N_{cr}}+\epsilon_0)^2\epsilon_1\psi_0^2\psi_1(2+e^{-2i(\Delta\theta)})+he^{i\theta_0}(\sqrt{N_{cr}}+\epsilon_0)^5\psi_0^5\\
&+he^{i\theta_1}\epsilon_1^5\psi_1^5+he^{i\theta_0}(\sqrt{N_{cr}}+\epsilon_0)^3\epsilon_1^2\psi_0^3\psi_1^2(6+e^{-2i(\Delta\theta)})\\
&+he^{i\theta_1}(\sqrt{N_{cr}}+\epsilon_0)^2\epsilon_1^3\psi_0^2\psi_1^3(6+e^{2i(\Delta\theta)})\\
&+3he^{i\theta_1}(\sqrt{N_{cr}}+\epsilon_0)^4\psi_0^4\epsilon_1\psi 1+2he^{i\theta_0}(\sqrt{N_{cr}}+\epsilon_0)\epsilon_1^4\psi_0\psi_1^4(\tfrac{3}{2}+e^{2i(\Delta\theta)})\\
&+3he^{i\theta_1}(\sqrt{N_{cr}}+\epsilon_0)^2\epsilon_1^3\psi_0^2\psi_1^3e^{-2i(\Delta\theta)}+3he^{i\theta_0}(\sqrt{N_{cr}}+\epsilon_0)^3\epsilon_1^2\psi_0^3\psi_1^2e^{-2i(\Delta\theta)}\\
&+2he^{i\theta_1}(\sqrt{N_{cr}}+\epsilon_0)^4\epsilon_1\psi_0^4\psi_1e^{2i(\Delta\theta)}\Big]
\end{aligned}
$$

$$
\begin{aligned}
&-2\Big[(\sqrt{N_{cr}}+\epsilon_0)^2\psi_0^2+2(\sqrt{N_{cr}}+\epsilon_0)\epsilon_1\psi_0\psi_1\cos(\theta_0-\theta_1)+\psi_1^2\epsilon_1^2\\
&-\tfrac{3}{2}h\Big((\sqrt{N_{cr}}+\epsilon_0)^4\psi_0^4+\epsilon_1^4\psi_1^4\Big)-6h(\sqrt{N_{cr}}+\epsilon_0)^2\psi_0^2\epsilon_1^2\psi_1^2\\
&-3h\,e^{i(\Delta\theta)}(\sqrt{N_{cr}}+\epsilon_0)^3\epsilon_1\psi_0^3\psi_1(1+e^{-2i(\Delta\theta)})\\
&-3h\,e^{i(\Delta\theta)}(\sqrt{N_{cr}}+\epsilon_0)\epsilon_1^3\psi_0\psi_1^3(1+e^{-2i(\Delta\theta)})\\
&-\tfrac{3}{2}h\,e^{2i(\Delta\theta)}(\sqrt{N_{cr}}+\epsilon_0)^2\epsilon_1^2\psi_0^2\psi_1^2(1+e^{-4i(\Delta\theta)})\Big]R\\
&-e^{i(\theta_1+\theta_0)}\Big[(\sqrt{N_{cr}}+\epsilon_0)^2\psi_0^2e^{-i(\Delta\theta)}+\epsilon_1^2\psi_1^2e^{i\Delta\theta}+2(\sqrt{N_{cr}}+\epsilon_0)\epsilon_1\psi_0\psi_1\\
&-6h(\sqrt{N_{cr}}+\epsilon_0)^2\epsilon_1^2\psi_1^2\psi_0^2e^{i(\Delta\theta)}-6h(\sqrt{N_{cr}}+\epsilon_0)^3\epsilon_1\psi_0^3\psi_1\\
&-6h(\sqrt{N_{cr}}+\epsilon_0)^2\epsilon_1^2\psi_1^2\psi_0^2e^{-i(\Delta\theta)}-2h\Big((\sqrt{N_{cr}}+\epsilon_0)^4\psi_0^4+\epsilon_1^4\psi_1^4\Big)e^{-i(\Delta\theta)}\\
&-2h(\sqrt{N_{cr}}+\epsilon_0)\epsilon_1^3\psi_0\psi_1^3(3+e^{-2i(\Delta\theta)})-2h(\sqrt{N_{cr}}+\epsilon_0)^3\epsilon_1\psi_0^3\psi_1e^{-2i(\Delta\theta)}\Big]\bar{R}\\
&-\Big[e^{-i\theta_0}(\sqrt{N_{cr}}+\epsilon_0)\psi_0+e^{-i\theta_1}\epsilon_1\psi_1-3he^{-i\theta_0}(\sqrt{N_{cr}}+\epsilon_0)^3\psi_0^3\\
&-3he^{-i\theta_1}\epsilon_1^3\psi_1^3-3he^{-i\theta_0}(\sqrt{N_{cr}}+\epsilon_0)\epsilon_1^2\psi_0\psi_1^2(2+e^{-2i(\Delta\theta)})\\
&-3he^{-i\theta_1}(\sqrt{N_{cr}}+\epsilon_0)^2\epsilon_1\psi_0^2\psi_1(2+e^{2i(\Delta\theta)})\Big]R^2\\
&+\Big[he^{3i\theta_0}(\sqrt{N_{cr}}+\epsilon_0)^3\psi_0^3+he^{3i\theta_1}\epsilon_1^3\psi_1^3+3he^{-i\theta_0}(\sqrt{N_{cr}}+\epsilon_0)\epsilon_1^2\psi_0\psi_1^2e^{2i(\theta_1+\theta_0)}\\
&+3he^{-i\theta_1}(\sqrt{N_{cr}}+\epsilon_0)^2\epsilon_1\psi_0^2\psi_1e^{2i(\theta_1+\theta_0)}\Big]\bar{R}^2\\
&+\Big[he^{-2i\theta_0}(\sqrt{N_{cr}}+\epsilon_0)^2\psi_0^2+2he^{-i(\theta_1+\theta_0)}(\sqrt{N_{cr}}+\epsilon_0)\epsilon_1\psi_1\psi_0+e^{-2i\theta_1}h\epsilon_1^2\psi_1^2\Big]R^3\\
&-\Big[2e^{i\theta_0}(\sqrt{N_{cr}}+\epsilon_0)\psi_0+2e^{i\theta_1}\epsilon_1\psi_1\\
&-6he^{i\theta_1}(\sqrt{N_{cr}}+\epsilon_0)^2\epsilon_1\psi_0^2\psi_1(2+e^{2i(\theta_0-\theta_1)})\\
&-6he^{i\theta_0}(\sqrt{N_{cr}}+\epsilon_0)\epsilon_1^2\psi_0\psi_1^2(2+e^{2i(\Delta\theta)})-6he^{i\theta_0}(\sqrt{N_{cr}}+\epsilon_0)^3\psi_0^3-6he^{i\theta_1}\epsilon_1^3\psi_1^3\Big]|R|^2\\
&-\Big[1-6h\Big((\sqrt{N_{cr}}+\epsilon_0)^2\psi_0^2+\epsilon_1^2\psi_1^2\Big)\\
&-6he^{i(\theta_0-\theta_1)}(\sqrt{N_{cr}}+\epsilon_0)\psi_1\epsilon_1\psi_0(1+e^{2i(\Delta\theta)})\Big]|R|^2R\\
&+\Big[3he^{2i\theta_0}(\sqrt{N_{cr}}+\epsilon_0)^2\psi_0^2+3he^{2i\theta_1}\epsilon_1^2\psi_1^2\\
&+6he^{i(\theta_0+\theta_1)}(\sqrt{N_{cr}}+\epsilon_0)\psi_0\epsilon_1\psi_1\Big]|R|^2\bar{R}\\
&+\Big[3h\Big(e^{i\theta_0}(\sqrt{N_{cr}}+\epsilon_0)\psi_0+e^{i\theta_1}\epsilon_1\psi_1\Big)\Big]|R|^4\\
&+h|R|^4R\\
=\;&(I)+(II)R+(III)\bar{R}+(IV)R^2+(V)\bar{R}^2+(VI)R^3+(VII)|R|^2+(VIII)|R|^2R\\
&+(IX)|R|^2\bar{R}+(X)|R|^4-h|R|^4R.
\end{aligned}
\tag{3.50}
$$

Notice that $P_c(I) = (I)$. Hence, in order to increase the existence time for the observed orbits, it seems natural to attempt to include a term in the ansatz to account for the linear behavior of such an operator. Specifically, we would like to to slightly alther our ansatz to include a term $\tilde{R}$ such that

$$(i\partial_t - H)\tilde{R} = (I).$$

In this case, it is particularly challenging as (I) is a function of x and t, meaning we must do a perturbative argument in order to pull out the leading order behavior of this term. Another possibility is to couple the ODE's to a term in the continuous spectrum, say R, which would add a term very similar to the above η equation. However, we would only see the observed Hamiltonian dynamics if R was small in relation to the leading order parameters. The leading order equation for R is precisely

$$(i\partial_t - H)R = (I).$$

Hence, in order to do a perturbative argument about the finite dimensial dynamics on the system of ODE's couple to the continuous spectrum, we would need to do it on a time scale for which R is small relative to the dynamical parameters.

Now, assuming we have an asymptotic parameter, say δ such that

$$\epsilon_0, \epsilon_1, N_{cr}, n \leq \delta,$$

we see

$$\begin{aligned}
(I) &\approx O(\delta^5), \\
(II) &\approx O(\delta^4), \\
(III) &\approx O(\delta^4), \\
(IV) &\approx O(\delta^3),
\end{aligned}$$

$$\begin{aligned}
(V) &\approx O(\delta^3),\\
(VI) &\approx O(\delta^2),\\
(VII) &\approx O(\delta^3),\\
(VIII) &\approx O(\delta^2),\\
(IX) &\approx O(\delta^2),\\
(X) &\approx O(\delta).
\end{aligned}$$

3.5 Perturbative analysis for cubic-quintic nonlinearity

In this section, we will linearize the solution about the finite dimensional ODE solutions above. To begin, we look at solutions of the form $n > 0, \epsilon_0, \epsilon_1, \Delta\theta$ small. In this case, linearising about the localised solution shows that the essential frequency of oscillation is the form

$$\frac{\pi}{2\left(N_{cr}^2 - N_{cr}n - n^2\right)^{\frac{1}{2}}}$$

Hence, it is on the time scale of multiple oscillations and we hope to control the difference between the observed finite dimensional periodic solutions and the full solution to the PDE. Consider again (3.15), where here we denote $F_\perp$ and G are $P_cF_b(c_0, c_1, \bar{c}_0, \bar{c}_1)$ and $P_cF_R(c_0, c_1, \bar{c}_0, \bar{c}_1; R, \bar{R})$ respectively.

Let c_0, c_1 be the periodic solutions to the finite dimensional system above, which is obtained by taking $F_0 = F_1 = 0$. Now, we wish to linearize about an infinite dimensional solution, namely ρ_0, ρ_1, and $\tilde{R}$. In other words, we further refine our

ansatz again such that

$$c_0(t) = \rho_0(t) + \eta_0(t), \tag{3.51a}$$

$$c_1(t) = \rho_1(t) + \eta_1(t), \tag{3.51b}$$

$$R(x,t) = \tilde{R}(x,t) + W(x,t), \tag{3.51c}$$

where

$$i\tilde{R}_t - H_L\tilde{R} + F_\perp(\rho_0, \rho_1, \bar{\rho}_0, \bar{\rho}_1) = 0,$$

or

$$\begin{aligned}\tilde{R} &= -i\int_0^t e^{iH_L(t-s)}P_cF_\perp(\rho_0, \rho_1, \bar{\rho}_0, \bar{\rho}_1)ds \\ &= -i\int_0^t e^{iH_L(t-s)}F_\perp(\rho_0, \rho_1, \bar{\rho}_0, \bar{\rho}_1)ds.\end{aligned}$$

If we plug equations (3.51) into equation (3.15), we obtain

$$\begin{aligned}
i\dot{\eta}_0 \;&-\; \Omega_0\eta_0 + \Omega\eta_0 + 2|\rho_0|^2\eta_0 + \rho_0^2\bar{\eta}_0 + \rho_1^2\bar{\eta}_0 + 2\bar{\rho}_0\rho_1\eta_1 + 2|\rho_1|^2\eta_0 + 2\rho_0\rho_1\bar{\eta}_1 + 2\rho_0\bar{\rho}_1\eta_1 \\
&-\; 2h\left(|\rho_0|^2\rho_0^2\bar{\eta}_0 + \rho_0^3\bar{\rho}_1\bar{\eta}_1 + \bar{\rho}_0\rho_1^3\bar{\eta}_1 + |\rho_1|^2\rho_1^2\bar{\eta}_0\right) - 3h\left(|\rho_0|^4\eta_0 + \rho_0^2\bar{\rho}_1^2\eta_0 + \bar{\rho}_0^2\rho_1^2\eta_0 + |\rho_1|^4\eta_0\right) \\
&-\; 6h\left(|\rho_0|^2\bar{\rho}_0\rho_1\eta_1 + |\rho_0|^2\rho_1^2\bar{\eta}_0 + |\rho_1|^2\bar{\rho}_1\rho_0\eta_1 + |\rho_1|^2\rho_1\rho_0\bar{\eta}_1 + |\rho_1|^2\rho_1\bar{\rho}_0\eta_1\right. \\
&+\; \left.|\rho_0|^2\rho_0\bar{\rho}_1\eta_1 + |\rho_0|^2\rho_0\rho_1\bar{\eta}_1 + |\rho_1|^2\rho_0^2\bar{\eta}_0\right) - 12h|\rho_0|^2|\rho_1|^2\eta_0 \\
&=\; F_0\left(\rho_0 + \eta_0, \rho_1 + \eta_1, \bar{\rho}_0 + \bar{\eta}_0, \bar{\rho}_1 + \bar{\eta}_1; \tilde{R} + W, \bar{\tilde{R}} + \bar{W}\right) + \text{h.o.t.}, \\
i\dot{\eta}_1 \;&-\; \Omega_1\eta_1 + \Omega\eta_1 + 2|\rho_1|^2\eta_1 + \rho_1^2\bar{\eta}_1 + \rho_0^2\bar{\eta}_1 + 2\bar{\rho}_1\rho_0\eta_0 + 2|\rho_0|^2\eta_1 + 2\rho_1\rho_0\bar{\eta}_0 + 2\rho_1\bar{\rho}_0\eta_0 \\
&-\; 2h\left(\rho_0^3\bar{\rho}_1\bar{\eta}_0 + |\rho_0|^2\rho_0^2\bar{\eta}_1 + \bar{\rho}_0\rho_1^3\bar{\eta}_0 + |\rho_1|^2\rho_1^2\bar{\eta}_1\right) - 3h\left(|\rho_0|^4\eta_1 + \bar{\rho}_0^2\rho_1^2\eta_1 + \rho_0^2\bar{\rho}_1^2\eta_1 + |\rho_1|^4\eta_1\right) \\
&-\; 6h\left(|\rho_0|^2\rho_1^2\bar{\eta}_1 + |\rho_1|^2\bar{\rho}_1\rho_0\eta_0 + |\rho_1|^2\rho_0^2\bar{\eta}_1 + |\rho_0|^2\bar{\rho}_0\rho_1\eta_0 + |\rho_0|^2\rho_0\rho_1\bar{\eta}_0\right. \\
&+\; \left.|\rho_0|^2\rho_0\bar{\rho}_1\eta_0 + |\rho_1|^2\rho_1\bar{\rho}_0\eta_0 + |\rho_1|^2\rho_1\rho_0\bar{\eta}_0\right) - 12h|\rho_0|^2|\rho_1|^2\eta_1 \\
&=\; F_1\left(\rho_0 + \eta_0, \rho_1 + \eta_1, \bar{\rho}_0 + \bar{\eta}_0, \bar{\rho}_1 + \bar{\eta}_1; \tilde{R} + W, \bar{\tilde{R}} + \bar{W}\right) + \text{h.o.t.},
\end{aligned}$$

$$\begin{aligned} iW_t &- H_L W + F_\perp(\rho_0+\eta_0,\rho_1+\eta_1,\bar{\rho}_0+\bar{\eta}_0,\bar{\rho}_1+\bar{\eta}_1) - F_\perp(\rho_0,\rho_1,\bar{\rho}_0,\bar{\rho}_1) \\ &= G\Big(\rho_0+\eta_0,\rho_1+\eta_1,\bar{\rho}_0+\bar{\eta}_0,\bar{\rho}_1+\bar{\eta}_1;\tilde{R}+W,\bar{\tilde{R}}+\bar{W}\Big), \end{aligned}$$

where F_0, F_1, G have higher order dependence on $\tilde{R}+W$.

Now, let us define again

$$\vec{\eta} = \begin{bmatrix} \eta_0 \\ \bar{\eta}_0 \\ \eta_1 \\ \bar{\eta}_1 \end{bmatrix}.$$

Then, we obtain

$$\begin{aligned} i\dot{\vec{\eta}} &= A(t)\vec{\eta} + F\Big(\vec{\eta};\tilde{R}+W,\bar{\tilde{R}}+\bar{W}\Big), \\ iW_t &- H_L W + F_\perp(\rho_0+\eta_0,\rho_1+\eta_1,\bar{\rho}_0+\bar{\eta}_0,\bar{\rho}_1+\bar{\eta}_1) - F_\perp(\rho_0,\rho_1,\bar{\rho}_0,\bar{\rho}_1) \\ &= G\Big(\rho_0+\eta_0,\rho_1+\eta_1,\bar{\rho}_0+\bar{\eta}_0,\bar{\rho}_1+\bar{\eta}_1;\tilde{R}+W,\bar{\tilde{R}}+\bar{W}\Big), \end{aligned}$$

where

$$\Big|F_\perp(\rho_0+\eta_0,\rho_1+\eta_1,\bar{\rho}_0+\bar{\eta}_0,\bar{\rho}_1+\bar{\eta}_1) - F_\perp(\rho_0,\rho_1,\bar{\rho}_0,\bar{\rho}_1)\Big| \approx \mathcal{O}(\vec{\eta}).$$

This system must then be analyzed. There are dispersive estimates for the infinite dimensional part of the system, but we need to understand the estimates on the linear part of the finite dimensional piece. In particular, we must understand the system

$$i\dot{\vec{\eta}} = A(t)\vec{\eta} + f(t)$$

using Floquet theory, where $A(t)$ is given by a matrix as follow:

$$\begin{bmatrix} A_{11} & A_{12} & A_{13} & A_{14} \\ A_{21} & A_{22} & A_{23} & A_{24} \\ A_{31} & A_{32} & A_{33} & A_{34} \\ A_{41} & A_{42} & A_{43} & A_{44} \end{bmatrix},$$

where

$$\begin{aligned}
A_{11} &= 2|\rho_0|^2 + 2|\rho_1|^2 - \Omega_0 - 3h\left(|\rho_0|^4 + \rho_0^2\bar{\rho}_1^2 + \bar{\rho}_0^2\rho_1^2 + |\rho_1|^4\right) - 12h|\rho_0|^2|\rho_1|^2, \\
A_{12} &= \rho_0^2 + \rho_1^2 - 16h\left(|\rho_0|^2\rho_0^2 + |\rho_1|^2\rho_1^2\right) - 6h\left(|\rho_0|^2\rho_1^2 + |\rho_1|^2\rho_0^2\right), \\
A_{13} &= 2\left(\bar{\rho}_0\rho_1 + \rho_0\bar{\rho}_1\right) - 6h\left(|\rho_0|^2\bar{\rho}_0\rho_1 + |\rho_1|^2\bar{\rho}_1\rho_0 + |\rho_1|^2\rho_1\bar{\rho}_0 + |\rho_0|^2\rho_0\bar{\rho}_1\right), \\
A_{14} &= 2\rho_0\rho_1 - 2h\left(\rho_0^3\bar{\rho}_1 + \bar{\rho}_0\rho_1^3\right) - 6h\left(|\rho_1|^2\rho_1\rho_0 + |\rho_0|^2\rho_0\rho_1\right), \\
A_{21} &= -\bar{\rho}_0^2 - \bar{\rho}_1^2 + 2h\left(|\rho_0|^2\bar{\rho}_0^2 + |\rho_1|^2\bar{\rho}_1^2\right) + 6h\left(|\rho_0|^2\bar{\rho}_1^2 + |\rho_1|^2\bar{\rho}_0^2\right), \\
A_{22} &= -2|\rho_0|^2 - 2|\rho_1|^2 + \Omega_0 + 3h\left(|\rho_0|^4 + \bar{\rho}_0^2\rho_1^2 + \rho_0^2\bar{\rho}_1^2 + |\rho_1|^4\right) + 12h|\rho_0|^2|\rho_1|^2, \\
A_{23} &= -2\bar{\rho}_0\bar{\rho}_1 + 2h\left(\bar{\rho}_0^3\rho_1 + \rho_0\bar{\rho}_1^3\right) + 6h\left(|\rho_1|^2\bar{\rho}_1\bar{\rho}_0 + |\rho_0|^2\bar{\rho}_0\bar{\rho}_1\right), \\
A_{24} &= -2(\rho_0\bar{\rho}_1 + \bar{\rho}_0\rho_1) + 6h\left(|\rho_0|^2\rho_0\bar{\rho}_1 + |\rho_1|^2\rho_1\bar{\rho}_0 + |\rho_1|^2\bar{\rho}_1\rho_0 + |\rho_0|^2\bar{\rho}_0\rho_1\right), \\
A_{31} &= 2(\bar{\rho}_1\rho_0 + \rho_1\bar{\rho}_0) - 6h\left(|\rho_1|^2\bar{\rho}_1\rho_0 + |\rho_0|^2\bar{\rho}_0\rho_1 + |\rho_0|^2\rho_0\bar{\rho}_1 + |\rho_1|^2\rho_1\bar{\rho}_0\right), \\
A_{32} &= 2\rho_0\rho_1 - 2h\left(\rho_0^3\bar{\rho}_1 + \bar{\rho}_0\rho_1^3\right) - 6h\left(|\rho_0|^2\rho_0\rho_1 + |\rho_1|^2\rho_1\rho_0\right), \\
A_{33} &= 2|\rho_0|^2 + 2|\rho_1|^2 - \Omega_1 - 3h\left(|\rho_0|^4 + \bar{\rho}_0^2\rho_1^2 + \rho_0^2\bar{\rho}_1^2 + |\rho_1|^4\right) - 12h|\rho_0|^2|\rho_1|^2, \\
A_{34} &= \rho_1^2 + \rho_0^2 - 2h\left(|\rho_0|^2\rho_0^2 + |\rho_1|^2\rho_1^2\right) - 6h\left(|\rho_0|^2\rho_1^2 + |\rho_1|^2\rho_0^2\right), \\
A_{41} &= -2\bar{\rho}_0\bar{\rho}_1 + 2h\left(\bar{\rho}_0^3\rho_1 + \rho_0\bar{\rho}_1^3\right) + 6h\left(|\rho_0|^2\bar{\rho}_0\bar{\rho}_1 + |\rho_1|^2\bar{\rho}_1\bar{\rho}_0\right), \\
A_{42} &= -2\left(\rho_1\bar{\rho}_0 + \bar{\rho}_1\rho_0\right) + 6h\left(|\rho_1|^2\rho_1\bar{\rho}_0 + |\rho_0|^2\rho_0\bar{\rho}_1 + |\rho_0|^2\bar{\rho}_0\rho_1 + |\rho_1|^2\bar{\rho}_1\rho_0\right), \\
A_{43} &= -\bar{\rho}_1^2 - \bar{\rho}_0^2 + 2h\left(|\rho_0|^2\bar{\rho}_0^2 + |\rho_1|^2\bar{\rho}_1^2\right) + 6h\left(|\rho_0|^2\bar{\rho}_1^2 + |\rho_1|^2\bar{\rho}_0^2\right), \quad \text{and} \\
A_{44} &= -2|\rho_0|^2 - 2|\rho_1|^2 + \Omega_1 + 3h\left(|\rho_0|^4 + \rho_0^2\bar{\rho}_1^2 + \bar{\rho}_0^2\rho_1^2 + |\rho_1|^4\right) + 12h|\rho_0|^2|\rho_1|^2.
\end{aligned}$$

Analysis of the phase diagram shows that the finite dimensional ODE system is nonlinearly stable. By linearizing about the radially symmetric ODE's, it is clear that the system is also linearly stable, hence A is a purely oscillatory matrix.

Now, we proceed to make the necessary asymptotic assumptions. From Sec. 5.4 above, we have

$$|\rho_0|^2 + |\rho_1|^2 = N_{cr} + n,$$

and for our analysis, we assume

$$0 < n \ll N_{cr} = n^{\alpha} \ll 1,$$

for some $\alpha < 1$ to be chosen later. Now, as $n > 0$, we are assuming ρ_0 and ρ_1 to be such that they are close to the equilibrium point as shown in the ODE analysis above. As a result, we have

$$|\rho_0| \approx n^{\frac{\alpha}{2}}, \ \ |\rho_1| \approx n^{\frac{1}{2}}.$$

As a result, we would like the error terms to be of size n^{β} for $\beta > \frac{1}{2}$. Also, we have the period T approximated by

$$\frac{\pi}{2\left(n^{2\alpha} - n^{\alpha+1} - n^2\right)^{\frac{1}{2}}} \approx \frac{\pi}{n^{\frac{\alpha+1}{2}}}.$$

Hence, we wish to prove the remainder terms are small on a time period $n^{-\gamma}$ where $\gamma > \alpha$.

To this end, let us first analyze the term $\tilde{R}$. Our analysis will both show the necessary bounds on $\tilde{R}$ and give us a natural time interval I on which to run our contraction argument for existence. Based on the expansion in the ansatz, we have:

$$\begin{aligned} F_{\perp}(\vec{\rho}) \ = \ & P_c\Big[|\rho_0|^2\rho_0\psi_0^3 + (\rho_0^2\bar{\rho}_1 + 2|\rho_0|^2\rho_1)\psi_0^2\psi_1 + (\rho_1^2\bar{\rho}_0 + 2\rho_0|\rho_1|^2)\psi_0\psi_1^2 + |\rho_1|^2\rho_1\psi_1^3 \\ & -h|\rho_0|^4\rho_0\psi_0^5 - h|\rho_1|^4\rho_1\psi_1^5 - h\Big(6|\rho_0|^2\rho_0|\rho_1|^2 + \rho_0^3\bar{\rho}_1^2\Big)\psi_0^3\psi_1^2 - h\Big(6|\rho_0||\rho_1|^2\rho_1 \\ & +h\bar{\rho}_0^2\rho_1^3\Big)\psi_0^2\psi_1^3 - 2h|\rho_1|^2\rho_1^2\bar{\rho}_0\psi_0\psi_1^4 - 2h|\rho_0|^2\rho_0^2\bar{\rho}_1\psi_0^4\psi_1 - 3h\Big(|\rho_0|^4\rho_1\psi_0^4\psi_1 \\ & -\rho_0|\rho_1|^4\psi_0\psi_1^4 - \rho_0^2|\rho_1|^2\bar{\rho}_1\psi_0^2\psi_1^3 - |\rho_0|^2\bar{\rho}_0\rho_1^2\psi_0^3\psi_1^2\Big)\Big]. \end{aligned}$$

The term of largest order in this expansion is $|\rho_0|^4\rho_0\psi_0^5$. The bounds on the remaining terms will follow similarly, so we look at

$$\int_0^t e^{iH_L(t-s)}P_c h(\sqrt{N_{cr}}+\epsilon_0)^5 e^{i\theta_0(s)}\psi_0^5 ds,$$

where we have expanded in radial coordinates. Hence, we must bound a term of the form

$$(\sqrt{N_{cr}})^5\int_0^t e^{iH_L(t-s)}e^{i\theta_0(s)}P_c\psi_0^5 ds = n^{\frac{5\alpha}{2}}\int_0^t e^{iH_L(t-s)}e^{i\theta_0(s)}P_c\psi_0^5 ds.$$

In particular, we would like

$$\left\| n^{\frac{5\alpha}{2}}\int_0^t e^{iH_L(t-s)}e^{i\theta_0(s)}P_c\psi_0^5 ds\right\|_{L^\infty_{t,x}} \lesssim n,$$

for $t\in I$ to be determined later. From above, we know

$$\begin{aligned}\dot\theta_0 &= \Omega_0-(\sqrt{N_{cr}}+\epsilon_0)^2-2\epsilon_1^2-\epsilon_1^2 cos(2\Delta\theta)+h(\sqrt{N_{cr}}+\epsilon_0)^4\\ &\quad +h(\sqrt{N_{cr}}+\epsilon_0)^2\epsilon_1^2(4cos(2\Delta\theta)+6)+h\epsilon_1^4(3+2cos(2\Delta\theta))\end{aligned}$$

From $\dot\theta_0$, we need the leading order constant term from the derivative. We have the leading order constant terms from the derivative is $\Omega_0-N_{cr}+hN_{cr}^2$.

We write

$$\begin{aligned}&n^{\frac{5\alpha}{2}}\int_0^t e^{iH_L(t-s)}e^{i\theta_0(s)}P_c\psi_0^5\,ds =\\ &n^{\frac{5\alpha}{2}}e^{iH_Lt}\int_0^t e^{-iH_Ls+i\Omega_0s-iN_{cr}s+ihN_{cr}^2s}e^{i\theta_0(s)-i\Omega_0s+iN_{cr}s-ihN_{cr}^2s}P_c\psi_0^5 ds =\\ &n^{\frac{5\alpha}{2}}e^{iH_Lt}\int_0^t e^{i\theta_0(s)-i\Omega_0s+iN_{cr}s-ihN_{cr}^2s}\frac{d}{ds}\frac{e^{-i(H_L-\Omega_0+N_{cr}-hN_{cr}^2)s}}{-i(H_L-\Omega_0+N_{cr}-hN_{cr}^2)}P_c\psi_0^5 ds,\end{aligned}$$

where the resolvent $(H-\Omega_0+N_{cr}-hN_{cr}^2)^{-1}$ is well-defined operator in H^1 on $P_c\psi_0^5$. We can see this explanation in Appendix C in [48], also see reference [95] for the

details. Using the estimates from that appendix and integrations by part, we have

$$\begin{aligned}
& n^{\frac{5\alpha}{2}} \left| e^{iH_L t} \int_0^t e^{-iH_L s + i\Omega_0 s - iN_{cr} s} e^{i\theta_0(s) - i\Omega_0 s + iN_{cr} s} P_c \psi_0^5 ds \right| \\
\lesssim\ & n^{\frac{5\alpha}{2}} \left| (H - \Omega_0 + N_{cr} - 8hN_{cr}^2)^{-1} P_c \psi_0^5 \right| + n^{\frac{5\alpha}{2}} \left| e^{iH_L t} (H - \Omega_0 + N_{cr} - hN_{cr}^2)^{-1} P_c \psi_0^5 \right| \\
& + n^{\frac{5\alpha}{2}} O(n) \int_0^t \left\| e^{iH_L s} (H_L - \Omega_0 + N_{cr} - hN_{cr}^2)^{-1} P_c \psi_0^5 \right\|_{L^\infty} ds \\
\lesssim\ & n^{\frac{5\alpha}{2}} \left\| (H - \Omega_0 + N_{cr})^{-1} P_c \psi_0^5 \right\|_{H^1} + hn^{\frac{5\alpha}{2}} \left\| e^{iH_L t} (H - \Omega_0 + N_{cr} - hN_{cr}^2)^{-1} P_c \psi_0^5 \right\|_{H^1} \\
& + n^{\frac{5\alpha}{2}} O(n) \int_0^t \left\| e^{iH_L s} (H - \Omega_0 + N_{cr} - hN_{cr}^2)^{-1} P_c \psi_0^5 \right\|_{H^1} ds \\
\lesssim\ & n^{\frac{5\alpha}{2}} + n^{\frac{5\alpha}{2}} + n^{\frac{5\alpha}{2}} O(n) t.
\end{aligned}$$

By selecting $\alpha > \frac{2}{5}$, we ensure that all terms resulting from integration by parts are bounded by n for all t and $t^{\frac{1}{2}} n^{\frac{5\alpha}{2}} \lesssim 1$, which implies that $t \lesssim n^{-5\alpha}$. Hence, we may allow $t \in I$, where $I \subset [0, n^{-2}]$. For reasons that will be become clear in below, let us set $I = [0, n^{-\frac{1+\alpha}{2} - \epsilon}]$, where $\epsilon > 0$ will be chosen small enough in the sequel and for simplicity, we set $\gamma = \frac{\alpha+1}{2}$. In other words, a time period allowing one to observe $n^{-\epsilon}$ oscillations of the finite dimensional system. Note, on this time scale, we have

$$|\tilde{R}| \lesssim n^{\frac{5\alpha+3}{4}} \lesssim n^{1+\delta}$$

for any $0 < \delta < \delta_0$, where δ_0 is determined by α.

Now that we have bounds of $\tilde{R}$, we can proceed with the contraction argument on η and W. To begin, let us assume

$$\|\vec{\eta}\|_{L_t^\infty} \lesssim n^{\alpha+\delta_1}, \ \ \|W\|_{L_t^\infty H_x^1} \lesssim n^{1+\delta_2},$$

for all $t \in I$ where $\delta_2 > \delta_1 > \epsilon > 0$ will be chosen later. Note, by Sobolev embeddings, we have

$$\|W\|_{L_{t,x}^\infty} \lesssim n^{1+\delta_2}.$$

Then, we must control terms of the form

$$\begin{aligned}\vec{\eta}(t) &= \int_0^t A(t-s)[f_0(\eta)+g_1(\vec{c})\langle R,\chi_1\rangle+g_2(\vec{c})\langle R^2,\chi_2\rangle+g_3(\vec{c})\langle R^3,\chi_3\rangle+\langle |R|^4R,\psi_0\rangle]ds\\ &= I+II+III+IV+V,\end{aligned}$$

where

$$\begin{aligned}f_0 &= O(\eta^4),\\ g_1 &= O(|\vec{c}|^4),\\ g_2 &= O(|\vec{c}|^3),\\ g_3 &= O(|\vec{c}|^2),\\ g_4 &= O(|\vec{c}|),\end{aligned}$$

and $\chi_1, \chi_2, \chi_3 \in \mathcal{S}$.

Using the bounds on η, $\tilde{R}$ and W, plus the fact that $\|A\| \lesssim 1$, we have

$$\begin{aligned}|I| &\lesssim n^{4\alpha+4\delta_1}t \ll n^{\alpha+\delta_1},\\ |II| &\lesssim n^{1+\delta_2}t \ll n^{\alpha+\delta_1},\\ |III| &\lesssim n^{2+2\delta_2}t \ll n^{\alpha+\delta_1},\\ |IV| &\lesssim n^{3+3\delta_2}t \ll n^{\alpha+\delta_1},\\ |V| &\lesssim n^{5+5\delta_2}t \ll n^{\alpha+\delta_1},\end{aligned}$$

for all $t \in I$ where $a \ll b$ implies $a \lesssim n^\beta b$ where $\beta > 0$ and we have implicitly assumed $\delta_2 - \epsilon > \delta_1$. Hence, the contraction argument works on the η equations.

For the W equation, we must bound terms of the form

$$\begin{aligned}&\int_0^t e^{iH_L(t-s)}P_c[(F_\perp(\vec{c})-F_\perp(\vec{\rho}))\chi_1+G_1(\vec{c})\chi_2 R+G_2(\vec{c})\chi_3R^2+G_3(\vec{c})\chi_4R^3+|R|^4R]ds\\ &= I+II+III+IV+V,\end{aligned}$$

where

$$\begin{aligned} F_\perp(\vec{c}) - F_\perp(\vec{\rho}) &= O(\eta), \\ G_1 &= O(|\vec{c}|^4), \\ G_2 &= O(|\vec{c}|^3), \\ G_3 &= O(|\vec{c}|^2), \\ G_4 &= O(|\vec{c}|), \end{aligned}$$

and $\chi_1, \chi_2, \chi_3, \chi_4 \in \mathcal{S}$, which is the Schwartz space.

Before we continue, using the theory of Strichartz estimates on linear dispersive operators, we have the following useful relation

$$\left\| \int_0^t e^{iH_L(t-s)} P_c f \right\|_{L^\infty H^1} \lesssim \left\| f(x,t) \right\|_{L_t^{\tilde{p}} W_x^{1,\tilde{q}}},$$

where $(\tilde{p},\tilde{q})$ is a dual Strichartz pair. In one dimension, it is useful to note we may take $\tilde{p} = \frac{4}{3}$ and $\tilde{q} = 1$. Then, we proceed similarly to above to see

$$\begin{aligned} \|I\|_{L^\infty H^1} &\lesssim n^{2\alpha+\delta_1} t^{\frac{3}{4}} \ll n^{1+\delta_2}, \\ |II| &\lesssim n^\alpha t^{\frac{3}{4}} \|W\|_{L^\infty H^1} \ll n^{1+\delta_2}, \\ |III| &\lesssim n^{2\alpha+2+2\delta_2} t \ll n^{1+\delta_2}, \\ |IV| &\lesssim n^{3+3\delta_2} t^{\frac{3}{4}} \|W\|_{L^\infty H^1} \ll n^{1+\delta_2}, \\ |V| &\lesssim n^{5\alpha+5+5\delta_2} \ll n^{1+\delta_2}. \end{aligned}$$

assuming α close enough to 1. Hence, the contraction argument holds on W and we have existence of a unique solution (η, W) for all $t \in I$.

This concludes our main result that for any sufficiently small amplitude periodic solution about an equilibrium state of the finite dimensional reduction, there is a solution of the PDE (NLS/GP), whose projection into the finite dimensional phase space, shadows this finite dimension orbit on very long time scales.

3.6 Numerical computations: stationary solutions

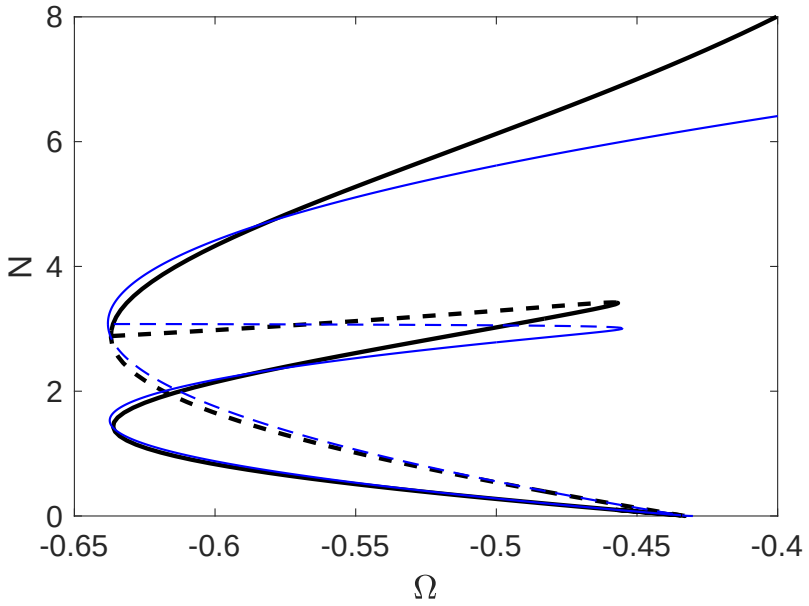

Figure 3.1. The stationary solution branches for $h = 1$. The analytical predictions are denoted with the blue (thin) line while the numerically determined solutions are denoted with the black (thick) line that is solid when it is stable and dashed otherwise.

We turn to the examination of our analysis against numerical computations of the NLS/GP equation. We focus here on stationary solutions as the dynamics of the case considered herein has been simulated elsewhere [69, 80] (see also, e.g., [86, 86] and references therein).

In our calculations, the stationary solutions are obtained by using a fixed-point Newton-Raphson iteration for a finite difference discretization of the relevant boundary value problem (3.5), with a choice of the grid spacing of $\Delta x = 0.1$ and employing a pseudo-arclength continuation of the solutions with respect to the bifurcation parameter Ω.

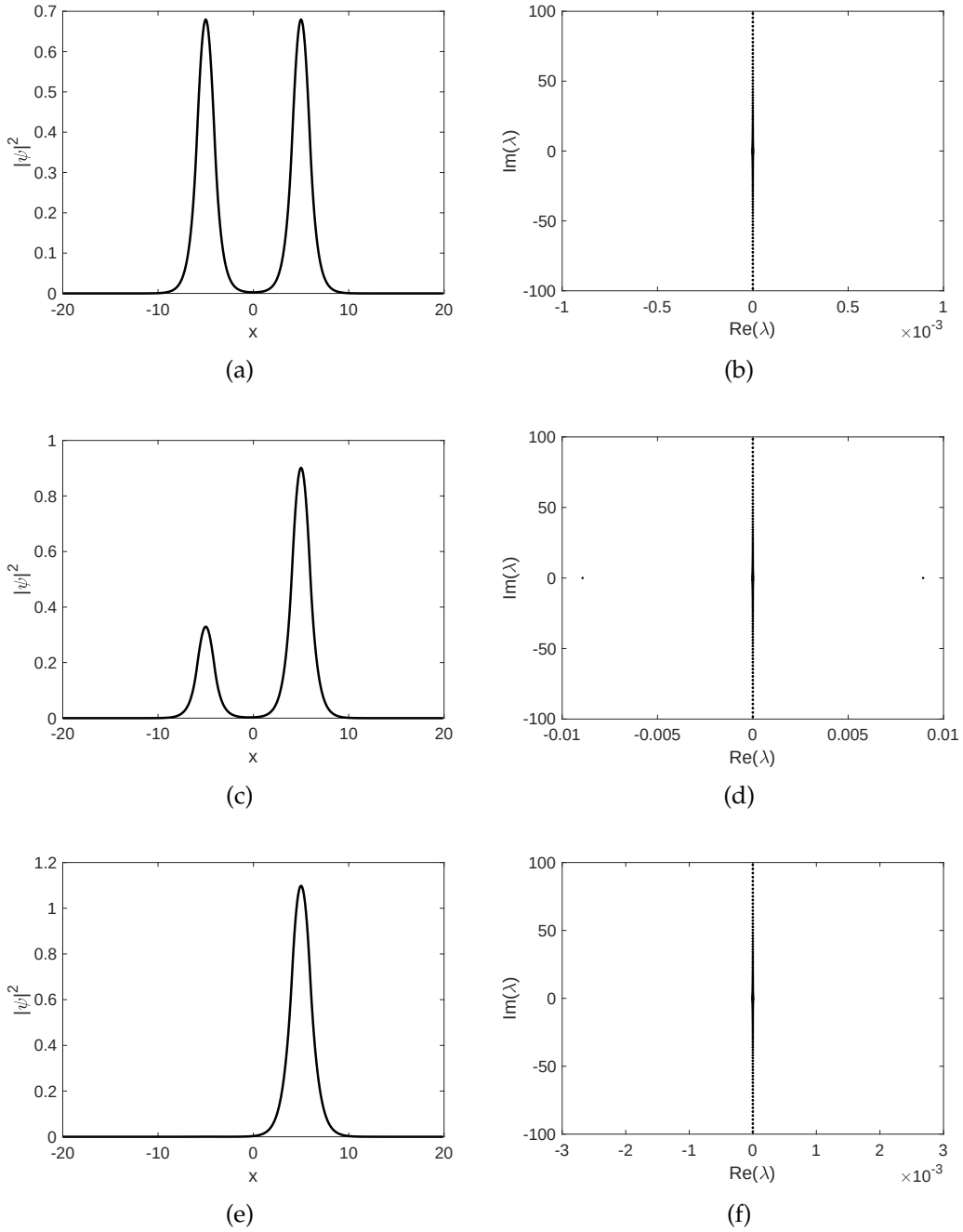

Figure 3.2. Corresponding solutions of the bifurcation diagram in Fig. 3.1 for the same power at $N = 3$ and their spectrum in the complex plane.

The linear stability is analyzed by considering the standard linearization around the stationary solutions $\hat{\psi}$ in the form

$$\psi(x,t) = \left(\hat{\psi} + \epsilon(a(x)e^{\lambda t} + b^*(x)e^{\lambda^* t})\right)e^{-i\Omega t}.$$

This yields the eigenvalue problem

$$\begin{pmatrix} L_1 & L_2 \\ -L_2^* & -L_1^* \end{pmatrix}\begin{pmatrix} a \\ b \end{pmatrix} = i\lambda\begin{pmatrix} a \\ b \end{pmatrix}, \tag{3.52}$$

where the operators are defined as

$$L_1\phi = -\partial_{xx} + V - \Omega + 2g\hat{\psi}^2 + 3h\hat{\psi}^4,\ L_2\phi = g\hat{\psi}^2 + 2h\hat{\psi}^4.$$

Because for our Hamiltonian system when λ is an eigenvalue, so are $-\lambda$, $\lambda^\star$ and $-\lambda^\star$, instability of $\hat{\psi}$ is guaranteed by the existence of any eigenvalues λ of the linearized operator with $\Re(\lambda) \neq 0$.

We present in Fig. 3.1 the bifurcation diagram of our ground state that is symmetric as a function of Ω. It bifurcates from Ω_0 as a marginally stable solution. As Ω decreases and the power increases, there is a critical value where the state becomes unstable. When Ω decreases further, there is a turning point where our symmetric state regains its stability. We plot the corresponding solution for $N = 3$ (i.e., past the turning point) in Fig. 3.2(a) and its spectrum in the complex plane in Fig. 3.2(b), obtained from solving the eigenvalue problem (3.52), showing its stability.

The point of stability change near Ω_0 is the symmetry breaking bifurcation. A stable asymmetric state emanates from the point. The corresponding branch is also depicted in Fig. 3.1. As we follow the branch, there are two turning points. In Fig. 3.2(c-f) we plot two asymmetric states for the same power $N = 3$ and their

corresponding spectrum. The figure shows that for high enough power, the system prefers states where almost all of it is concetrated in one of the wells only.

In Fig. 3.1, we also plot the equilibria of the finite dimensional reduction. It is clear that in accordance with the theory, the coupled mode approximation captures the full system very well near the bifurcation point Ω_0. For relatively large N, the approximation deviates rather rapidly. For this reason, our shadowing result is only applicable for solutions along the lower symmetric and asymmetric branches. To obtain a better comparison between numerical results and the approximations, especially for the asymetric states, one needs to 'force' the system to admit them at low powers, which can be achieved by considering a higher value of h.

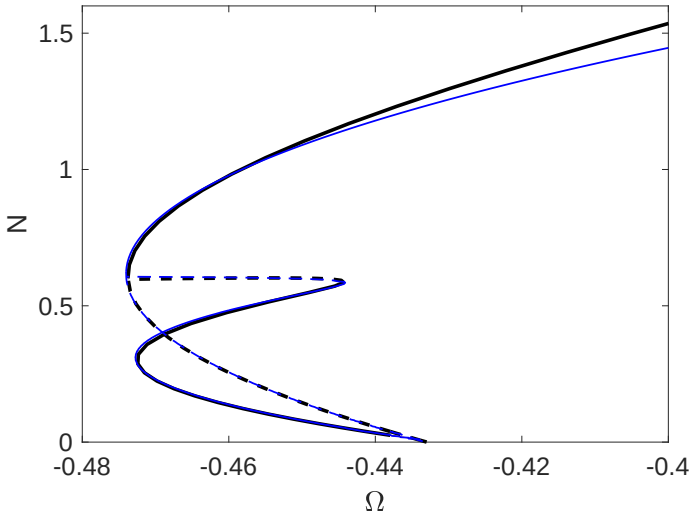

Figure 3.3. The same as Fig. 3.1, but for for $h = 5$.

We compute the bifurcation diagram of the symmetric and asymmetric states for $h = 5$ and plot the results in Fig. 3.3. As we expected, in this case our finite dimensional reduction provides a better approximation. In addition to the lower branches, in this case we can also show that the shadowing result applies to the asymmetric states in their entire existence region. The challange in here is that the solutions may not be representable conveniently in closed expressions.

Chapter 4

Justification of the discrete nonlinear Schrödinger equation from a parametrically driven damped nonlinear Klein-Gordon equation and numerical comparisons

4.1 Introduction

We consider the following parametrically driven discrete Klein-Gordon (dKG) equation with damping

$$\ddot{u}_j = -u_j - \xi u_j^3 + \varepsilon^2 \Delta u_j - \alpha \dot{u}_j + H\cos(2\Omega t)\, u_j, \tag{4.1}$$

where $u_j \equiv u_j(t)$ is a real-valued wave function at site j, the overdot denotes the time derivative and ε^2 represents the coupling constant between two adjacent sites, with $\Delta u_j = u_{j+1} - 2u_j + u_{j-1}$ being the one dimensional discrete Laplacian.

The positive parameters α and H denote the damping coefficient and the strength of the parametric drive, respectively. The real constant ξ is the nonlinearity coefficient and Ω is the driving frequency. The governing equation (4.1) is relevant to the experimental study of localised structures in coupled pendula [25, 27] and micromechanical arrays [18].

To analyse the equation, one usually uses a multiple scale expansion and the rotating wave approximation under the assumption of small wave amplitudes, that lead to a damped, parametrically driven discrete nonlinear Schrödinger (dNLS) equation [28, 63, 72, 79]. Using the scaling $\alpha = \varepsilon^2\hat{\alpha}$, $H = 2\varepsilon^2 h$, $\Omega = 1 + \varepsilon^2\Lambda/2$, and a slow time variable $\tau = \varepsilon^2 t/2$, we consider a $(2:1)$ parametric resonance and define a slowly varying approximation to the solutions of the dKG lattice equation (4.1)

$$u_j(t) \approx \phi_j(t) = \varepsilon\, A_j(\tau)e^{i\Omega t} + \frac{\varepsilon^3}{8}\Big[\xi A_j(\tau)^3 - hA_j(\tau)\Big]e^{3i\Omega t} + \text{c.c.}, \tag{4.2}$$

that will yield the dNLS equation

$$i\dot{A}_j = \Delta A_j - i\hat{\alpha}A_j + \Lambda A_j - 3\xi|A_j|^2 A_j + h\bar{A}_j\,. \tag{4.3}$$

Here, the dot denotes derivative with respect to the slow time τ, which implies that the approximation (4.2)-(4.3) is expected to be valid until $t \sim O(2/\varepsilon^2)$. The abbreviation c.c. means the complex conjugate of the preceding terms. It should be clear by now that the coupling constant (i.e., the prefactor of the discrete Laplacian term) is scaled to ε^2 only for the sake of convenience, so that $u_j = O(\varepsilon)$. Replacing $\varepsilon \to \sqrt{\varepsilon}$ will yield the standard scaling used, e.g., in [75]. Our scaling may also be interpreted that instead of using the coupling constant as a measure of the smallness, we use the solution amplitude.

The presence of parametric drive and damping in the dNLS equation was possibly first studied in [46], where the existence of localised solutions was

discussed using a nonlinear map approach. It was shown that numerous types of localised states emerge from the system depending on the strength of the parametric driving. The parametrically driven dNLS equation (4.3) was studied in [87, 88], where it was shown that the parametric drive can change the stability of fundamental discrete solitons, i.e., it can destroy onsite solitons as well as restore the stability of intersite discrete solitons, both for bright and dark cases. In [89], breathers of (4.3), i.e., spatially localised solutions with periodically time varying $|A_j(\tau)|$ emanating from Hopf bifurcations, were studied systematically.

Despite the wide interests in both equations (4.1) and (4.3), the reduction from the former to the latter has not been rigorously justified. Without damping and parametric drive, the analysis was provided rather recently by Pelinovsky, Penati and Paleari [75]. However, as the presence of damping and drive will certainly require modifications in the justification of the reduction, here we address the problem, which will be the primary aim of the chapter. Following [75], we use an energy estimate method. The method has been used as well in various systems of differential equations, see, e.g., [8, 13, 31, 39, 83].

This chapter is organized as follows. Mathematical formulations to obtain the uniqueness and global existence of solutions to the dNLS equation (4.3) are given in Section 4.2. In Section 4.3, we discuss an error bound estimation of the rotating wave approximation, which leads to the main result of the paper, i.e., Theorem 4.3.1. Finally, in Section 4.4 we illustrate the main results by considering the evolution of errors made by the rotating wave approximation for two different initial conditions, with one of them corresponding to discrete solitons of the nonlinear Schrödinger equation (4.3).

4.2 Analytical formulation and preliminary results

Substituting the slowly varying approximation ansatz (4.2) into the original dKG equation (4.1) and taking into account the dNLS equation (4.3), we obtain the residual terms in the form of

$$
\begin{aligned}
R_j(t) := \varepsilon^5 \Bigg[& \frac{e^{i\Omega t}}{8}\Big(-3h\xi A_j\bar{A}_j^2 + 3\xi^2 A_j^3\bar{A}_j^2 + h^2 A_j - h\xi A_j^3 + 4i\alpha\Lambda A_j + 4\alpha\dot{A}_j \\
& -2\Lambda^2 A_j + 4i\Lambda\dot{A}_j + 2\ddot{A}_j\Big) \\
& + \frac{e^{3i\Omega t}}{8}\Big(-6h\xi A_j^2\bar{A}_j + 6\xi^2 A_j^4\bar{A}_j - 3i\alpha h A_j + 9h\Lambda A_j - 3ih\dot{A}_j \\
& -2hA_j + hA_{j-1} + \frac{1}{8}hA_{j+1} + 3i\alpha\xi A_j^3 - 9\xi\Lambda A_j^3 + 9i\xi A_j^2\dot{A}_j \\
& +2\xi A_j^3 - \xi A_{j-1}^3 - \xi A_{j+1}^3\Big) + \frac{e^{5i\Omega t}}{8}\Big(h^2 A_j - 4h\xi A_j^3 + 3\xi^2 A_j^5\Big)\Bigg] \\
& + \varepsilon^7\Bigg[\frac{3e^{i\Omega t}}{32}\Big(h^2\xi A_j^2\bar{A}_j - h\xi^2 A_j^4\bar{A}_j - h\xi^2 A_j^2\bar{A}_j^3 + \xi^3 A_j^4\bar{A}_j^3\Big) \\
& + \frac{e^{3i\Omega t}}{32}\Big(-6i\alpha h\Lambda A_j - 2\alpha h\dot{A}_j - h\ddot{A}_j + 9h\Lambda^2 A_j - 6ih\Lambda\dot{A}_j + 6i\alpha\xi\Lambda A_j^3 \\
& +6\alpha\xi A_j^2\dot{A}_j - 9\xi\Lambda^2 A_j^3 + 18i\xi\Lambda A_j^2\dot{A}_j + 6\xi A_j\dot{A}_j^2 + 3\xi A_j^2\ddot{A}_j\Big) \\
& + \frac{e^{5i\Omega t}}{64}\Big(3h^2\xi A_j^2\bar{A}_j - 6h\xi^2 A_j^4\bar{A}_j + 3\xi^3 A_j^6\bar{A}_j\Big) \\
& + \frac{e^{7i\Omega t}}{64}\Big(3h^2\xi A_j^3 - 6h\xi^2 A_j^5 + 3\xi^3 A_j^7\Big)\Bigg] \\
& + \varepsilon^9\Bigg[\frac{e^{3i\Omega t}}{512}\Big(-3h^3\xi A_j^2\bar{A}_j + 6h^2\xi^2 A_j^4\bar{A}_j + 6h^2\xi^2 A_j^2\bar{A}_j^3 - 3h\xi^3 A_j^6\bar{A}_j \\
& -6h\xi^3 A_j^4\bar{A}_j^3 + 3\xi^4 A_j^6\bar{A}_j^3\Big) + \frac{e^{9i\Omega t}}{512}\Big(-h^3\xi A_j^3 + 3h^2\xi^2 A_j^5 \\
& -3h\xi^3 A_j^7 + \xi^4 A_j^9\Big)\Bigg] + \text{c.c.}
\end{aligned}
\tag{4.4}
$$

Note that the dNLS equation (4.3) is obtained from removing the resonant terms at $O(\varepsilon^3)$. The usual rotating frame ansatz, where one uses only the first term of (4.2) and its complex conjugate, i.e., $u_j(t) \approx \varepsilon\, A_j(\tau)e^{i\Omega t} + \text{c.c.}$, will also yield (4.3),

but it leaves a larger residue:

$$R_j(t) \;:=\; \varepsilon^3(\xi A_j^3 - hA_j)e^{3i\Omega t} + \varepsilon^5\Big(\tfrac{1}{2}i\hat{\alpha}\Lambda A_j - \tfrac{1}{4}\Lambda^2 A_j + \tfrac{1}{2}\hat{\alpha}\dot{A}_j + \tfrac{1}{2}i\Lambda\dot{A}_j + \tfrac{1}{2}\ddot{A}_j\Big)e^{i\Omega t} + c.c.$$

Over a long time, this can yield an error that is of the same order as the approximation itself, which will be problematic for the expansion. Thus, R_j needs to be smaller. It might be made small only if ξ and h were both to be very small. However, this cannot be the case since they have been derived from scaling the original "physical" parameters properly with respect to ε, i.e., their smallness have already been exploited. The only way to reduce the residue is therefore by modifying the rotating ansatz, which following [30] (see Chapter 5) yields (4.2).

In the followings, we denote by A the sequence $(A_j)_{j\in\mathbb{Z}}$ in $\ell^2(\mathbb{Z})$, which is a Banach space equipped with norm,

$$\|A\|_{\ell^2(\mathbb{Z})} = \left(\sum_{j\in\mathbb{Z}} |A_j|^2\right)^{1/2}. \tag{4.5}$$

First, we prove the preliminary estimates on the global solutions of the dNLS equation (4.3) in $\ell^2(\mathbb{Z})$-space, the leading order approximation (4.2), and the residual term (4.4).

Lemma 4.2.1. *For every $A(0) = \varphi \in \ell^2(\mathbb{Z})$, the dNLS equation* (4.3) *admits a unique global solution $A(\tau)$ on $[0,\infty)$ which belongs to $C^k\Big([0,+\infty), \ell^2(\mathbb{Z})\Big)$. Furthermore, the unique solution $A(\tau)$ satisfies the estimate*

$$\|A(\tau)\|_{\ell^2(\mathbb{Z})} \le \|\varphi\|_{\ell^2(\mathbb{Z})}\, e^{-(\hat{\alpha}-2|h|)\tau}. \tag{4.6}$$

Proof. We split the proof into four parts.

1. Local existence. Let us rewrite Eq. (4.3) in its equivalent integral form

$$A_j(\tau) = \varphi_j - i\int_0^\tau \Big(\Delta A_j - i\alpha A_j + \Lambda A_j - 3\xi|A_j|^2 A_j + h\bar{A}_j\Big)ds. \tag{4.7}$$

Define a Banach space,

$$\mathcal{B} = \{A \in C\Big([0,\tilde{\tau}], \ell^2(\mathbb{Z})\Big) | \|A\|_{\ell^2(\mathbb{Z})} \leq \delta\}\,, \tag{4.8}$$

equipped with norm,

$$\|A\|_{\mathcal{B}} = \sup_{\tau\in[0,\tilde{\tau}]} \|A(\tau)\|_{\ell^2(\mathbb{Z})}. \tag{4.9}$$

For $A \in \ell^2(\mathbb{Z})$, we define a nonlinear operator

$$K_j[A(\tau)] = \varphi_j - i\int_0^\tau \Big(\Delta A_j - i\alpha A_j + \Lambda A_j - 3\xi|A_j|^2 A_j + h\bar{A}_j\Big)ds. \tag{4.10}$$

We want to prove that the operator K is a contraction mapping on $\mathcal{B}$. Because the discrete Laplacian Δ is a bounded operator on $\ell^2(\mathbb{Z})$, we have

$$\|\Delta A\|_{\ell^2(\mathbb{Z})} \leq C_\Delta \|A\|_{\ell^2(\mathbb{Z})}. \tag{4.11}$$

To be precise, $C_\Delta = 4$ because the operator is a self-adjoint and its continuous spectrum lies within the interval $[-4, 0]$.

Since $\ell^2(\mathbb{Z})$ is an algebra, there is a constant $C > 0$ such that for every $A, B \in \ell^2(\mathbb{Z})$, we have

$$\|AB\|_{\ell^2(\mathbb{Z})} \leq C\|A\|_{\ell^2(\mathbb{Z})}\|B\|_{\ell^2(\mathbb{Z})}. \tag{4.12}$$

From Eq. (4.10) and using the estimate (4.12), we obtain the following bound

$$\|K(A)\|_{\mathcal{B}} \leq \delta_0 + \tilde{\tau}(C\delta + \hat{\alpha}\delta + \Lambda\delta + 3|\xi|\delta^3 + |h|\delta). \tag{4.13}$$

We can pick $\delta_0 < \frac{\delta}{2}$ and $\tilde{\tau} \leq \frac{\delta}{2(C\delta+\hat{\alpha}\delta+\Lambda\delta+3|\xi|\delta^3+|h|\delta)}$ to conclude that $K : \mathcal{B} \to \mathcal{B}$.

Let $A, B \in \mathcal{B}$. Then we have

$$\begin{aligned} K_j[A(\tau)] - K_j[B(\tau)] &= -i\int_0^\tau \Big[\Delta(A_j - B_j) - i\hat{\alpha}(A_j - B_j) + \Lambda(A_j - B_j) \\ &\quad -3\xi(|A_j|^2 A_j - |B_j|^2 B_j) + h(\bar{A}_j - \bar{B}_j)\Big]\, ds\,. \end{aligned} \tag{4.14}$$

Noting that

$$\begin{aligned} |A_j|^2 A_j - |B_j|^2 B_j &= |A_j|^2 A_j - |A_j|^2 B_j + |A_j|^2 B_j - |B_j|^2 B_j \\ &= |A_j|^2 (A_j - B_j) + B_j(|A_j|^2 - |B_j|^2) \\ &= |A_j|^2 (A_j - B_j) + B_j(A_j\bar{A}_j - A_j\bar{B}_j + A_j\bar{B}_j - B_j\bar{B}_j) \\ &= |A_j|^2 (A_j - B_j) + B_j[A_j(\bar{A}_j - \bar{B}_j) + (A_j - B_j)\bar{B}_j], \end{aligned} \tag{4.15}$$

we obtain that

$$\|K(A) - K(B)\|_{\mathcal{B}} \leq \tilde{\tau}\left(C_\Delta + \hat{\alpha} + \Lambda + 3|\xi|C\delta^2 + |h|\right)\|A - B\|_{\mathcal{B}}. \tag{4.16}$$

By taking

$$\tilde{\tau} < \min\left(\frac{1}{C_\Delta + \hat{\alpha} + \Lambda + 3|\xi|C\delta^2 + |h|}, \frac{\delta}{2(C\delta + \hat{\alpha}\delta + \Lambda\delta + 3|\xi|\delta^3 + |h|\delta)}\right), \tag{4.17}$$

then K is a contraction mapping on $\mathcal{B}$. Therefore, by Banach fixed point theorem, there exists a unique fixed point of operator K, which is a unique solution of (4.7).

2. Smoothness. From Eq. (4.3), we obtain that

$$\sup_{\tau\in[0,\tilde{\tau}]} \|\dot{A}\|_{\ell^2(\mathbb{Z})} \leq \left(C_\Delta + \hat{\alpha} + \Lambda + |h| + 3|\xi|\delta^2\right)\delta\,, \tag{4.18}$$

which shows that the solution belongs to $C^1\left([0,\tilde{\tau}), \ell^2(\mathbb{Z})\right)$.

Furthermore, by writing $\eta = (A, \bar{A})$, we have

$$i\frac{d\eta}{d\tau} = L\eta + N(\eta) + F(\eta)\,, \tag{4.19}$$

where

$$L\eta = \begin{bmatrix} \Delta - i\hat{\alpha} + \Lambda \\ -\Delta - i\hat{\alpha} - \Lambda \end{bmatrix}\eta\,, \qquad N(\eta) = \frac{3\xi}{2}|\eta|^2\eta\,, \qquad F(\eta) = \begin{bmatrix} 0, h \\ h, 0 \end{bmatrix}\eta\,. \tag{4.20}$$

Differentiating (4.19), we obtain

$$i\frac{d^2\eta}{d\tau^2} = L\frac{d\eta}{d\tau} + DN(\eta)\cdot\frac{d\eta}{d\tau} + DF(\eta)\cdot\frac{d\eta}{d\tau}\,. \tag{4.21}$$

Since $N(\eta)$ and $F(\eta)$ are smooth on $\ell^2(\mathbb{Z})$ and $\frac{d\eta}{d\tau} \in C\Big([0,\tilde{\tau}), \ell^2(\mathbb{Z})\Big)$, then we have

$$\frac{d^2\eta}{d\tau^2} \in C\Big([0,\tilde{\tau}), \ell^2(\mathbb{Z})\Big)\,, \tag{4.22}$$

which implies that $A \in C^2\Big([0,\tilde{\tau}), \ell^2(\mathbb{Z})\Big)$. Using a similar procedure for higher derivatives, we conclude that

$$A \in C^k\Big([0,\tilde{\tau}), \ell^2(\mathbb{Z})\Big)\,. \tag{4.23}$$

3. Maximal solutions. We can construct a maximal solution by repeating the steps above with the initial condition $A(\tilde{\tau} - \tau_0)$ for some $0 < \tau_0 < \tilde{\tau}$ and by using the uniqueness result to glue the solutions.

4. Global existence. To prove the global existence, first we multiply the dNLS equation (4.3) with $\bar{A}_j$ and use its complex conjugate to obtain

$$i\frac{d}{d\tau}\left(A_j\bar{A}_j\right)-\left(\bar{A}_j\Delta A_j-A_j\Delta\bar{A}\right)=-2i\hat{\alpha}|A_j|^2+h(\bar{A}_j^2-A_j^2)\,. \tag{4.24}$$

Note that

$$\sum_{j\in\mathbb{Z}}\left(A_j\Delta\bar{A}_j-\bar{A}_j\Delta A_j\right)=0. \tag{4.25}$$

Summing up (4.24) over j, we then get

$$\frac{d}{d\tau}\|A\|^2_{\ell^2(\mathbb{Z})}=-2\hat{\alpha}\|A\|^2_{\ell^2(\mathbb{Z})}+4\,h\sum_{j\in\mathbb{Z}}\mathrm{Im}(\bar{A}_j)\mathrm{Re}(\bar{A}_j). \tag{4.26}$$

For the last term in the above equation, we have the estimate

$$h\sum_{j\in\mathbb{Z}}\mathrm{Im}(\bar{A}_j)\mathrm{Re}(\bar{A}_j)\le|h|\sum_{j\in\mathbb{Z}}\left|\mathrm{Im}(\bar{A}_j)\right|\left|\mathrm{Re}(\bar{A}_j)\right|\le|h|\|A\|^2_{\ell^2_k(\mathbb{Z})}\,, \tag{4.27}$$

which leads to

$$\frac{d}{d\tau}\|A\|^2_{\ell^2(\mathbb{Z})}+2(\hat{\alpha}-2h)\|A\|^2_{\ell^2(\mathbb{Z})}\le 0\,. \tag{4.28}$$

Integrating the inequality, we get

$$\|A(\tau)\|_{\ell^2(\mathbb{Z})}\le\|\varphi\|_{\ell^2(\mathbb{Z})}\,e^{-(\hat{\alpha}-2|h|)\tau}, \tag{4.29}$$

which shows that $A(\tau)$ cannot blow up in finite time. Thus, the dNLS equation (4.3) admits global solutions. ■

It is worth mentioning that due to the damping term, the dNLS equation (4.3) does not possess a constant of motion. However, we can define a Hamiltonian

(i.e., an energy function) associated with equation (4.3) as

$$\mathrm{H}_{\mathrm{dNLS}}[A](\tau) = \sum_{j\in\mathbb{Z}} \left(|\nabla A_j|^2 - \Lambda |A_j|^2 + \frac{3\xi}{2}|A_j|^4 - h\mathrm{Re}(A_j^2) \right), \tag{4.30}$$

with $\nabla A_j = A_{j+1} - A_j$. The Hamiltonian function satisfies the differential equation,

$$\frac{d}{d\tau}\mathrm{H}_{\mathrm{dNLS}}[A](\tau) + 2\alpha \mathrm{H}_{\mathrm{dNLS}}[A](\tau) = -3\alpha\xi \sum_{j\in\mathbb{Z}} |A_j(\tau)|^4 . \tag{4.31}$$

When $\alpha = 0$ (i.e., there is no damping present), $\mathrm{H}_{\mathrm{dNLS}}$ is conserved.

Now we provide estimates for the leading order approximation (4.2) and the residual terms (4.4) in the following lemmas.

Lemma 4.2.2. *For every $A(0) = \varphi \in \ell^2(\mathbb{Z})$, there exists a ε-independent positive constant C_ϕ that depends on $\|\varphi\|_{\ell^2(\mathbb{Z})}, h, \hat{\alpha}$ and τ_0, such that the leading-order approximation (4.2) satisfies*

$$\|\phi(t)\|_{\ell^2(\mathbb{Z})} + \|\dot{\phi}(t)\|_{\ell^2(\mathbb{Z})} \leq \varepsilon\, C_\phi, \tag{4.32}$$

for all $t \in [0, 2\tau_0/\varepsilon^2]$ and $\varepsilon \in (0,1)$.

Proof. From the global existence in Lemma 4.2.1 and using the Banach algebra property of $\ell^2(\mathbb{Z})$, we obtain

$$\begin{aligned}
\left\|\phi(t)\right\|_{\ell^2(\mathbb{Z})} &= \Big\| \varepsilon \left(A_j e^{i\Omega t} + \bar{A}_j e^{-i\Omega t} \right) + \tfrac{\varepsilon^3}{8} \Big[\left(\xi A_j^3 - h A_j \right) e^{3i\Omega t} \\
&\qquad + \left(\xi \bar{A}_j^3 - h \bar{A}_j \right) e^{-3i\Omega t} \Big] \Big\|_{\ell^2(\mathbb{Z})} \\
&\leq \left\| \varepsilon \left(A_j e^{i\Omega t} + \bar{A}_j e^{-i\Omega t} \right) \right\|_{\ell^2(\mathbb{Z})} + \left\| \tfrac{\varepsilon^3}{8} \left(\xi A_j^3 e^{3i\Omega t} - h A_j e^{3i\Omega t} \right) \right\|_{\ell^2(\mathbb{Z})} \\
&\qquad + \left\| \tfrac{\varepsilon^3}{8} \left(\xi \bar{A}_j^3 e^{-3i\Omega t} - h \bar{A}_j e^{-3i\Omega t} \right) \right\|_{\ell^2(\mathbb{Z})} \\
&\leq \varepsilon \left(2\|A\|_{\ell^2(\mathbb{Z})} + \tfrac{1}{4}|\xi|\varepsilon^2 \left\|A^3\right\|_{\ell^2(\mathbb{Z})} + \tfrac{1}{4}|h|\varepsilon^2 \|A\|_{\ell^2(\mathbb{Z})} \right) \\
&\leq \varepsilon\, C_{\phi_1}
\end{aligned} \tag{4.33}$$

and

$$\begin{aligned}\left\|\dot{\phi}(t)\right\|_{\ell^2(\mathbb{Z})} = \Big\| & \frac{3}{16}ih\Lambda\varepsilon^5 e^{-3i\Omega t}\bar{A}_j - \frac{1}{16}h\varepsilon^5 e^{-3i\Omega t}\dot{\bar{A}}_j + \frac{3}{8}ih\varepsilon^3 e^{-3i\Omega t}\bar{A}_j \\ & -\frac{3}{16}i\xi\Lambda\varepsilon^5 e^{-3i\Omega t}\bar{A}_j^3 + \frac{3}{16}\xi\varepsilon^5 e^{-3i\Omega t}\bar{A}_j^2\dot{\bar{A}}_j - \frac{3}{8}i\xi\varepsilon^3 e^{-3i\Omega t}\bar{A}_j^3 \\ & -\frac{1}{2}i\Lambda\varepsilon^3 e^{-i\Omega t}\bar{A}_j + \frac{1}{2}\varepsilon^3 e^{-i\Omega t}\dot{\bar{A}}_j - i\varepsilon e^{-i\Omega t}\bar{A}_j \\ & -\frac{3}{16}ih\Lambda\varepsilon^5 e^{3i\Omega t}A_j - \frac{1}{16}h\varepsilon^5 e^{3i\Omega t}\dot{A}_j - \frac{3}{8}ih\varepsilon^3 e^{3i\Omega t}A_j \\ & +\frac{3}{16}i\xi\Lambda\varepsilon^5 e^{3i\Omega t}A_j^3 + \frac{3}{16}\xi\varepsilon^5 e^{3i\Omega t}A_j^2\dot{A}_j + \frac{3}{8}i\xi\varepsilon^3 e^{3i\Omega t}A_j^3 \\ & +\frac{1}{2}i\Lambda\varepsilon^3 e^{i\Omega t}A_j + \frac{1}{2}\varepsilon^3 e^{i\Omega t}\dot{A}_j + i\varepsilon e^{i\Omega t}A_j\Big\|_{\ell^2(\mathbb{Z})}.\end{aligned} \tag{4.34}$$

Since $A \in C^1\left([0,+\infty), \ell^2(\mathbb{Z})\right)$, then we have

$$\left\|\dot{\phi}(t)\right\|_{\ell^2(\mathbb{Z})} \leq \varepsilon\, C_{\phi_2}\,. \tag{4.35}$$

From Eqs. (4.33) and (4.35), we obtain the inequality (4.32), which concludes the proof. ∎

Lemma 4.2.3. *For every $A(0) = \varphi \in \ell^2(\mathbb{Z})$, there exists a positive $\varepsilon-$independent constant $\tilde{C}_R$ that depends on $\|A_0\|_{\ell^2}, h, \hat{\alpha}$ and τ_0, such that for every $\varepsilon \in (0,1)$ and every $t \in [0, 2\tau_0/\varepsilon^2]$, the residual terms in (4.4) is estimated by*

$$\|R(t)\|_{\ell^2(\mathbb{Z})} \leq \tilde{C}_R\varepsilon^5. \tag{4.36}$$

Proof. To prove this lemma, we can use the result from Lemma (4.2.1) as well as the property of Banach algebra in $\ell^2(\mathbb{Z})$, such that from the global existence and smoothness of the solution $A(\tau)$ of the discrete nonlinear Schrödinger equation (4.3) in Lemma (4.2.1), we obtain the result (4.36). ∎

4.3 Main Results

We are now ready to formulate the main result of the chapter that is stated in the following theorem:

Theorem 4.3.1. *Let $u = (u_j)_{j\in\mathbb{Z}}$ be a solution of the dNLS equation* (4.1) *and let $\phi = (\phi_j)_{j\in\mathbb{Z}}$ be the leading approximation terms given by* (4.2)*. For every $\tau_0 > 0$, there are a small $\varepsilon_0 > 0$ and positive constants C_0 and C such that for every $\varepsilon \in (0, \varepsilon_0)$ with*

$$\|u(0) - \phi(0)\|_{\ell^2(\mathbb{Z})} + \|\dot{u}(0) - \dot{\phi}(0)\|_{\ell^2(\mathbb{Z})} \leq C_0\varepsilon^3\,, \tag{4.37}$$

the inequality

$$\|u(t) - \phi(t)\|_{\ell^2(\mathbb{Z})} + \|\dot{u}(t) - \dot{\phi}(t)\|_{\ell^2(\mathbb{Z})} \leq C\varepsilon^3\,, \tag{4.38}$$

holds for $t \in [0, 2\tau_0\varepsilon^{-2}]$.

Proof. Write

$$u_j(t) = \phi_j(t) + y_j(t), \tag{4.39}$$

where $\phi_j(t)$ is the leading-order approximation (4.2) and $y_j(t)$ is the error term. The error will give us a description of how good $\phi_j(t)$ is as an approximation to solutions of the dKG equation.

Plugging the decomposition (4.39) into equation (4.1), we obtain the evolution problem for the error term as

$$\ddot{y}_j + y_j + \xi\left(y_j^3 + 3\phi_j^2 y_j + 3\phi_j y_j^2\right) - \varepsilon^2\Delta y_j + \epsilon^2\hat{\alpha}\dot{y}_j - 2\varepsilon^2 h\cos(2\Omega t)\, y_j + R_j(t) = 0\,. \tag{4.40}$$

Associated with equation (4.40), we can define the energy of the error term as

$$E(t) := \frac{1}{2}\sum_{j\in\mathbb{Z}}\left[\dot{y}_j^2 + y_j^2 - 2\varepsilon\left(y_j y_{j+1} - y_j^2\right)\right]. \tag{4.41}$$

Note that from the Cauchy-Schwartz inequality, we have

$$\sum_{j\in\mathbb{Z}} y_j y_{j+1} \le \left(\sum_{j\in\mathbb{Z}} y_j^2\right)^{1/2}\left(\sum_{j\in\mathbb{Z}} y_{j+1}^2\right)^{1/2} = \|y\|^2_{\ell^2(\mathbb{Z})}, \tag{4.42}$$

and

$$-2\varepsilon\sum_{j\in\mathbb{Z}} y_j y_{j+1} + 2\varepsilon\sum_{j\in\mathbb{Z}} y_j^2 \ge -2\varepsilon\|y\|^2_{\ell^2(\mathbb{Z})} + 2\varepsilon\|y\|^2_{\ell^2(\mathbb{Z})} = 0\,. \tag{4.43}$$

Thus the energy is always positive for all t on which the solution $y(t)$ is defined. We also have the inequality

$$\|\dot{y}(t)\|^2_{\ell^2(\mathbb{Z})} + \|y(t)\|^2_{\ell^2(\mathbb{Z})} \le 2E(t). \tag{4.44}$$

From the energy (4.41) and the error term (4.40), we obtain that

$$\begin{aligned}
\frac{dE}{dt} &= \frac{1}{2}\sum_{j\in\mathbb{Z}}\left[2\ddot{y}_j\dot{y}_j + 2\dot{y}_j y_j - 2\varepsilon^2\left(\dot{y}_j y_{j+1} + y_j\dot{y}_{j+1} - 2y_j\dot{y}_j\right)\right] \\
&= \sum_{j\in\mathbb{Z}}\left[\ddot{y}_j + y_j - \varepsilon^2(y_{j+1} + y_j - 2y_j)\right]\dot{y}_j \\
&= -\sum_{j\in\mathbb{Z}}\left[R_j(t) + \xi\left(y_j^3 + 3\phi_j^2 y_j + 3\phi_j y_j^2\right) + \epsilon^2\hat{\alpha}\dot{y}_j - 2\varepsilon^2 h\cos(2\Omega t)\, y_j\right]\dot{y}_j
\end{aligned} \tag{4.45}$$

Setting $E = Q^2$ and using the Cauchy-Schwarz inequality, we have

$$\begin{aligned}
\left|\frac{dQ}{dt}\right| \le\ & \frac{1}{\sqrt{2}}\|R(t)\|_{\ell^2(\mathbb{Z})} + \left[|\xi|\left(2Q^3 + 3\|\phi\|^2_{\ell^2(\mathbb{Z})}Q + 3\sqrt{2}\|\phi\|_{\ell^2(\mathbb{Z})}Q^2\right) + \frac{\varepsilon^2\hat{\alpha}}{2}Q\right. \\
&\left. + 2\varepsilon^2|h|Q^2\right].
\end{aligned} \tag{4.46}$$

Take $\tau_0 > 0$ arbitrarily. Assume that the initial norm of the perturbation term satisfies the bound

$$Q(0) \le C_0\varepsilon^3, \tag{4.47}$$

where C_0 is a positive constant. Define

$$T_0 = \sup\left\{t_0 \in [0, 2\tau_0\varepsilon^{-2}] : \sup_{t\in[0,t_0]} Q(t) \le C_Q\varepsilon^3\right\}, C_R = \sup_{\tau\in[0,\tau_0]} \tilde{C}_R, \tag{4.48}$$

on the time scale $[0, 2\tau_0\varepsilon^{-2}]$. Then, we can rewrite the energy estimate (4.46) by applying Lemma 4.2.2–4.2.3 and the definition (4.48) as

$$\left|\frac{dQ}{dt}\right| \leq \frac{1}{\sqrt{2}} C_R \varepsilon^5 + \left(4|\xi| C_Q^2 \varepsilon^4 + 6|\xi| C_\phi^2 + 6|\xi|\sqrt{2} C_\phi C_Q \varepsilon^2 + \hat{\alpha} + 4|h|\right) \frac{\varepsilon^2 Q}{2}. \tag{4.49}$$

Thus, for every $t \in [0, T_0]$ and suffeciently small $\varepsilon > 0$, we can find a positive constant K_0, which is independent of ε, such that

$$4|\xi| C_Q^2 \varepsilon^4 + 6|\xi| C_\phi^2 + 6|\xi|\sqrt{2} C_\phi C_Q \varepsilon^2 + \hat{\alpha} + 4|h| \leq K_0. \tag{4.50}$$

By simplifying and integrating (4.49), we get

$$Q(t) e^{-\frac{\varepsilon^2 K_0 t}{2}} - Q(0) \leq \int_0^t \frac{C_R \varepsilon^5}{\sqrt{2}} e^{-\frac{\varepsilon^2 K_0 s}{2}} ds \leq \frac{\sqrt{2} C_R \varepsilon^3}{K_0}. \tag{4.51}$$

By using (4.47), then we obtain

$$Q(t) \leq \varepsilon^3 \left(C_0 + \frac{\sqrt{2} C_R}{K_0}\right) e^{K_0 \tau_0}. \tag{4.52}$$

Therefore, we can define $C_Q := \left(C_0 + 2^{1/2} K_0^{-1} C_R\right) e^{K_0 \tau_0}$ and this concludes the proof.

■

4.4 Numerical comparisons: Breather solutions

In Section 4.2, we have discussed that small-amplitude solutions of the parametrically driven dKG equation (4.1) can be approximated by ansatz (4.2), that satisfies the dNLS equation (4.3) with a residue of order $O(\varepsilon^5)$. We then showed in Section 4.3 that the difference between solutions of Eqs. (4.1) and (4.3), that are initially of at most order $O(\varepsilon^3)$, will be of the same order for some finite time. In this section, we will illustrate the results numerically.

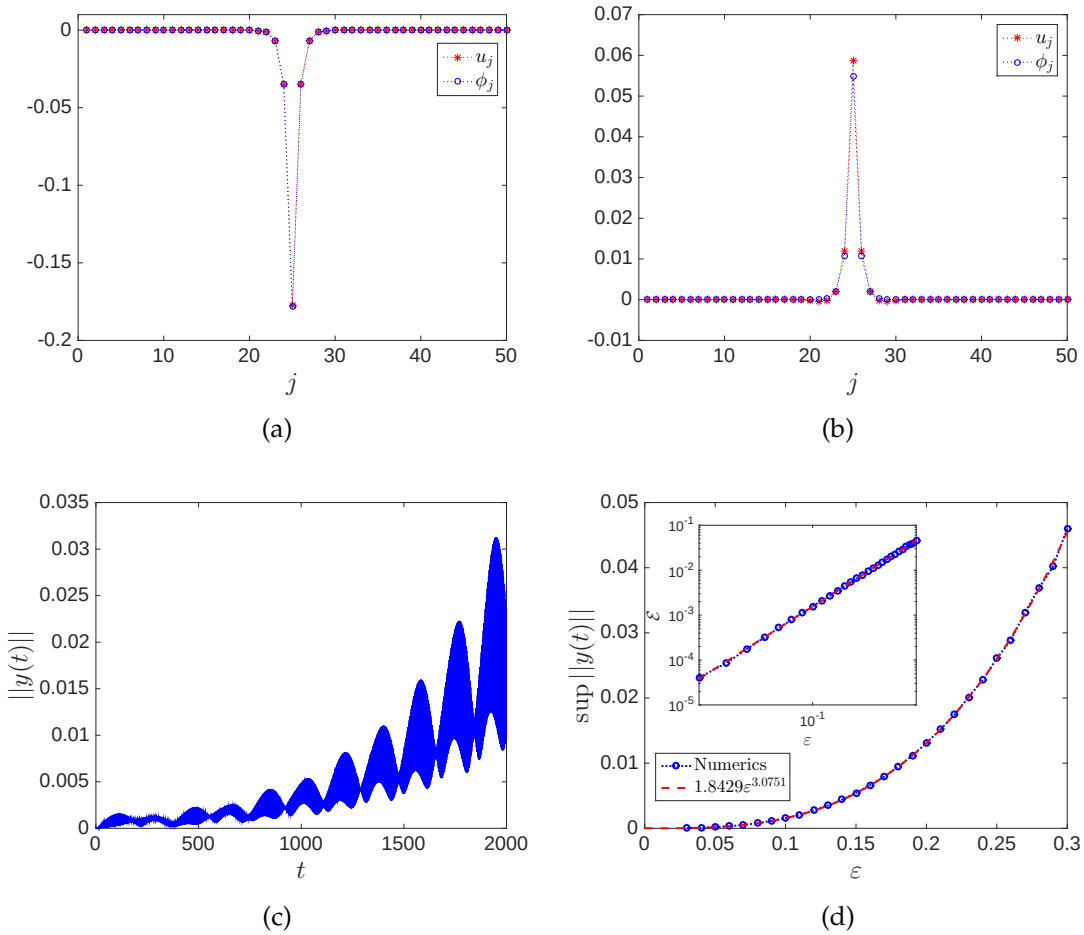

Figure 4.1. Panels (a,b) show numerical solutions of the dKG equation (blue circles) and the corresponding rotating wave approximations from the dNLS equation (red stars) at two time instances $t = 100$ and $t = 1000$. Here, $\varepsilon = 0.1$. Panel (c) is the time dynamics of the error. Panel (d) is the maximum error of the dNLS approximation within the interval $t \in [0, 2/\varepsilon^2]$ for varying $\varepsilon \to 0$. In the picture, we also plot the best power fit of the error, showing the same order as in Theorem 4.3.1.

We consider Eq. (4.1) as an initial value problem in the domain $D = \{(n,t)|(n,t) \in [1,N]\times[0,\widetilde{T}]\}$, $N \in \mathbb{N}, \widetilde{T} \in \mathbb{R}$. The differential equation is then integrated using the fourth order Runge-Kutta method. Simultaneously we also need to integrate Eq. (4.3). As the initial data of the dKG equation, we take

$$u_j(0) = \phi_j(0), \quad \dot{u}_j(0) = \dot{\phi}_j(t)\big|_{t=0}. \tag{4.53}$$

In this way, the initial error $y(0)$ between $u_j(0)$ and $\phi_j(0)$ (see (4.39)) will satisfy $\|y(0)\|_{\ell^2} = 0 < C_0\varepsilon^3$, for any $C_0 > 0$.

In the following, we take the parameter values $\Lambda = -3$, $h = -0.5$, and $\hat{\alpha} = 0.1$. The nonlinearity is considered to be 'softening', which without loss of generality is taken to be $\xi = -1$. This choice of nonlinearity coefficient will yield the dNLS equation (4.3) with a 'focusing' or 'attractive' nonlinearity. The case $\xi = +1$, i.e., 'stiffening' nonlinearity, corresponds to the 'defocusing' or 'repulsive' dNLS equation (4.3). In the dNLS description, the attractive and repulsive cases are mathematically equivalent through a "staggering" transformation $(-1)^j$, that reverses the phases in every second lattice.

In our first simulation, we consider the fundamental site-centred discrete soliton of the dNLS equation, that has been considered before in, e.g., [46, 87–89]. Such solutions will satisfy (4.3) with $\dot{A}_j = 0$ and can be obtained rather straightforwardly using Newton's method.

In Fig. 5.1(a) and 5.1(b) we plot the solutions $u_j(t)$ and $\phi_j(t)$ for $\varepsilon = 0.1$ at two different subsequent times. In panel (c) of the same figure, we plot the error $\|y(t)\|$ between the two solutions, which shows that it increases. However, the increment is bounded within the proven estimate $\sim C\epsilon^3$ for quite a long while.

We have performed similar computations for several different values of $\varepsilon \to 0$. Taking $\tau_0 = 1$, we record $\sup_{t\in[0,2\tau_0/\varepsilon^2]}\|y(t)\|$ for each ε. We plot in Fig. 5.1(d) the

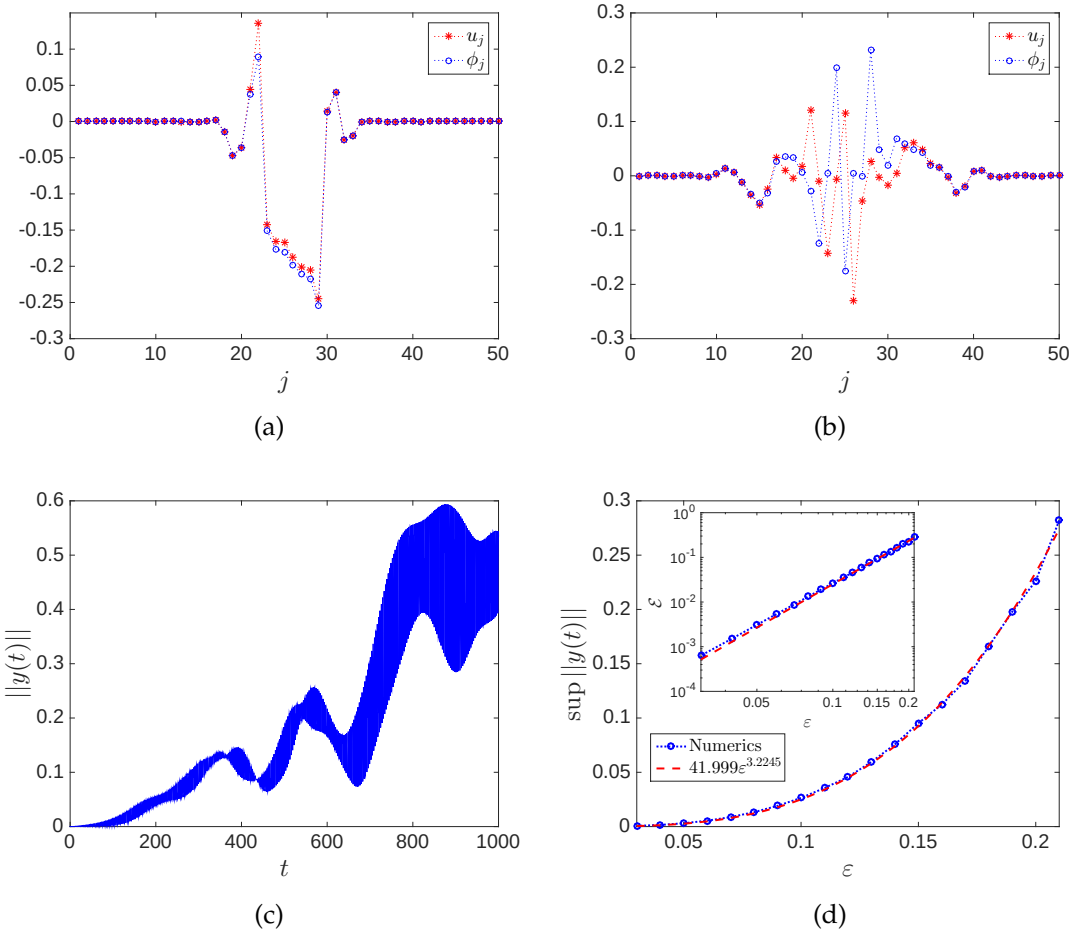

Figure 4.2. The same as Fig. 3.1, but for the initial data (4.54).

maximum error as a function of ε. We also plot in the same panel the best power fit in the nonlinear least squares sense, which agrees with Theorem 4.3.1.

Discrete solitons of the dNLS equation expectedly approximate discrete breathers of the dKG equation. Our simulations above indicate this as well. Yet, how close are they with each other? In Appendix B, we show numerically that they are $O(\varepsilon^3)$-apart, which interestingly seem to follow the result in Theorem 4.3.1.

In our second simulations, we consider a perhaps more interesting initial condition in the form of a clustered state:

$$A_j = e^{0.05ij},\ j = 21,\ldots,30, \tag{4.54}$$

and A_j vanishes elsewhere. The dynamics at some instances are shown in Fig. 3.2. We also computed the maximum error made by the rotating wave approximation within the time interval $[0, 2\tau_0/\varepsilon^2]$, with τ_0 taken to be 1, and plotted it in Fig. 4.2(d) for several values of ε. The best power fit to the error also shows the same behaviour, i.e., the error is $O(\varepsilon^3)$.

Chapter 5

Reduction of damped, driven Klein-Gordon equations into a discrete nonlinear Schrödinger equation: justification and numerical comparisons

5.1 Introduction

Nonlinear lattices are a set of nonlinear evolution equations that are coupled spatially. Prominent classes of nonlinear lattices are discrete Klein-Gordon [94] and Frenkel-Kontorova equations [17] that serve as possibly the simplest models for many complex physical and biological systems. While Frenkel-Kontorova type systems correspond to coupled equations with harmonic on-site potential, the discrete Klein-Gordon equations do with the anharmonic one.

Small-amplitude wave packets of nonlinear lattices are usually explored via reduction to an amplitude or modulation equation in the form of either continuous or discrete nonlinear Schrödinger equations. The method is usually referred to as the rotating wave approximation. If one is interested in solution profiles with a much larger length scale than the typical distance between the lattices, they can aim for a continuous approximation and obtain nonlinear Schrödinger equations (see, e.g., [7, 53, 57]). When one is instead interested in waves with the same scale of the typical lattice distance, one will obtain an approximation in the form of a discrete nonlinear Schrödinger equation (see, e.g., [26, 38, 49, 58, 59, 72, 88]) with the corresponding wave properties quite distinct from those in the continuous limit.

Despite their widespread use, rigorous justifications of the rotating wave procedures are more sparse, with an early example being [57], wherein Hamiltonian Klein-Gordon lattices are approximated by nonlinear Schrödinger equations (see also [30, 60]). A justification for the discrete nonlinear Schrödinger approximation was provided rather recently in [75].

In this chapter, we consider a Klein-Gordon equation with external damping and drive. Our present work will be relevant to models appearing in the study of, e.g., superconducting Josephson junctions [4], mechanical oscillators [62], electrical lattices [33], etc. Using the rotating-wave approximation, we will show that the corresponding modulation equation is a damped, driven discrete nonlinear Schrödinger equation. The similar approximation has been used to reduce an externally driven sine-Gordon equation into a damped, driven continuous nonlinear Schrödinger equation [9, 90]. In here, we are going to provide a rigorous justification of the discrete Schrödinger equation. Note that our work here is significantly different from the aforementioned published works in the sense that our original governing equation as well as the modulation one are not Hamiltonian.

Moreover, the external drive yields a constant term that can be challenging to control in providing boundedness of the error, i.e., the solution does not lie in ℓ^2-space of $\mathbb{Z}$. Without external damping and drive, the initial value problem for the discrete nonlinear Schrödinger equation with power nonlinearity in weighted ℓ^2-space has been shown to be globally well-posed in [74]. N'Guérékata and Pankov [73] provides a stronger result of global well-posedness in spaces of exponentially decaying data. Here, by considering the problem with damping and drive in a periodic domain, we are able to provide the global existence of the discrete nolinear Schrd̈inger equation as well as the error bound of the rotating wave approximation.

This chapter is organized as follows. We define the governing equation and formulate preliminary results on the unique global solution and error estimate in Section 5.2. The main result on the error bound of the rotating-wave approximation as time evolves is presented in Section 5.3. In Section 5.4 we describe the computation of the error made by the Schrödinger approximation numerically. The comparison is provided for localised waves, i.e., breather solutions.

5.2 Mathematical formulation and preliminary results

Consider the following model of coupled oscillators with damping and drive on a finite lattice

$$\ddot{u}_j = -u_j - \xi u_j^3 + \epsilon(\Delta_2 u_j) - \alpha \dot{u}_j + \frac{h}{2}(e^{i\Omega t} + e^{-i\Omega t}), \quad j \in \mathbb{Z}_N = \{1, \dots, N\}, \tag{5.1}$$

where $u_j \equiv u_j(t)$ is a real-valued wave function at site j, the overdot is the time derivative and ϵ represents the coupling constant between two adjacent sites, with $\Delta_2 u_j = u_{j+1} - 2u_j + u_{j-1}$ being the discrete Laplacian in one dimension. The parameters α and h denote the damping coefficient and the strength of the external

drive, respectively. The driving frequency is taken to be $\Omega = 1 - \frac{\epsilon\omega}{2}$, i.e., it is close to the natural frequency of the uncoupled linear oscillator. We also consider a periodic boundary condition,

$$u_{j+N}(t) = u_j(t), \qquad \text{for all} j \in \mathbb{Z}_N. \tag{5.2}$$

Considering small-amplitude oscillations, one commonly uses the rotating wave approximation

$$u_j(t) \approx X_j(t) = \sqrt{\epsilon} A_j(\tau) e^{i\Omega t} + \frac{1}{8}\xi\epsilon^{3/2} A_j^3(\tau) e^{3i\Omega t} + c.c., \tag{5.3}$$

i.e., $X_j(t)$ is the leading order approximation of $u_j(t)$ and $\tau = \frac{\epsilon t}{2}$ is the slow time variable. Substituting the ansatz (5.3) into Eq. (5.1) and removing the resonant terms $e^{\pm i\Omega t}$ at the leading order of $O(\epsilon^{3/2})$, we obtain the damped, driven discrete nonlinear Schrödinger equation

$$i\dot{A}_j + 3\xi|A_j|^2 A_j - \Delta_2 A_j + i\hat{\alpha} A_j - \hat{h} + \omega A_j = 0, \tag{5.4}$$

where $\alpha = \epsilon\hat{\alpha}$, $h = 2\epsilon^{3/2}\hat{h}$, and $A_{j+N}(t) = A_j(t)$, i.e., the periodic boundary condition.

Using Eqs. (5.3) and (5.4) to approximate the solutions of (5.1) will yield the residual terms

$$\begin{aligned} \mathrm{Res}_j(t) \quad := \quad & \epsilon^{5/2}\Bigg[\frac{e^{i\Omega t}}{2}\left(\frac{3}{4}\xi^2 A_j^3 \bar{A}_j^2 - i\hat{\alpha}\omega A_j + \hat{\alpha}\dot{A}_j - \frac{\omega^2 A_j}{2} - i\omega\dot{A}_j + \frac{\ddot{A}_j}{2}\right) \\ & + \frac{e^{3i\Omega t}}{8}\Big(6\xi^2 A_j^4 \bar{A}_j + 3i\hat{\alpha}\xi A_j^3 + 9\xi\omega A_j^3 + 9i\xi A_j^2 \dot{A}_j + 2\xi A_j^3 \\ & - \xi A_{j-1}^3 - \xi A_{j+1}^3\Big) + \frac{e^{5i\Omega t}}{8}\left(3\xi^2 A_j^5\right)\Bigg] \end{aligned}$$

$$
\begin{aligned}
&+\epsilon^{7/2}\Bigg[\frac{e^{i\Omega t}}{32}\left(3\xi^3 A_j^3\bar{A}_j^4\right)+\frac{e^{3i\Omega t}}{32}\Big(-6i\hat{\alpha}\xi\omega A_j^3+6\hat{\alpha}\xi A_j^2\dot{A}_j-9\xi\omega^2 A_j^3 x\\
&\quad+3i\hat{\alpha}\xi A_j^3+9\xi\omega A_j^3+9i\xi A_j^2\dot{A}_j+2\xi A_j^3+6\xi A_j\left(\dot{A}_j\right)^2+3\xi A_j^2\ddot{A}_j\Big)\\
&\quad+\frac{e^{5i\Omega t}}{64}\left(3\xi^3 A_j^6\bar{A}_j\right)+\frac{e^{7i\Omega t}}{64}\left(3\xi^3 A_j^7\right)\Bigg]\\
&+\epsilon^{9/2}\left[\frac{e^{3i\Omega t}}{512}\left(3\xi^4 A_j^6\bar{A}_j^3\right)+\frac{e^{9i\Omega t}}{512}\left(\xi^4 A_j^9\right)\right]+\text{c.c.}
\end{aligned}
\tag{5.5}
$$

The terms with derivatives of A_j can be changed into those without derivative using Eq. (5.4), provided that $\left(A_j\right)_{j\in\mathbb{Z}_N}$ is a twice differentiable sequence with respect to time. Because of the periodic boundary condition, we consider the sequence space $\ell^2(\mathbb{Z}_N)$ and we will simply denote $\left(A_j\right)_{j\in\mathbb{Z}_N}\in\ell^2(\mathbb{Z}_N)$ by A. The space $\ell^2(\mathbb{Z}_N)$ is a Hilbert space equipped with norm,

$$
\|A\|_{\ell^2(\mathbb{Z}_N)}=\sum_{j=1}^{N}|A_j|^2\,. \tag{5.6}
$$

The following lemma gives us a preliminary result on the global solutions of the discrete nonlinear Schrödinger equation (5.4).

Lemma 5.2.1. *For every $\phi\in\ell^2(\mathbb{Z}_N)$, there exists a unique global solution $A(\tau)$ of the discrete nonlinear Schrödinger equation (5.4) in $\ell^2(\mathbb{Z}_N)$ such that $A(0)=\phi$. Moreover, the solution $A(\tau)$ is smooth in τ and there is a real constant C_A, that depends on the initial value, $\hat{h}$, $\hat{\alpha}$ and N such that $\|A(\tau)\|_{\ell^2(\mathbb{Z}_N)}\le C_A$.*

Proof. Let us rewrite Eq. (5.4) in the following equivalent integral form

$$
A_j(\tau)=A_j(0)-i\int_0^\tau\left(\Delta_2 A_j-i\hat{\alpha}A_j-3\xi|A_j|^2A_j-\omega A_j+\hat{h}\right)ds\,. \tag{5.7}
$$

Define a Banach space,

$$
\mathcal{B}=\left\{A\in C\left([0,\tau_m],\ell^2(\mathbb{Z}_N)\right)\mid\|A(\tau)\|_{\ell^2(\mathbb{Z}_N)}\le\delta\right\}, \tag{5.8}
$$

equipped with the norm

$$\|A\|_{\mathcal{B}} = \sup_{\tau\in[0,T]} \|A(\tau)\|_{\ell^2(\mathbb{Z}_N)}.$$

For $A \in \ell^2(\mathbb{Z}_N)$, we define a nonlinear operator,

$$K_j[A(\tau)] = \phi - i\int_0^\tau \Big(\Delta_2 A_j - i\hat{\alpha}A_j - 3\xi|A_j|^2A_j - \omega A_j + \hat{h}\Big)ds. \tag{5.9}$$

We want to prove that K is contraction mapping on $\mathcal{B}$.

Due to the periodic boundary condition, $A_j = A_{N+j}$, we get

$$\|\Delta_2 A\|_{\ell^2(\mathbb{Z}_N)} \le C_{\Delta_2}\|A\|_{\ell^2(\mathbb{Z}_N)}. \tag{5.10}$$

Therefore, the discrete Laplacian Δ_2 is a bounded operator in $\ell^2(\mathbb{Z}_N)$. From the Banach algebra property of the $\ell^2(\mathbb{Z}_N)$-space, there is a constant $C > 0$ such that for every $A, B \in \ell^2(\mathbb{Z}_N)$ we have

$$\|AB\|_{\ell^2(\mathbb{Z}_N)} \le C\|A\|_{\ell^2(\mathbb{Z}_N)}\|B\|_{\ell^2(\mathbb{Z}_N)}. \tag{5.11}$$

From (5.9) and using the estimate (5.11) we obtain the following bound

$$\|K(A)\|_{\mathcal{B}} \le \delta_0 + T(C\delta + \alpha\delta + 3C\delta^3 + \omega\delta).$$

We can pick $\delta_0 < \frac{\delta}{2}$ and $T \le \frac{\delta}{2(C\delta+\alpha\delta+3C\delta^3+\omega\delta)}$. Thus, K is a mapping from $\overline{B}_\delta$ to itself.

For $A, B \in \overline{B}_\delta$, we have

$$K_j[A(\tau)] - K_j[B(\tau)] = -i \int_0^\tau \Big[\Delta_2(A_j - B_j) - i\hat{\alpha}(A_j - B_j) - 3\xi(|A_j|^2 A_j - |B_j|^2 B_j) \\ -\omega(A_j - B_j)\Big] ds.$$

Therefore, we obtain

$$\|K(A) - K(B)\|_{\mathcal{B}} \leq T\{C_\Delta + \hat{\alpha} + 3C\hat{\alpha}^2 + \omega\}\|A - B\|_{\mathcal{B}}.$$

By taking $T < \min\left(\frac{1}{C_\Delta + \hat{\alpha} + 3C\hat{\alpha}^2 + \omega}, \frac{\delta}{2(C\delta + \alpha\delta + 3C\delta^3 + \omega\delta)}\right)$, then K is a contraction mapping. Therefore, there exists a constant T such that the discrete nonlinear Schrödinger equation has a local unique solution $A \in C\left([0,T], \ell^2(\mathbb{Z}_N)\right)$ with $\sup_{\tau\in[0,T]}\|A(\tau)\|_{\ell^2(\mathbb{Z}_N)} \leq \delta$.

Now, we will prove the global well-posedness of the discrete nonlinear Schrödinger equation (5.4). Multiplying the jth-component of the equation by $\bar{A}_j$, taking the imaginary part and summing over j, we obtain

$$\frac{d}{d\tau}\|A\|^2_{\ell^2(\mathbb{Z}_N)} + 2\hat{\alpha}\|A\|^2_{\ell^2(\mathbb{Z}_N)} = 2|\hat{h}| \sum_{j=1}^{N} \mathrm{Im}(\bar{A}_j) \leq 2|\hat{h}|\|A\|_{\ell^2(\mathbb{Z}_N)}\,. \tag{5.12}$$

Integrating the inequality, we get

$$\begin{aligned} \|A\|^2_{\ell^2(\mathbb{Z}_N)} &\leq \frac{|\hat{h}|}{\hat{\alpha}} + \left(\|A_0\|_{\ell^2(\mathbb{Z}_N)} - \frac{|\hat{h}|}{\hat{\alpha}}\right) e^{-\hat{\alpha}\tau} \\ &\leq C_A\left(\|A_0\|_{\ell^2(\mathbb{Z}_N)}, \hat{h}, \hat{\alpha}, N\right), \end{aligned} \tag{5.13}$$

which provides a global bound to the solutions and hence, conclude the proof of the lemma. ■

The following lemma will give us an estimate for the leading order approximation (5.3).

Lemma 5.2.2. *For every $A_0 \in \ell^2(\mathbb{Z}_N)$, there exits a positive constant $C_X(\|A_0\|_{\ell^2(\mathbb{Z}_N)}, \hat{h}, \hat{\alpha}, N)$ such that the leading-order approximation (5.3) is estimated by*

$$\|X(t)\|_{\ell^2(\mathbb{Z}_N)} + \|\dot{X}(t)\|_{\ell^2(\mathbb{Z}_N)} \leq \sqrt{\epsilon}\, C_X(\|A_0\|_{\ell^2(\mathbb{Z}_N)}, \hat{h}, \hat{\alpha}, N)\,, \tag{5.14}$$

for all $t \in [0, \infty)$ and $\epsilon \in (0,1)$.

Proof. From the global existence in Lemma 5.2.1 and using the Banach algebra property of $\ell^2(\mathbb{Z}_N)$, we obtain

$$\begin{aligned}
\|X(t)\|_{\ell^2(\mathbb{Z}_N)} &= \left\| \sqrt{\epsilon}\left(Ae^{i\Omega t} + \bar{A}e^{-i\Omega t}\right) + \frac{1}{8}\xi\epsilon^{3/2}\left(A^3e^{3i\Omega t} + \bar{A}^3e^{-3i\Omega t}\right)\right\|_{\ell^2(\mathbb{Z}_N)} \\
&\leq \left\| \sqrt{\epsilon}\left(Ae^{i\Omega t} + \bar{A}e^{-i\Omega t}\right)\right\|_{\ell^2(\mathbb{Z}_N)} + \left\|\frac{1}{8}\xi\epsilon^{3/2}\left(A^3e^{3i\Omega t} + \bar{A}^3e^{-3i\Omega t}\right)\right\|_{\ell^2(\mathbb{Z}_N)} \\
&\leq 2\sqrt{\epsilon}\|A\|_{\ell^2(\mathbb{Z}_N)} + \frac{1}{4}\xi\epsilon^{3/2}\left\|A^3\right\|_{\ell^2(\mathbb{Z}_N)} \\
&\leq \sqrt{\epsilon}\, C_{X_1}(\|A_0\|_{\ell^2(\mathbb{Z}_N)}, \hat{h}, \hat{\alpha}, N)
\end{aligned} \tag{5.15}$$

and

$$\begin{aligned}
\left\|\dot{X}(t)\right\|_{\ell^2(\mathbb{Z}_N)} = \Bigg\| &\frac{1}{8}\xi\epsilon^{3/2}\left(\frac{3}{2}\epsilon\bar{A}^2e^{-3i\Omega t}\dot{\bar{A}} - 3i\Omega\bar{A}^3e^{-3i\Omega t} + \frac{3}{2}\epsilon A^2\dot{A}e^{3i\Omega t} + 3i\Omega A^3e^{3i\Omega t}\right) \\
&+ \sqrt{\epsilon}\left(\frac{1}{2}\epsilon e^{-i\Omega t}\dot{\bar{A}} - i\Omega\bar{A}e^{-i\Omega t} + \frac{1}{2}\epsilon\dot{A}e^{i\Omega t} + i\Omega Ae^{i\Omega t}\right)\Bigg\|_{\ell^2(\mathbb{Z}_N)}.
\end{aligned} \tag{5.16}$$

From (5.4), we have that

$$\begin{aligned}\left\|\dot{A}(\tau)\right\|_{\ell^2(\mathbb{Z}_N)} &= \left\|3i\xi A^2\bar{A} - \hat{\alpha}A + i\omega A - i(\Delta_2 A) - i\hat{h}\right\|_{\ell^2(\mathbb{Z}_N)} \\ &\leq 3\xi C_A^3\left(\|A_0\|_{\ell^2(\mathbb{Z}_N)},\hat{h},\hat{\alpha}\right) + \alpha C_A\left(\|A_0\|_{\ell^2(\mathbb{Z}_N)},\hat{h},\hat{\alpha}\right) + \omega C_A\left(\|A_0\|_{\ell^2(\mathbb{Z}_N)},\hat{h},\hat{\alpha}\right) \\ &\quad + C_{\Delta_2}C_A\left(\|A_0\|_{\ell^2(\mathbb{Z}_N)},\hat{h},\hat{\alpha}\right) + C\hat{h} \\ &\leq \tilde{C}_A\left(\|A_0\|_{\ell^2(\mathbb{Z}_N)},\hat{h},\hat{\alpha},N\right).\end{aligned} \tag{5.17}$$

Therefore, Eq. (5.16) becomes

$$\left\|\dot{X}(t)\right\|_{\ell^2(\mathbb{Z}_N)} \leq \sqrt{\epsilon}\, C_{X_2}(\|A_0\|_{\ell^2(\mathbb{Z}_N)},\hat{h},\hat{\alpha},N) \tag{5.18}$$

and

$$\|X(t)\|_{\ell^2(\mathbb{Z}_N)} + \|\dot{X}(t)\|_{\ell^2(\mathbb{Z}_N)} \leq \sqrt{\epsilon}\, C_X(\|A_0\|_{\ell^2(\mathbb{Z}_N)},\hat{h},\hat{\alpha},N)$$

■

Next, we have the following result on the bound of the residual terms Eq. (5.5).

Lemma 5.2.3. *For every $A_0 \in \ell^2(\mathbb{Z}_N)$, there exists a positive $\epsilon-$independent constant $C_R(\|A_0\|_{\ell^2(\mathbb{Z}_N)},\hat{h},\hat{\alpha},N)$, such that for every $\epsilon \in (0,1)$ and every $t \in \mathbb{R}$, the residual term in (5.5) is estimated by*

$$\|\mathrm{Res}(t)\|_{\ell^2(\mathbb{Z}_N)} \leq C_R\left(\|A_0\|_{\ell^2(\mathbb{Z}_N)},\hat{h},\hat{\alpha},N\right)\epsilon^{5/2}. \tag{5.19}$$

Proof. To prove this lemma, we can use the result from Lemma 5.2.1 as well as the property of Banach algebra in $\ell^2(\mathbb{Z}_N)$, such that from the global existence and smoothness of the solution $A(\tau)$ of the discrete nonlinear Schrödinger equation (5.4) in Lemma 5.2.1, we obtain (5.19). ■

5.3 Main Results

In this section we will develop the main result on the time evolution of the rotating-wave approximation error by writing $u_j(t) = X_j(t) + y_j(t)$, where $X_j(t)$ is the leading-order approximation (5.3) and $y_j(t)$ is the error term. Plugging the decomposition into Eq. (5.1), we obtain the evolution problem for the error term:

$$\ddot{y}_j + y_j + \xi\left(y_j^3 + 3X_j^2 y_j + 3X_j y_j^2\right) - \epsilon\Delta_2 y_j + \epsilon\hat{\alpha}\dot{y}_j + \mathrm{Res}_j(t) = 0, \quad j \in \mathbb{Z}_N, \tag{5.20}$$

where the residual term $\mathrm{Res}_j(t)$ is given by (5.5) if $A(\tau)$ satisfies Eq. (5.4). Since u and X satisfy periodic boundary conditions, the error term y also satisfies the same condition $y_{j+N}(t) = y_j(t)$.

Associated with Eq. (5.20), we can define the energy of the error term as

$$E(t) := \frac{1}{2}\sum_{j=1}^{N}\left[\dot{y}_j^2 + y_j^2 - 2\epsilon\left(y_j y_{j+1} - y_j^2\right)\right]. \tag{5.21}$$

For every t for which the solution $y(t)$ is defined, we have $E(t) \geq 0$ and the following inequality,

$$\|\dot{y}(t)\|^2_{\ell^2(\mathbb{Z}_N)} + \|y(t)\|^2_{\ell^2(\mathbb{Z}_N)} \leq 2E(t). \tag{5.22}$$

The rate of change for the energy (5.21) is found from the evolution problem (5.20) as follows

$$\frac{dE}{dt} = -\sum_{j=1}^{N}\left[\mathrm{Res}_j(t) + \epsilon\hat{\alpha}\dot{y}_j + \xi(y_j^3 + 3X_j^2 y_j + 3X_j y_j^2)\right]\dot{y}_j. \tag{5.23}$$

Using the Cauchy-Schwarz inequality and setting $E = Q^2$, we get

$$\begin{aligned}\left|\frac{dQ}{dt}\right| \leq \frac{1}{\sqrt{2}}\|\mathrm{Res}(t)\|_{\ell^2(\mathbb{Z}_N)} + \Big[\epsilon\hat{\alpha} + 2|\xi|Q^2 + 3|\xi|\sqrt{2}\|X(t)\|_{\ell^2(\mathbb{Z}_N)}Q \\ +3|\xi|\sqrt{2}\|X(t)\|^2_{\ell^2(\mathbb{Z}_N)}\Big]Q. \end{aligned} \tag{5.24}$$

Take $\tau_0 > 0$ arbitrarily. Assume that the initial norm of the perturbation term satisfies the following bound

$$Q(0) \leq C_0\epsilon^{3/2}, \tag{5.25}$$

where C_0 is a positive constant, and define

$$T_0 = \sup\left\{t_0 \in [0, 2\tau_0\epsilon^{-1}] : \sup_{t\in[0,t_0]} Q(t) \leq C_Q\epsilon^{3/2}\right\}, \tag{5.26}$$

on the time scale $[0, 2\tau_0\epsilon^{-1}]$.

Applying Lemmas 5.2.2-5.2.3 and the definition (5.26), we have

$$\left|\frac{dQ}{dt}\right| \leq \frac{\epsilon^{5/2}C_R}{\sqrt{2}} + \left(2\hat{\alpha} + 4|\xi|C_Q^2\epsilon^2 + 6|\xi|\sqrt{2}C_QC_X\epsilon + 6|\xi|C_X^2\right)\frac{\epsilon Q}{2}. \tag{5.27}$$

Thus, for every $t \in [0, T_0]$ and $\epsilon > 0$ which is sufficiently small, we can find a positive constant K_0, which is independent of ϵ, such that

$$2\hat{\alpha} + 4|\xi|C_Q^2\epsilon^2 + 6|\xi|\sqrt{2}C_QC_X\epsilon + 6|\xi|C_X^2 \leq K_0. \tag{5.28}$$

Integrating (5.27), we get

$$Q(t)e^{-\frac{\epsilon K_0 t}{2}} - Q(0) \leq \int_0^t \frac{C_R\epsilon^{5/2}}{\sqrt{2}}e^{-\frac{\epsilon K_0 s}{2}}ds \leq \frac{\sqrt{2}C_R\epsilon^{3/2}}{K_0}. \tag{5.29}$$

Since we assume (5.25) holds, then we obtain

$$Q(t) \leq \epsilon^{3/2}\left(C_0 + \frac{\sqrt{2}C_R}{K_0}\right)e^{K_0\tau_0}. \tag{5.30}$$

Therefore, we can define $C_Q := \left(C_0 + 2^{1/2}K_0^{-1}C_R\right)e^{K_0\tau_0}$.

Based on the above analysis, we can state the main result of this paper in the following theorem.

Theorem 5.3.1. *For every $\tau_0 > 0$, there are a small $\epsilon_0 > 0$ and positive constants C_0 and C such that for every $\epsilon \in (0,\epsilon_0)$, for which the initial data satisfies*

$$\|y(0)\|_{\ell^2(\mathbb{Z}_N)} + \|\dot{y}(0)\|_{\ell^2(\mathbb{Z}_N)} \leq C_0\epsilon^{3/2}, \tag{5.31}$$

the solution of the discrete Klein-Gordon equation (5.1) satisfies for every $t \in [0, 2\tau_0\epsilon^{-1}]$,

$$\|y(t)\|_{\ell^2(\mathbb{Z}_N)} + \|\dot{y}(t)\|_{\ell^2(\mathbb{Z}_N)} \leq C\epsilon^{3/2}. \tag{5.32}$$

Remark 5.3.2. *The error bound that is of order $O(\epsilon^{3/2})$ in Theorem 5.3.1 is linked to the choice of our rotating wave ansatz* (5.3) *that creates a residue of order $O(\epsilon^{5/2})$. If we include a higher-order correction term in the ansatz* (5.3)*, see Chapter 5.3 of [30] for the procedure to do it, we will obtain a smaller residue and in return a smaller error bound.*

5.4 Numerical Discussions

We have discussed in Section 5.2, that as an approximate solution of the Klein-Gordon equation (5.1), the rotating wave approximation (5.3) and (5.4) yields a residue of order $O\left(\epsilon^{5/2}\right)$. Following on the result, we proved in Section 5.3 that the difference between solutions of Eqs. (5.1) and (5.4) that are initially of at most order $O\left(\epsilon^{3/2}\right)$ will be of the same order for some finite time $2\tau_0/\epsilon$, for $\tau_0 > 0$.

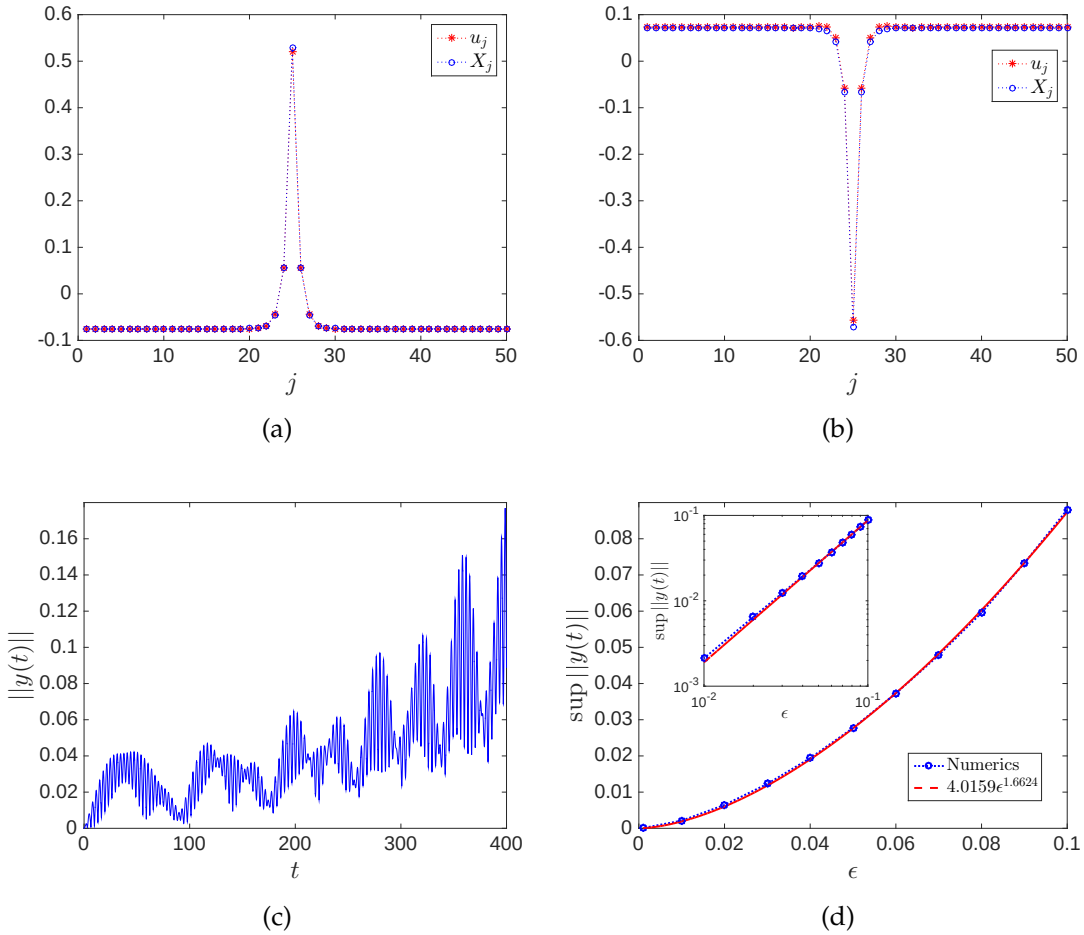

Figure 5.1. (a,b) Numerical solutions of the Klein-Gordon equation (blue circles) and the corresponding rotating wave approximations from the Schrödinger equation (red stars) at two time instances $t = 75$ and $t = 200$. Here, $\epsilon = 0.05$. (c) Time dynamics of the error. (d) Maximum error of the Schrödinger approximation within the interval $t \in [0, 2/\epsilon]$ for varying $\epsilon \to 0$. In the picture, we also plot the best power fit of the error, showing that the error approximately has the same order as in Theorem 5.3.1.

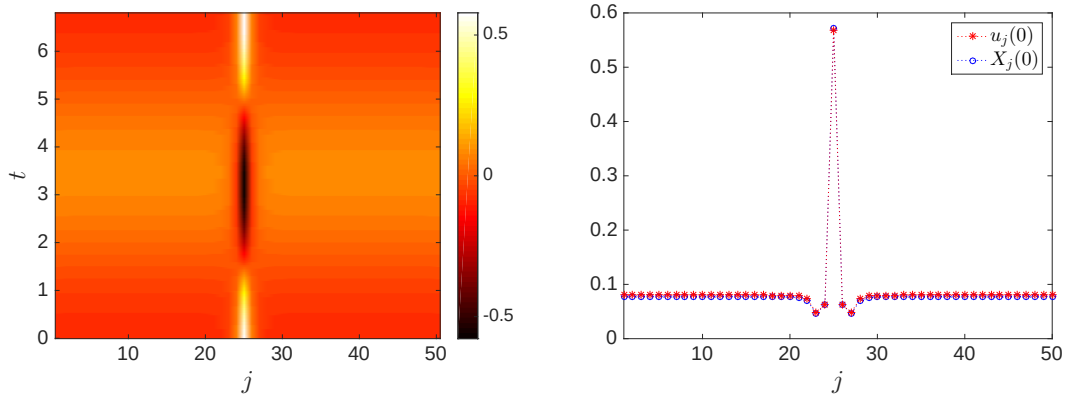

(a) (b)

Figure 5.2. Breather solution of (5.1) for $\epsilon = 0.05$. Panel (a) shows the dynamics of the solution in one period, while panel (b) presents the comparison of the breather and its approximation (5.3), with A_j obtained from solving the Schrödinger equation (5.4).

In this section, we will illustrate the analytical result on the error bound above numerically.

5.4.1 Error growth

We consider Eq. (5.1) as an initial value problem, that is then integrated using the fourth-order Runge-Kutta method. To compare solutions of Eq. (5.1) and the rotating wave approximation (5.3), simultaneously we also need to integrate Eq. (5.4). As the initial data of the Klein-Gordon equation, we take

$$\begin{aligned} u_j(0) &= \epsilon^{1/2} A_j + \frac{1}{8}\xi\epsilon^{3/2} A_j^3\Big|_{t=0} + c.c., \\ \dot{u}_j(0) &= \epsilon^{1/2}\left[A_{j_\tau} + i\Omega A_j\right] + \frac{1}{8}\xi\epsilon^{3/2} A_j^2\left[3A_{j_\tau} + 3i\Omega A_j\right]\Big|_{t=0} + c.c., \end{aligned}$$

where $A_{j_\tau}(0)$ can be obtained from the Schrödinger equation (5.4). In this way, the error $y(t) = u_j(t) - X_j(t)$ will satisfy the initial condition $\|y(0)\|_{\ell^2} = 0$. In the following, we take the parameter values $\omega = 3$, $\hat{h} = -0.5$, $\hat{\alpha} = 0.1$, and the nonlinearity coefficient $\xi = -1$. We also take the number of sites $N = 50$.

For our illustration, we consider a discrete soliton, i.e., a special standing wave solution of the Schrödinger equation (5.4) that is localised in space. Such a solution can be obtained rather immediately from solving the time-independent equation of (5.4) using, e.g., Newton's method.

In Fig. 5.1(a) and 5.1(b) we plot the solutions $u_j(t)$ and $X_j(t)$ for $\epsilon = 0.05$ at two different subsequent times. In panel (c) of the same figure, we plot the error $\|y(t)\|$ between the two solutions, which shows that it increases. However, the increment is bounded within the prediction $\sim C\epsilon^{3/2}$ for quite a long while.

We have performed similar computations for several different values of $\epsilon \to 0$. Taking $\tau_0 = 1$, we record $\sup_{t\in[0,2\tau_0/\epsilon]}\|y(t)\|$ for each ϵ. We plot in Fig. 5.1(d) the maximum error within the time interval as a function of ϵ. We also plot in the same panel the best power fit in the nonlinear least squares sense, showing that the error is approximately of order $O(\epsilon^{3/2})$ in agreement with Theorem 5.3.1.

5.4.2 Discrete solitons vs. discrete breathers

Our simulations in Fig. 3.1 indicate that discrete solitons of the Schrödinger equation shall approximate breathers, i.e., solutions that are periodic in time but localised in space, of the discrete Klein-Gordon equation. Yet, how close are the actual discrete breathers from the solitons? If they are quite close, do they share the same stability characteristics?

To answer the questions, we need to look for breathers of (5.1). Due to the temporal periodicity of the solutions, we can write $u_j(t)$ in trigonometric series:

$$u_j(t) = \sum_{k=1}^{K} a_{j,k}\cos\left((k-1)\,\Omega t\right) + b_{j,k}\sin\left(k\Omega t\right),\ j = 1,2,\ldots,N, \tag{5.33}$$

where $a_{j,k}$ and $b_{j,k}$ are the Fourier coefficients and K is the number of Fourier modes we will use in our numerics. Herein, we use $K = 3$ and $N = 50$, even though larger

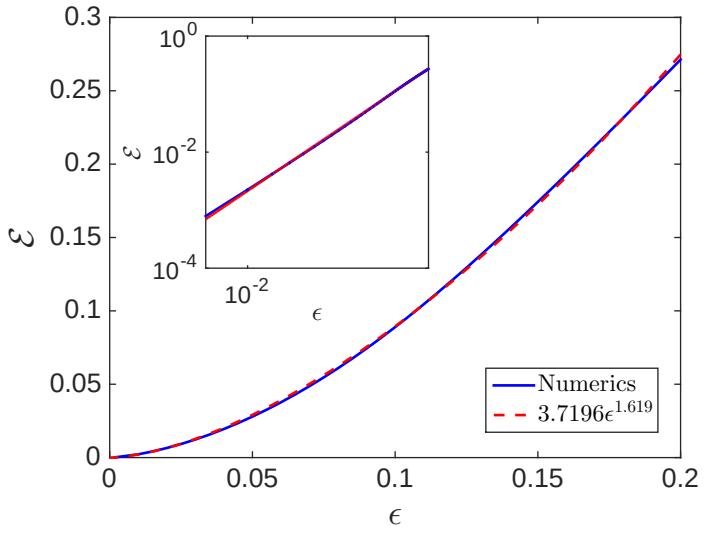

Figure 5.3. Plot of the estimated error of the discrete Schrödinger approximation (5.4) for various $\epsilon \to 0$. The dashed line is the best power fit, indicated in the legend.

numbers have been used as well to make sure that the results are independent of the lattice size and the number of modes.

Substituting the series (5.33) into Eq. (5.1) and integrating the resulting equation over the time-period $2\pi/\Omega$, one will obtain coupled nonlinear equations for the coefficients $a_{j,k}$ and $b_{j,k}$. We then use Newton's method to solve the resulting equations. Breathers will be obtained by properly choosing the initial guess for the coefficients.

Once a solution, e.g., $\hat{u}_j(t)$, is obtained, we determine its linear stability using Floquet theory. Defining $u_j(t) = \hat{u}_j(t) + \delta Y_j(t)$, substituting it into Eq. (5.1), and linearising about $\delta = 0$, we obtain the linear second-order differential-difference equation

$$\begin{aligned} \dot{Y}_j &= Z_j, \\ \dot{Z}_j &= -Y_j - 3\xi\hat{u}_j^2 Y_j + \epsilon\Delta_2 Y_j - \alpha Z_j. \end{aligned} \tag{5.34}$$

By integrating the system of linear equations until $t = 2\pi/\Omega$, and using a standard basis in $\mathbb{R}^{2N}$, i.e., $\left\{e_1^0, e_2^0, ..., e_{2N}^0\right\}$ as the initial condition at $t = 0$, we obtain a collection

of solutions at $t = 2\pi/\Omega$:

$$M = \{E_1, E_2, ..., E_{2N}\} \in \mathbb{R}^{2N\times 2N}, \tag{5.35}$$

as a monodromy matrix. The solution $\hat{u}_j(t)$ is said to be linearly stable when all the eigenvalues λ of the monodromy matrix lies inside or on the unit circle and unstable when there exists at least one λ that is outside the unit circle.

As for discrete solitons of the Schrödinger equation (5.4), after a standing wave solution $\tilde{A}_j = (\tilde{x}_j + i\tilde{y}_j)$ is obtained, its linear stability can also be determined from solving the linear eigenvalue problem

$$\lambda \begin{pmatrix} \hat{x}_j \\ \hat{y}_j \end{pmatrix} = \begin{pmatrix} -6\xi x_j y_j - \alpha & \Delta - \omega - 3\xi\left(x_j^2 + 3y_j^2\right) \\ \omega - \Delta + 3\xi\left(3x_j^2 + y_j^2\right) & 6\xi x_j y_j - \alpha \end{pmatrix} \begin{pmatrix} \hat{x}_j \\ \hat{y}_j \end{pmatrix}, \tag{5.36}$$

that is derived straightforwardly as above from substituting $A_j = \tilde{A}_j + \delta(\hat{x}_j + i\hat{y}_j)e^{\lambda\tau}$ into Eq. (5.4) and linearising the equation about $\delta = 0$. Solution $\tilde{A}_j$ is said to be linearly stable when all of the eigenvalues have $\mathrm{Re}(\lambda) \leq 0$ and unstable when there is an eigenvalue with $\mathrm{Re}(\lambda) > 0$.

We present in Fig. 5.2(a) a breather solution and its time-dynamics in one period for $\epsilon = 0.05$. We also compare in Fig. 5.2(b) the breather in panel (a) and the approximation (5.3) where A_j is the discrete soliton solution obtained from solving Eq. (5.4). One can see the good agreement between them.

By defining the error between breathers of (5.1) and the approximation (5.3) using discrete solitons of (5.4) as

$$\mathcal{E} = \sup_{0\leq t<2\pi/\Omega} \|y(t)\|_{\ell^2(\mathbb{Z}_N)},$$

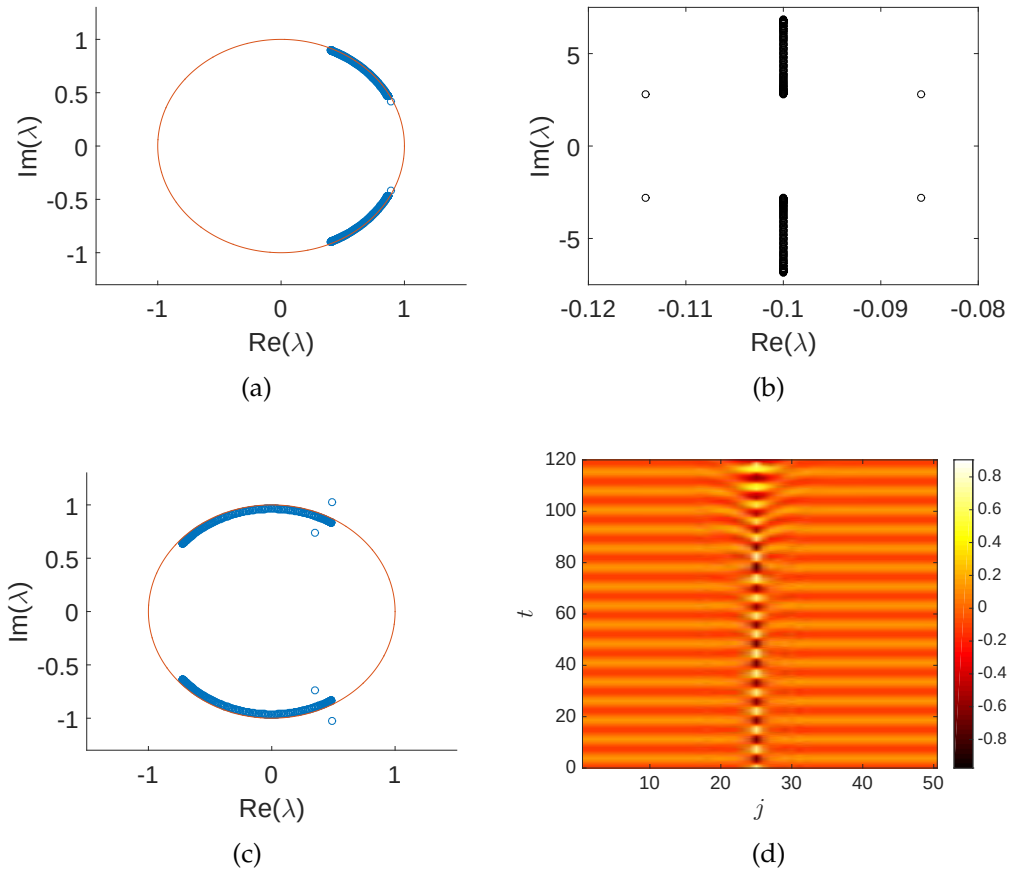

Figure 5.4. (a) Characteristic multipliers, i.e., eigenvalues of the monodromy matrix, of the breather in Fig. 5.2(a), showing the linear stability of the solution. (b) Eigenvalues of the corresponding discrete soliton. Because all of the eigenvalues are on the left half-plane, the solution is linearly stable. (c) The same as panel (a), but for $\epsilon = 0.1$, i.e., the breather is linearly unstable. (d) Time dynamics of the unstable breather with multipliers shown in panel (c).

we plot the error in Fig. 5.3 for varying ϵ. We also depict in the same picture, the best power fit, which interestingly shows an algebraic power that follows the estimated error in Theorem 5.3.1, i.e., $\sim \epsilon^{3/2}$.

For the sake of completeness, we show in Fig. 5.4(a) the Floquet multipliers of the solution in Fig. 5.2(a) for $\epsilon = 0.05$, that are obtained from solving the linear equations (5.34). Because all the eigenvalues are inside the unit circle, the breather is stable. We plot the eigenvalues of the corresponding discrete soliton in Fig. 5.4(b), also showing stability. Because both solutions are stable, the error between them, that is initially of order $O(\epsilon^{3/2})$, will stay the same as time evolves until at least $t = 2\tau_0/\epsilon$, for some $\tau_0 > 0$.

When ϵ is taken to be larger, we observe that breathers of Eq. (5.1) can become unstable. Shown in Fig. 5.4(c) are the Floquet multipliers of the breather when $\epsilon = 0.1$. Because there is an eigenvalue outside the unit circle, the localised solution is unstable. The unstable eigenvalue bifurcates from the collision of an eigenvalue with the continuous spectrum. Note that the corresponding localised solution of the approximating Schrödinger equation (5.4) is still the same as that shown in Fig. 5.2(a), i.e., it is a stable solution.

We show in Fig. 5.4(d) the dynamics of the unstable solution. One can observe that it maintains its shape in the form of periodic oscillations for a while, i.e., $t \sim 2\tau_0/\epsilon$. After that, the breather starts to deform and break up. Eventually the solution will collapse, i.e. unbounded blow-up, which is typical for the Klein-Gordon equation (5.1), even when it is undriven [2] (see also a related work [29]).

Chapter 6

Conclusion and future work

In this thesis, we studied the long-time dynamics near a symmetry breaking bifurcation for the cubic-quintic nonlinear Schrödinger/Gross-Pitaevskii equation, and the rotating wave approximations in lattice models. Moreover, we showed the justification of that approximation by finding the error bound. Now, let us conclude the work that we have gained and delivered in the previous chapters as well as bring up a certain problem that might be interesting to be considered in the future.

6.1 Conclusion

We presented background information of coupled mode reduction, symmetry breaking bifurcation and the rotating wave approximation in Chapter 1. In this chapter, some analytical methods used throughout this thesis were also reviewed briefly. We closed this chapter by delivering the outline of the thesis. Next, proceed with Chapter 2 which discussed definitions, examples and calculation of eigenvalue problems to support Chapter 3.

In Chapter 3 we investigated the long-time dynamics near a symmetry breaking bifurcation for the cubic-quintic nonlinear Schrödinger/Gross-Pitaevskii equation.

Moreover, we studied the applicability of the coupled mode theory in the cubic-quintic NLS/GP with a linear double-well potential.

In Chapter 4 we discussed a parametrically driven discrete nonlinear Schrödinger equation derived from a discrete nonlinear Klein-Gordon equation with damping and parametric drive terms. Here, using a small amplitude ansatz, we justified the approximation by getting the error bound. We proved the global existence and error bound of the rotating wave approximation in ℓ^2-space of $\mathbb{Z}$.

Next, in Chapter 5 we used a similar method, we studied an externally driven nonlinear Klein-Gordon equation with a discrete nonlinear Schrödinger equation with damping and external drive. In addition, as well as Chapter 4, we provided a justification of the approximation by finding the error bound using an energy estimate. Moreover, we found that with external damping and drive, the solutions do not lie in ℓ^2-space of $\mathbb{Z}$, while without external damping and drive, the initial value problem for the discrete nonlinear Schrödinger equation with power nonlinearity is in weighted ℓ^2-space.

6.2 Future work

One of interesting problems that we can investigate in the future is from [21], where the Swift-Hohenberg equation is studied using multiple scale analysis.

Consider the equation [12, 66]

$$\frac{\partial E}{\partial t} = \mathcal{Y} + CE - E^3 - \left(1 + \frac{\partial^2}{\partial x^2}\right)^2 E, \tag{6.1}$$

where in the context of nonlinear optics, E is the amplitude of the optical electric field, $\mathcal{Y}$ is the injection field, and C is the cooperativity parameter. Here, the homogeneous steady state E_{hg} is given by $Y = E_{hg}^3 - CE_{hg} + E_{hg}$. Looking for steady

perturbations to E_{hg}, we set

$$C = 3E_{hg}^2 - \epsilon^2, \qquad E(x,t) = E_{hg} + \epsilon f(x),$$

where $0 < \epsilon \ll 1$, to give the classical Swift-Hohenberg equation

$$\left(1 + \frac{d^2}{dx^2}\right)^2 f + \epsilon^2 f + 3\epsilon E_{hg} f^2 + \epsilon^2 f^3 = 0. \tag{6.2}$$

We can also set

$$C = 3E_{hg}^2 - \epsilon^4, \qquad E(x,t) = E_{hg} + \epsilon f(x),$$

to obtain

$$\left(1 + \frac{d^2}{dx^2}\right)^2 f + \epsilon^4 f + 3\epsilon E_{hg} f^2 + \epsilon^2 f^3 = 0. \tag{6.3}$$

Equations (6.2) and (6.3) correspond to the so-called conditions far and near from the Maxwell point, respectively. Rotating wave approximations have been used to analyse the equations [21].

Consider Eq. (6.2). Let $X = \epsilon x$ and treat x and X as independent variables to give

$$\begin{aligned} &\frac{\partial^4 f}{\partial x^4} + 4\epsilon \frac{\partial^4 f}{\partial x^3 \partial X} + 6\epsilon^2 \frac{\partial^4 f}{\partial x^2 \partial X^2} + 4\epsilon^3 \frac{\partial^4 f}{\partial x \partial X^3} + \epsilon^4 \frac{\partial^4 f}{\partial X^4} + 2\frac{\partial^2 f}{\partial x^2} + 4\epsilon \frac{\partial^2 f}{\partial x \partial X} \\ &+2\epsilon^2 \frac{\partial^2 f}{\partial X^2} + f = -\epsilon^2 f - 3\epsilon E_{hg} f^2 - \epsilon^2 f^3. \end{aligned} \tag{6.4}$$

We expand f in powers of ϵ as

$$f = f_0(x,X) + \epsilon f_1(x,X) + \epsilon^2 f_2(x,X) + \cdots. \tag{6.5}$$

Substituting the expansion (6.5) into (6.4), at $O(\epsilon^0)$ we obtain

$$\frac{\partial^4 f_0}{\partial x^4} + 2\frac{\partial^2 f_0}{\partial x^2} + f_0 = 0, \tag{6.6}$$

so that

$$f_0 = A_0(X)e^{i\tilde{x}} + \tilde{A}_0(X)e^{-i\tilde{x}}, \tag{6.7}$$

where $\tilde{x} = x - \varphi$, with $0 \leq \varphi < 2\pi$. Here, φ is an arbitrary constant which determines the relative phase between the fast oscillation and the slow amplitude modulation.

At $O(\epsilon)$, Eq. (6.4) gives

$$\mathcal{L}f_1 = -3E_{hg}f_0^2. \tag{6.8}$$

Using (6.7), we have

$$f_1 = -\frac{E_{hg}A_0^2e^{2i\tilde{x}}}{3} - \frac{E_{hg}\tilde{A}_0^2e^{-2i\tilde{x}}}{3} - 6E_{hg}|A_0|^2. \tag{6.9}$$

At $O\left(\epsilon^2\right)$, Eq. (6.4) gives

$$\mathcal{L}f_2 = 4\frac{\partial^2 f_0}{\partial X^2} - f_0^3 - f_0 - 6E_{hg}f_0f_1. \tag{6.10}$$

To avoid secular terms, the coefficients of $e^{\pm i\tilde{x}}$ on the right hand side must be zero, which gives the solvability condition

$$4\ddot{A}_0 + (38E_{hg}^2 - 3)|A_0|^2A_0 - A_0 = 0. \tag{6.11}$$

So far, the error made in approximating Eq. (6.2) using Eq. (6.11) is still lacking, which we address for future work. The energy method we presented in Chapters 3 and 4 should be readily applicable.

Now, consider Eq. (6.3), i.e., near the Maxwell point. This time we consider the slow scale as $X = \epsilon^2 x$. We develop a multiple scale solution

$$f \sim \sum_{n=0}^{N-1} \epsilon^n f_n(x, X) + R_N(x - \varphi, X). \tag{6.12}$$

We also expand

$$E_{hg} \sim E_0 + \epsilon E_1 + \epsilon^2 E_2 + \cdots + \delta E. \tag{6.13}$$

Now, substituting (6.12) into (6.3) and performing the same calculations as before, we will obtain the solvability condition at $O(\epsilon^4)$ to be given by

$$4\ddot{A}_0 + \frac{16i\dot{A}_0|A_0|^2}{19} - \frac{8820|A_0|^4 A_0}{361} + 2\sqrt{114}E_2|A_0|^2 A_0 - A_0 = 0. \tag{6.14}$$

Again, here we ask whether the energy method we used in the previous chapters can be applied in this case. Can we find an error bound and decrease the error? This question is particularly challenging because Eq. (6.14) admits a front solution that is not square integrable.

Bibliography

[1] Ablowitz, M. J. and Zhu, Y. (2013). Nonlinear dynamics of bloch wave packets in honeycomb lattices. In *Spontaneous Symmetry Breaking, Self-Trapping, and Josephson Oscillations*, pages 1–26. Springer.

[2] Achilleos, V., Álvarez, A., Cuevas, J., Frantzeskakis, D. J., Karachalios, N. I., Kevrekidis, P. G., and Sánchez-Rey, B. (2013). Escape dynamics in the discrete repulsive $\phi 4$ model. *Physica D: Nonlinear Phenomena*, 244(1):1–24.

[3] Akhiezer, N. I. and Glazman, I. M. (2013). *Theory of linear operators in Hilbert space*. Courier Corporation.

[4] Ali, A., Susanto, H., and Wattis, J. A. (2013). Rapidly oscillating ac-driven long josephson junctions with phase-shifts. *Physica D: Nonlinear Phenomena*, 246(1):15–22.

[5] Aschbacher, W., Frohlich, J., Graf, G., Schnee, K., and Troyer, M. (2002). Symmetry breaking regime in the nonlinear hartree equation. *Journal of Mathematical Physics*, 43(8):3879–3891.

[6] Ball, K. (2012). Functional analysis II. Lecture note.

[7] Bambusi, D., Paleari, S., and Penati, T. (2010). Existence and continuous approximation of small amplitude breathers in 1d and 2d Klein–Gordon lattices. *Applicable Analysis*, 89(9):1313–1334.

[8] Bambusi, D. and Ponno, A. (2006). On metastability in FPU. *Communications in mathematical physics*, 264(2):539–561.

[9] Barashenkov, I. and Smirnov, Y. S. (1996). Existence and stability chart for the ac-driven, damped nonlinear Schrödinger solitons. *Physical Review E*, 54(5):5707.

[10] Bender, C. M. and Orszag, S. A. (2013). *Advanced mathematical methods for scientists and engineers I: Asymptotic methods and perturbation theory*. Springer Science & Business Media.

[11] Berkolaiko, G. and Comech, A. (2012). On spectral stability of solitary waves of nonlinear dirac equation in 1d. *Reviews in Mathematical Physics*, 7(2):13–31.

[12] Berre, M. L., Ressayre, E., and Tallet, A. (1995). Why does a Ginzburg-Landau diffraction equation become a diffusion equation in the passive ring cavity? *Quantum and Semiclassical Optics: Journal of the European Optical Society Part B*, 7(1):1–4.

[13] Bidégaray-Fesquet, B., Dumas, E., and James, G. (2013). From Newton's cradle to the discrete p-Schrödinger equation. *SIAM Journal on Mathematical Analysis*, 45(6):3404–3430.

[14] Birnbaum, Z. and Malomed, B. (2008). *Physica D: Nonlinear Phenomena*, 237:3252–3262.

[15] Boudebs, G., Cherukulappurath, S., Leblond, H., Troles, J., Smektala, F., and Sanchez, F. (2003). Experimental and theoretical study of higher-order nonlinearities in chalcogenide glasses. *Optics Communications*, 219(1-6):427–433.

[16] Boyd, R. W. (2003). *Nonlinear optics*. Elsevier.

[17] Braun, O. M. and Kivshar, Y. S. (2004). *The Frenkel-Kontorova Model: Concepts, Methods, and Applications*. Springer Science & Business Media.

[18] Buks, E. and Roukes, M. L. (2002). Electrically tunable collective response in a coupled micromechanical array. *Journal of Microelectromechanical Systems*, 11(6):802–807.

[19] Castellani, E. (2003). On the meaning of symmetry breaking. *Symmetries in physics: Philosophical reflections*, pages 321–334.

[20] Cataliotti, F., Burger, S., Fort, C., Maddaloni, P., Minardi, F., Trombettoni, A., Smerzi, A., and Inguscio, M. (2001). Josephson junction arrays with Bose-Einstein condensates. *Science*, 293(5531):843–846.

[21] Chapman, S. J. and Kozyreff, G. (2009). Exponential asymptotics of localised patterns and snaking bifurcation diagrams. *Physica D: Nonlinear Phenomena*, 238(3):319–354.

[22] Chen, W. (2001). Linear functional analysis.

[23] Chris Eilbeck, J. and Johansson, M. (2003). The discrete nonlinear Schrödinger equation—20 years on. In *Localization and energy transfer in nonlinear systems*, pages 44–67. World Scientific.

[24] Christodoulides, D. and Joseph, R. (1988). Discrete self-focusing in nonlinear arrays of coupled waveguides. *Optics letters*, 13(9):794–796.

[25] Cuevas, J., English, L., Kevrekidis, P., and Anderson, M. (2009). Discrete breathers in a forced-damped array of coupled pendula: modeling, computation, and experiment. *Physical Review Letters*, 102(22):224101.

[26] Daumont, I., Dauxois, T., and Peyrard, M. (1997). Modulational instability: first step towards energy localization in nonlinear lattices. *Nonlinearity*, 10(3):617.

[27] Denardo, B., Galvin, B., Greenfield, A., Larraza, A., Putterman, S., and Wright, W. (1992a). Observations of localized structures in nonlinear lattices: Domain walls and kinks. *Physical Review Letters*, 68(5-6):1730.

[28] Denardo, B., Larraza, A., Putterman, S., and Roberts, P. (1992b). Nonlinear theory of localized standing waves. *Physical Review Letters*, 69(4):597.

[29] Diblík, J., Fečkan, M., Pospíšil, M., Rothos, V., and Susanto, H. (2014). Travelling waves in nonlinear magnetic metamaterials. In *Localized Excitations in Nonlinear Complex Systems*, pages 335–358. Springer.

[30] Dörfler, W., Lechleiter, A., Plum, M., Schneider, G., and Wieners, C. (2011). *Photonic crystals: Mathematical analysis and numerical approximation*, volume 42. Springer Science & Business Media.

[31] Dumas, E. and Pelinovsky, D. (2014). Justification of the log–KdV equation in granular chains: The case of precompression. *SIAM Journal on Mathematical Analysis*, 46(6):4075–4103.

[32] Eisenberg, H., Silberberg, Y., Morandotti, R., Boyd, A., and Aitchison, J. (1998). Discrete spatial optical solitons in waveguide arrays. *Physical Review Letters*, 81(16):3383.

[33] English, L. Q., Palmero, F., Candiani, P., Cuevas, J., Carretero-González, R., Kevrekidis, P. G., and Sievers, A. J. (2012). Generation of localized modes in an electrical lattice using subharmonic driving. *Physical review letters*, 108(8):084101.

[34] Erdős, L., Schlein, B., and Yau, H.-T. (2007). Rigorous derivation of the Gross-Pitaevskii equation. *Physical review letters*, 98(4):040404.

[35] Faye, G. (2011). An introduction to bifurcation theory. *NeuroMathComp Laboratory, INRIA, Sophia Antipolis, CNRS, ENS Paris, France*.

[36] Flach, S. (2004). Computational studies of discrete breathers. In *Energy Localisation And Transfer*, pages 1–71. World Scientific.

[37] Flach, S. and Gorbach, A. V. (2008). Discrete breathers advances in theory and applications. *Physics Reports*, 467(1):1–116.

[38] Flach, S. and Willis, C. R. (1998). Discrete breathers. *Physics reports*, 295(5):181–264.

[39] Friesecke, G. and Pego, R. L. (1999). Solitary waves on FPU lattices: I. qualitative properties, renormalization and continuum limit. *Nonlinearity*, 12(6):1601.

[40] Fujii, K. (2013). Introduction to the rotating wave approximation (rwa): two coherent oscillations. *arXiv preprint arXiv:1301.3585*.

[41] Gelfreich, V. (2015). Functional analysis 1. Lecture note.

[42] Gerlach, U. (2007). Linear mathematics in infinite dimensions. *Department of Mathematics, Ohaio*.

[43] Glotzer, S. (2000). Spatially heterogeneous dynamics in liquids: insights from simulation. *J. Non-Cryst. Solids*, 274:342.

[44] Goodman, R. M. (2013). Hamiltonian normal form expansions and application to NLS equations with multiple potentials. *Journal of Physics A: Mathematical and Theoretical*, 44:425101.

[45] Harrell, E. M. (1980). Double wells. *Communications in Mathematical Physics*, 75(3):239–261.

[46] Hennig, D. (1999). Periodic, quasiperiodic, and chaotic localized solutions of a driven, damped nonlinear lattice. *Physical Review E*, 59(2):1637.

[47] Hennig, D. and Tsironis, G. P. (1999). Wave transmission in nonlinear lattices. *Physics Reports*, 307(5):333–432.

[48] Jackson, R. K. and Weinstein, M. I. (2004). Geometric analysis of bifurcation and symmetry breaking in a Gross—Pitaevskii equation. *Journal of statistical physics*, 116(1-4):881–905.

[49] Johansson, M. (2006). Discrete nonlinear Schrödinger approximation of a mixed Klein–Gordon/Fermi–Pasta–Ulam chain: Modulational instability and a statistical condition for creation of thermodynamic breathers. *Physica D: Nonlinear Phenomena*, 216(1):62–70.

[50] Kapitula, T., Kevrekidis, P. G., and Chen, Z. (2006). Three is a crowd: Solitary waves in photorefractive media with three potential wells. *SIAM Journal on Applied Dynamical Systems*, 5(4):598–633.

[51] Kapitula, T. and Promislow, K. (2013). *Spectral and dynamical stability of nonlinear waves*. Springer.

[52] Kelley, W. G. and Peterson, A. C. (2010). *The theory of differential equations: classical and qualitative*. Springer Science & Business Media.

[53] Kenig, E., Malomed, B. A., Cross, M., and Lifshitz, R. (2009). Intrinsic localized modes in parametrically driven arrays of nonlinear resonators. *Physical Review E*, 80(4):046202.

[54] Kevorkian, J. K. and Cole, J. D. (2012). *Multiple scale and singular perturbation methods*, volume 114. Springer Science & Business Media.

[55] Kirr, E., Kevrekidis, P., and Pelinovsky, D. (2011). Symmetry-breaking bifurcation in the nonlinear Schrödinger equation with symmetric potentials. *Communications in mathematical physics*, 308(3):795–844.

[56] Kirr, E., Kevrekidis, P., Shlizerman, E., and Weinstein, M. I. (2008). Symmetry-breaking bifurcation in nonlinear Schrödinger/Gross–Pitaevskii equations. *SIAM Journal on Mathematical Analysis*, 40(2):566–604.

[57] Kirrmann, P., Schneider, G., and Mielke, A. (1992). The validity of modulation equations for extended systems with cubic nonlinearities. *Proceedings of the Royal Society of Edinburgh Section A: Mathematics*, 122(1-2):85–91.

[58] Kivshar, Y. S. (1993). Localized modes in a chain with nonlinear on-site potential. *Physics Letters A*, 173(2):172–178.

[59] Kivshar, Y. S. and Peyrard, M. (1992). Modulational instabilities in discrete lattices. *Physical Review A*, 46(6):3198.

[60] Kramer, P. (2013). *The Method of Multiple Scales for nonlinear Klein-Gordon and Schrödinger Equations*. PhD thesis, Karlsruhe Institute of Technology.

[61] L Herman, R. (2014). *A course in mathematical methods for physicist*. CRC Press.

[62] Lifshitz, R. and Cross, M. (2008). Nonlinear dynamics of nanomechanical and micromechanical resonators. *Review of nonlinear dynamics and complexity*, 1:1–52.

[63] Lifshitz, R. and Cross, M. C. (2003). Response of parametrically driven nonlinear coupled oscillators with application to micromechanical and nanomechanical resonator arrays. *Physical Review B*, 67(13):134302.

[64] MacKay, R. and Aubry, S. (1994). Proof of existence of breathers for time-reversible or Hamiltonian networks of weakly coupled oscillators. *Nonlinearity*, 7(6):1623.

[65] Malomed, B. A. (2013). *Spontaneous Symmetry Breaking, Self-Trapping, and Josephson Oscillations*. Springer.

[66] Mandel, P. (2005). *Theoretical problems in cavity nonlinear optics*, volume 21. Cambridge University Press.

[67] Marin, J., Falo, F., Martinez, P., and Floria, L. (2001). Discrete breathers in dissipative lattices. *Physical Review E*, 63(6):066603.

[68] Martınez, P., Meister, M., Floria, L., and Falo, F. (2003). Dissipative discrete breathers: Periodic, quasiperiodic, chaotic, and mobile. *Chaos: An Interdisciplinary Journal of Nonlinear Science*, 13(2):610–623.

[69] Marzuola, J. L. and Weinstein, M. I. (2009). Long time dynamics near the symmetry breaking bifurcation for nonlinear Schrödinger/Gross-Pitaevskii equations. *arXiv preprint arXiv:0912.1706*.

[70] Miransky, V. A. (1993). *Dynamical symmetry breaking in quantum field theories*. World Scientific.

[71] Moloney, J. V. and Newell, A. C. (2004). Nonlinear optics.

[72] Morgante, A. M., Johansson, M., Kopidakis, G., and Aubry, S. (2002). Standing wave instabilities in a chain of nonlinear coupled oscillators. *Physica D: Nonlinear Phenomena*, 162(1):53–94.

[73] N'Guérékata, G. M. and Pankov, A. (2010). Global well-posedness for discrete non-linear Schrödinger equation. *Applicable Analysis*, 89(9):1513–1521.

[74] Pacciani, P., Konotop, V., and Menzala, G. P. (2005). On localized solutions of discrete nonlinear Schrödinger equation: An exact result. *Physica D: Nonlinear Phenomena*, 204(1):122–133.

[75] Pelinovsky, D., Penati, T., and Paleari, S. (2016). Approximation of small-amplitude weakly coupled oscillators by discrete nonlinear Schrödinger equations. *Reviews in Mathematical Physics*, 28(07):1650015.

[76] Pelinovsky, D. and Phan, T. (2012). Normal form for the symmetry-breaking bifurcation in the nonlinear Schrödinger equation. *Journal of Differential Equations*, 253(10):2796–2824.

[77] Pelinovsky, D. and Sakovich, A. (2012). Multi-site breathers in Klein–Gordon lattices: stability, resonances and bifurcations. *Nonlinearity*, 25(12):3423.

[78] Pitaevskii, L. and Stringari, S. (2016). *Bose-Einstein condensation and superfluidity*, volume 164. Oxford University Press.

[79] Putterman, S. J. and Roberts, P. H. (1993). Nonlinear theory of modulated standing waves; domain walls, kinks and breathers. *Proc. R. Soc. Lond. A*, 440(1908):135–148.

[80] R Goodman, Marzuola, J. L. and I, W. M. (2015). Shadowing theorems for NLS equations with multiple well potentials. *Discrete and Continuous Dynamical Systems-A*, 35:225–246.

[81] Reed, M. and Simon, B. (1978). Analysis of operators, vol. iv of methods of modern mathematical physics.

[82] Sakovich, A. (2013). *Nonlinear waves in weakly-coupled lattices*. PhD thesis.

[83] Schneider, G. and Wayne, C. E. (2000). Counter-propagating waves on fluid surfaces and the continuum limit of the Fermi-Pasta-Ulam model. In *Equadiff 99: (In 2 Volumes)*, pages 390–404. World Scientific.

[84] Sideris, T. C. (2013). Ordinary differential equations and dynamical systems.

[85] Simon, B. and Dicke, A. (1970). Coupling constant analyticity for the anharmonic oscillator. *Annals of Physics*, 58(1):76–136.

[86] Susanto, H., Cuevas, J., and Krüger, P. (2011). Josephson tunnelling of dark solitons in a double-well potential. *Journal of Physics B: Atomic, Molecular and Optical Physics*, 44(9):095003.

[87] Susanto, H., Hoq, Q., and Kevrekidis, P. (2006). Stability of discrete solitons in the presence of parametric driving. *Physical Review E*, 74(6):067601.

[88] Syafwan, M., Susanto, H., and Cox, S. (2010). Discrete solitons in electromechanical resonators. *Physical Review E*, 81(2):026207.

[89] Syafwan, M., Susanto, H., and Cox, S. (2012). Solitons in a parametrically driven damped discrete nonlinear Schrödinger equation. In *Spontaneous Symmetry Breaking, Self-Trapping, and Josephson Oscillations*, pages 601–638. Springer.

[90] Terrones, G., McLaughlin, D. W., Overman, E. A., and Pearlstein, A. J. (1990). Stability and bifurcation of spatially coherent solutions of the damped-driven NLS equation. *SIAM Journal on Applied Mathematics*, 50(3):791–818.

[91] Trombettoni, A. and Smerzi, A. (2001). Discrete solitons and breathers with dilute Bose-Einstein condensates. *Physical Review Letters*, 86(11):2353.

[92] Tsilifis, P. A., Kevrekidis, P. G., and Rothos, V. M. (2013). Cubic–quintic long-range interactions with double well potentials. *Journal of Physics A: Mathematical and Theoretical*, 47(3):035201.

[93] Van Dyke, M. (1964). *Perturbation methods in fluid mechanics*, volume 136. Academic press New York.

[94] V.Z. Enolskii, Fatkhulla Kh. Abdullaev, V. V. K. e. (2005). *Nonlinear Waves: Classical and Quantum Aspects*. Springer Science & Business Media.

[95] Weder, R. (1999). The W k, p-continuity of the Schrödinger wave operators on the line. *Communications in Mathematical Physics*, 208(2):507–520.

[96] Zhan, C., Zhang, D., Zhu, D., Wang, D., Li, Y., Li, D., Lu, Z., Zhao, L., and Nie, Y. (2002). Third-and fifth-order optical nonlinearities in a new stilbazolium derivative. *JOSA B*, 19(3):369–375.

[97] Zhao, J.-H., Wang, H.-L., Li, B., and Zhou, H.-Q. (2010). Spontaneous symmetry breaking and bifurcations in ground-state fidelity for quantum lattice systems. *Physical Review E*, 82(6):061127.

Appendix A

The error for the finite dimensional ansatz

We assume we are near the symmetry breaking equilibrium point, meaning we may take $\alpha(t), \beta(t) \ll \Gamma(t)$ and $\Gamma(t) > 0$. Then, we have

$$
\begin{aligned}
(i\dot{\Gamma} - \dot{\theta}\Gamma - \Omega_0\Gamma)\psi_0 + (i\dot{\alpha} - \dot{\beta} - \dot{\theta}(\alpha + i\beta) - (\alpha + i\beta)\Omega_1)\psi_1 + i\dot{R} - HR - \dot{\theta}R = \\
-\Big[\Gamma^3\psi_0^3 + (\alpha^2+\beta^2)(\alpha+i\beta)\psi_1^3 + \Gamma(\alpha+i\beta)^2\psi_1^2\psi_0 + 2\Gamma(\alpha^2+\beta^2)\psi_1^2\psi_0 + \\
\Gamma^2(\alpha - i\beta)\psi_0^2\psi_1 + 2\Gamma^2(\alpha+i\beta)\psi_0^2\psi_1 - h\Gamma^5\psi_0^5 - h(\alpha^2+\beta^2)^2(\alpha+i\beta)\psi_1^5 - \\
h\Gamma^3(\alpha - i\beta)^2\psi_0^3\psi_1^2 - h\Gamma^2(\alpha+i\beta)^3\psi_0^2\psi_1^3 - 2h\Gamma^3(\alpha - i\beta)\psi_0^4\psi_1 - \\
2h\Gamma(\alpha^2+\beta^2)(\alpha+i\beta)^2\psi_0\psi_1^4 - 3h\Gamma^4(\alpha+i\beta)\psi_0^4\psi_1 - 3h\Gamma(\alpha^2+\beta^2)^2\psi_0\psi_1^4 - \\
3h\Gamma^3(\alpha+i\beta)^2\psi_0^3\psi_1^2 - 3h\Gamma^2(\alpha^2+\beta^2)(\alpha - i\beta)\psi_0^2\psi_1^3 - \\
6h\Gamma^2(\alpha^2+\beta^2)(\alpha+i\beta)\psi_0^2\psi_1^3 - 6h\Gamma^3(\alpha^2+\beta^2)\psi_0^3\psi_1^2\Big] \\
-\Big[2\Gamma^2\psi_0^2 + 4\Gamma\alpha\psi_0\psi_1 + 2(\alpha^2+\beta^2)\psi_1^2 - 3h\Gamma^4\psi_0^4 - 3h(\alpha^2+\beta^2)^2\psi_1^4 - \\
6h\Gamma^2(\alpha^2+\beta^2)\psi_0^2\psi_1^2 - 12h\Gamma^3\alpha\psi_0^3\psi_1 - 12h\Gamma(\alpha^3+\alpha\beta^2)\psi_0\psi_1^3 - 12h\Gamma^2(\alpha^2+\beta^2)\psi_0^2\psi_1^2\Big]R \\
-\Big[\Gamma^2\psi_0^2 + (\alpha+i\beta)^2\psi_1^2 + 2\Gamma(\alpha+i\beta)\psi_0\psi_1 - 2h\Gamma^4\psi_0^4 - 2h(\alpha^2+\beta^2)(\alpha+i\beta)^2\psi_1^4 - \\
2h\Gamma^3(\alpha - i\beta)\psi_0^3\psi_1 - 2h\Gamma(\alpha+i\beta)^3\psi_0\psi_1^3 - 12h\Gamma^2\alpha(\alpha+i\beta)\psi_0^2\psi_1^2 - \\
6h\Gamma^3(\alpha+i\beta)\psi_0^3\psi_1 - 6h\Gamma(\alpha^2+\beta^2)(\alpha+i\beta)\psi_0\psi_1^3\Big]\bar{R}
\end{aligned}
$$

$$-\Big[\Gamma\psi_0+(\alpha-i\beta)\psi_1-3h\Gamma(\alpha-i\beta)^2\psi_0\psi_1^2-3h\Gamma^2(\alpha+i\beta)\psi_0^2\psi_1-3h\Gamma^3\psi_0^3-$$
$$3h(\alpha^2+\beta^2)(\alpha-i\beta)\psi_1^3-6h\Gamma^2(\alpha-i\beta)\psi_0\psi_1-6h\Gamma(\alpha^2+\beta^2)\psi_0\psi_1^2\Big]R^2$$
$$-\Big[2\Gamma\psi_0+2(\alpha+i\beta)\psi_1-6h\Gamma^2(\alpha-i\beta)\psi_0^2\psi_1-6h\Gamma(\alpha+i\beta)^2\psi_0\psi_1^2-$$
$$6h\Gamma^3\psi_0^3-6h(\alpha^2+\beta^2)(\alpha+i\beta)\psi_1^3-12h\Gamma^2(\alpha+i\beta)\psi_0^2\psi_1-12h\Gamma(\alpha^2+\beta^2)\psi_0\psi_1^2\Big]|R|^2$$
$$-\Big[1-6h\Gamma^2\psi_0^2-6h(\alpha^2+\beta^2)\psi_1^2-12h\Gamma\alpha\psi_0\psi_1\Big]|R|^2R$$
$$+\Big[h\Gamma^3\psi_0^3+3h\Gamma^2(\alpha+i\beta)\psi_0^2\psi_1+3h\Gamma(\alpha+i\beta)^2\psi_0\psi_1^2+h(\alpha+i\beta)^3\psi_1^3\Big]\bar{R}^2$$
$$+\Big[h\bar{c}_0^2\psi_0^2+h\bar{c}_1^2\psi_1^2+2h\bar{c}_0\bar{c}_1\psi_0\psi_1\Big]R^3$$
$$+\Big[3h\Gamma^2\psi_0^2+3h(\alpha+i\beta)^2\psi_1^2+6h\Gamma(\alpha+i\beta)\psi_0\psi_1\Big]|R|^2\bar{R}$$
$$+\big[3h\Gamma\psi_0+3h(\alpha+i\beta)\psi_1\big]|R|^4+h|R|^4R$$

Hence,

$$\Big(i\dot{\Gamma}-\dot{\theta}\Gamma-\Omega_0\Gamma+\Gamma^3+\Gamma(\alpha+i\beta)^2+2\Gamma(\alpha^2+\beta^2)-h\Gamma^5-h\Gamma^3(\alpha-i\beta)^2-$$
$$2h\Gamma(\alpha^2+\beta^2)(\alpha+i\beta)^2-3h\Gamma(\alpha^2+\beta^2)^2-3h\Gamma^3(\alpha+i\beta)^2-6h\Gamma^3(\alpha^2+\beta^2)\Big)=$$
$$-\Big[\Gamma\langle\psi_0^2,R^2\rangle+(\alpha-i\beta)\langle\psi_0\psi_1,R^2\rangle-3h\Gamma(\alpha-i\beta)^2\langle\psi_0^2\psi_1^2,R^2\rangle-3h\Gamma^2(\alpha+i\beta)\langle\psi_0^3\psi_1,R^2\rangle-$$
$$3h\Gamma^3\langle\psi_0^4,R^2\rangle-3h(\alpha^2+\beta^2)(\alpha-i\beta)\langle\psi_0\psi_1^3,R^2\rangle-$$
$$6h\Gamma^2(\alpha-i\beta)\langle\psi_0^2\psi_1,R^2\rangle-6h\Gamma(\alpha^2+\beta^2)\langle\psi_0^2\psi_1^2,R^2\rangle\Big]$$
$$-\Big[2\Gamma\langle\psi_0^2,|R|^2\rangle+2(\alpha+i\beta)\langle\psi_0\psi_1,|R|^2\rangle-6h\Gamma^2(\alpha-i\beta)\langle\psi_0^3\psi_1,|R|^2\rangle-$$
$$6h\Gamma(\alpha+i\beta)^2\langle\psi_0^2\psi_1^2,|R|^2\rangle-6h\Gamma^3\langle\psi_0^4,|R|^2\rangle-6h(\alpha^2+\beta^2)(\alpha+i\beta)\langle\psi_0\psi_1^3,|R|^2\rangle-$$
$$12h\Gamma^2(\alpha+i\beta)\langle\psi_0^3\psi_1,|R|^2\rangle-12h\Gamma(\alpha^2+\beta^2)\langle\psi_0^2\psi_1^2,|R|^2\rangle\Big]$$
$$-\Big[\langle\psi_0,|R|^2R\rangle-6h\Gamma^2\langle\psi_0^3,|R|^2R\rangle-6h(\alpha^2+\beta^2)\langle\psi_0\psi_1^2,|R|^2R\rangle-12h\Gamma\alpha\langle\psi_0^2\psi_1,|R|^2R\rangle\Big]$$
$$+\Big[h\Gamma^3\langle\psi_0^4,\bar{R}^2\rangle+3h\Gamma^2(\alpha+i\beta)\langle\psi_0^3\psi_1,\bar{R}^2\rangle+3h\Gamma(\alpha+i\beta)^2\langle\psi_0^2\psi_1^2,\bar{R}^2\rangle+h(\alpha+i\beta)^3\langle\psi_0\psi_1^3,\bar{R}^2\rangle\Big]$$
$$+\Big[h\Gamma^2\langle\psi_0^3,R^3\rangle+h(\alpha-i\beta)^2\langle\psi_0\psi_1^2,R^3\rangle+2h\Gamma(\alpha-i\beta)\langle\psi_0^2\psi_1,R^3\rangle\Big]$$
$$+\Big[3h\Gamma^2\langle\psi_0^3,|R|^2\bar{R}\rangle+3h(\alpha+i\beta)^2\langle\psi_0\psi_1^2,|R|^2\bar{R}\rangle+6h\Gamma(\alpha+i\beta)\langle\psi_0^2\psi_1,|R|^2\bar{R}\rangle\Big]$$
$$+\Big[3h\Gamma\langle\psi_0^2,|R|^4\rangle+3h(\alpha+i\beta)\langle\psi_0\psi_1,|R|^4\rangle\Big]+\Big[h\langle\psi_0,|R|^4R\rangle\Big]$$

As a result, we have

$$\Big(i\dot{\alpha}-\dot{\beta}-\dot{\theta}(\alpha+i\beta)-(\alpha+i\beta)\Omega_1+(\alpha^2+\beta^2)(\alpha+i\beta)+\Gamma^2(\alpha-i\beta)+2\Gamma^2(\alpha+i\beta)-$$
$$h(\alpha^2+\beta^2)^2(\alpha+i\beta)-h\Gamma^2(\alpha+i\beta)^3-2h\Gamma^3(\alpha-i\beta)-3h\Gamma^4(\alpha+i\beta)-$$
$$3h\Gamma^2(\alpha^2+\beta^2)(\alpha-i\beta)-6h\Gamma^2(\alpha^2+\beta^2)(\alpha+i\beta)\Big)=$$
$$-\Big[\Gamma\langle\psi_0\psi_1,R^2\rangle+(\alpha-i\beta)\langle\psi_1^2,R^2\rangle-3h\Gamma(\alpha-i\beta)^2\langle\psi_0\psi_1^3,R^2\rangle-3h\Gamma^2(\alpha+i\beta)\langle\psi_0^2\psi_1^2,R^2\rangle-$$
$$3h\Gamma^3\langle\psi_0^3\psi_1,R^2\rangle-3h(\alpha^2+\beta^2)(\alpha-i\beta)\langle\psi_1^4,R^2\rangle-$$
$$6h\Gamma^2(\alpha-i\beta)\langle\psi_0\psi_1^2,R^2\rangle-6h\Gamma(\alpha^2+\beta^2)\langle\psi_0\psi_1^3,R^2\rangle\Big]$$
$$-\Big[2\Gamma\langle\psi_0\psi_1,|R|^2\rangle+2(\alpha+i\beta)\langle\psi_1^2,|R|^2\rangle-6h\Gamma^2(\alpha-i\beta)\langle\psi_0^2\psi_1^2,|R|^2\rangle-$$
$$6h\Gamma(\alpha+i\beta)^2\langle\psi_0\psi_1^3,|R|^2\rangle-6h\Gamma^3\langle\psi_0^3\psi_1,|R|^2\rangle-6h(\alpha^2+\beta^2)(\alpha+i\beta)\langle\psi_1^4,|R|^2\rangle-$$
$$12h\Gamma^2(\alpha+i\beta)\langle\psi_0^2\psi_1^2,|R|^2\rangle-12h\Gamma(\alpha^2+\beta^2)\langle\psi_0\psi_1^3,|R|^2\rangle\Big]$$
$$-\Big[\langle\psi_1,|R|^2R\rangle-6h\Gamma^2\langle\psi_0^2\psi_1,|R|^2R\rangle-6h(\alpha^2+\beta^2)\langle\psi_1^3,|R|^2R\rangle-12h\Gamma\alpha\langle\psi_0\psi_1^2,|R|^2R\rangle\Big]$$
$$+\Big[h\Gamma^3\langle\psi_0^3\psi_1,\bar{R}^2\rangle+3h\Gamma^2(\alpha+i\beta)\langle\psi_0^2\psi_1^2,\bar{R}^2\rangle+3h\Gamma(\alpha+i\beta)^2\langle\psi_0\psi_1^3,\bar{R}^2\rangle+h(\alpha+i\beta)^3\langle\psi_1^4,\bar{R}^2\rangle\Big]$$
$$+\Big[h\Gamma^2\langle\psi_0^2\psi_1,R^3\rangle+h(\alpha-i\beta)^2\langle\psi_1^3,R^3\rangle+2h\Gamma(\alpha-i\beta)\langle\psi_0\psi_1^2,R^3\rangle\Big]$$
$$+\Big[3h\Gamma^2\langle\psi_0^2\psi_1,|R|^2\bar{R}\rangle+3h(\alpha+i\beta)^2\langle\psi_1^3,|R|^2\bar{R}\rangle+6h\Gamma(\alpha+i\beta)\langle\psi_0\psi_1^2,|R|^2\bar{R}\rangle\Big]$$
$$+\Big[3h\Gamma\langle\psi_0\psi_1,|R|^4\rangle+3h(\alpha+i\beta)\langle\psi_1^2,|R|^4\rangle\Big]+\Big[h\langle\psi_1,|R|^4R\rangle\Big]$$

and

$$
\begin{aligned}
&iR_t - HR - \dot{\theta}R = \\
&-P_c\Big[\Gamma^3\psi_0^3 + (\alpha^2+\beta^2)(\alpha+i\beta)\psi_1^3 + \Gamma(\alpha+i\beta)^2\psi_1^2\psi_0 + 2\Gamma(\alpha^2+\beta^2)\psi_1^2\psi_0 + \\
&\Gamma^2(\alpha-i\beta)\psi_0^2\psi_1 + 2\Gamma^2(\alpha+i\beta)\psi_0^2\psi_1 - h\Gamma^5\psi_0^5 - h(\alpha^2+\beta^2)^2(\alpha+i\beta)\psi_1^5 - \\
&h\Gamma^3(\alpha-i\beta)^2\psi_0^3\psi_1^2 - h\Gamma^2(\alpha+i\beta)^3\psi_0^2\psi_1^3 - 2h\Gamma^3(\alpha-i\beta)\psi_0^4\psi_1 - \\
&2h\Gamma(\alpha^2+\beta^2)(\alpha+i\beta)^2\psi_0\psi_1^4 - 3h\Gamma^4(\alpha+i\beta)\psi_0^4\psi_1 - 3h\Gamma(\alpha^2+\beta^2)^2\psi_0\psi_1^4 - \\
&3h\Gamma^3(\alpha+i\beta)^2\psi_0^3\psi_1^2 - 3h\Gamma^2(\alpha^2+\beta^2)(\alpha-i\beta)\psi_0^2\psi_1^3 - \\
&6h\Gamma^2(\alpha^2+\beta^2)(\alpha+i\beta)\psi_0^2\psi_1^3 - 6h\Gamma^3(\alpha^2+\beta^2)\psi_0^3\psi_1^2\Big] \\
&-P_c\Big[2\Gamma^2\psi_0^2 + 4\Gamma\alpha\psi_0\psi_1 + 2(\alpha^2+\beta^2)\psi_1^2 - 3h\Gamma^4\psi_0^4 - 3h(\alpha^2+\beta^2)^2\psi_1^4 - \\
&6h\Gamma^2(\alpha^2+\beta^2)\psi_0^2\psi_1^2 - 12h\Gamma^3\alpha\psi_0^3\psi_1 - 12h\Gamma(\alpha^3+\alpha\beta^2)\psi_0\psi_1^3 - 12h\Gamma^2(\alpha^2+\beta^2)\psi_0^2\psi_1^2\Big]R \\
&-P_c\Big[\Gamma^2\psi_0^2 + (\alpha+i\beta)^2\psi_1^2 + 2\Gamma(\alpha+i\beta)\psi_0\psi_1 - 2h\Gamma^4\psi_0^4 - 2h(\alpha^2+\beta^2)(\alpha+i\beta)^2\psi_1^4 - \\
&2h\Gamma^3(\alpha-i\beta)\psi_0^3\psi_1 - 2h\Gamma(\alpha+i\beta)^3\psi_0\psi_1^3 - 12h\Gamma^2\alpha(\alpha+i\beta)\psi_0^2\psi_1^2 - \\
&6h\Gamma^3(\alpha+i\beta)\psi_0^3\psi_1 - 6h\Gamma(\alpha^2+\beta^2)(\alpha+i\beta)\psi_0\psi_1^3\Big]\bar{R} \\
&-P_c\Big[\Gamma\psi_0 + (\alpha-i\beta)\psi_1 - 3h\Gamma(\alpha-i\beta)^2\psi_0\psi_1^2 - 3h\Gamma^2(\alpha+i\beta)\psi_0^2\psi_1 - 3h\Gamma^3\psi_0^3 - \\
&3h(\alpha^2+\beta^2)(\alpha-i\beta)\psi_1^3 - 6h\Gamma^2(\alpha-i\beta)\psi_0\psi_1 - 6h\Gamma(\alpha^2+\beta^2)\psi_0\psi_1^2\Big]R^2 \\
&-P_c\Big[2\Gamma\psi_0 + 2(\alpha+i\beta)\psi_1 - 6h\Gamma^2(\alpha-i\beta)\psi_0^2\psi_1 - 6h\Gamma(\alpha+i\beta)^2\psi_0\psi_1^2 - \\
&6h\Gamma^3\psi_0^3 - 6h(\alpha^2+\beta^2)(\alpha+i\beta)\psi_1^3 - 12h\Gamma^2(\alpha+i\beta)\psi_0^2\psi_1 - 12h\Gamma(\alpha^2+\beta^2)\psi_0\psi_1^2\Big]|R|^2 \\
&-P_c\Big[1 - 6h\Gamma^2\psi_0^2 - 6h(\alpha^2+\beta^2)\psi_1^2 - 12h\Gamma\alpha\psi_0\psi_1\Big]|R|^2R \\
&+P_c\Big[h\Gamma^3\psi_0^3 + 3h\Gamma^2(\alpha+i\beta)\psi_0^2\psi_1 + 3h\Gamma(\alpha+i\beta)^2\psi_0\psi_1^2 + h(\alpha+i\beta)^3\psi_1^3\Big]\bar{R}^2 \\
&+P_c\Big[h\bar{c}_0^2\psi_0^2 + h\bar{c}_1^2\psi_1^2 + 2h\bar{c}_0\bar{c}_1\psi_0\psi_1\Big]R^3 \\
&+P_c\Big[3h\Gamma^2\psi_0^2 + 3h(\alpha+i\beta)^2\psi_1^2 + 6h\Gamma(\alpha+i\beta)\psi_0\psi_1\Big]|R|^2\bar{R} \\
&+P_c\big[3h\Gamma\psi_0 + 3h(\alpha+i\beta)\psi_1\big]|R|^4 + P_c\Big[h|R|^4R\Big]
\end{aligned}
$$

or

$$iR_t - HR - \dot{\theta}R = [F_b(A,\alpha,\beta,\theta) + F_R(A,\alpha,\beta,\theta;R,\bar{R})],$$

where we have assumed

$$P_c F_b = F_b,\ P_c F_R = F_R.$$

Let us take $\Gamma > 0$. Then, we see

$$\begin{aligned}
\dot{\Gamma} &= \left[-2\alpha\beta + 32h\alpha\beta^3 + 32h\alpha^3\beta + 32h\alpha\beta\Gamma^2\right]\Gamma + \mathrm{Error}'_\Gamma \\
\dot{\alpha} &= \left[\Omega_1 - (\alpha^2+\beta^2) - \Gamma^2 + \dot{\theta} + 8h(\alpha^4+\beta^4) + 16h\beta^2(\alpha^2+\Gamma^2) + 8h\Gamma^2(6\alpha^2+\Gamma^2)\right]\beta \\
&\quad + \mathrm{Error}'_\alpha, \\
\dot{\beta} &= -\left[\Omega_1 - (\alpha^2+\beta^2+\Gamma^2) - 2\Gamma^2 + \dot{\theta} + 8h(\alpha^4+\beta^4) + 16h(\alpha^2\beta^2 + 3\beta^2\Gamma^2 + 5\alpha^2\Gamma^2)\right. \\
&\quad \left. + 40h\Gamma^4\right]\alpha + \mathrm{Error}'_\beta, \\
\Gamma\dot{\theta} &= -\Omega_0\Gamma + \Gamma^3 + (3\alpha^2+\beta^2)\Gamma - 8h(\beta^4+\Gamma^4+5\alpha^4)\Gamma - 16h(\beta^2\Gamma^2 + 3\alpha^2\beta^2 + 5\alpha^2\Gamma^2)\Gamma \\
&\quad + \mathrm{Error}'_\theta,
\end{aligned}$$

$$i\dot{R} - HR - \dot{\theta}R = F_b(\Gamma,\alpha,\beta) + F_R(\Gamma,\alpha,\beta;R,\bar{R}).$$

Specifically, we have (3.20) - (3.20e) with

$$\begin{aligned}
\mathrm{Error}_\Gamma(R,\bar{R},\vec{\alpha}) = \Im\Big(-\Big\langle\Big[&2\Gamma^2\psi_0^3 + 4\Gamma\alpha\psi_0^2\psi_1 + 2(\alpha^2+\beta^2)\psi_1^2\psi_0 - 3h\Gamma^4\psi_0^5 - 3h(\alpha^2+\beta^2)^2\psi_0\psi_1^4 \\
&- 6h\Gamma^2(\alpha^2+\beta^2)\psi_0^3\psi_1^2 - 12h\Gamma^3\alpha\psi_0^4\psi_1 - 12h\Gamma(\alpha^3+\alpha\beta^2)\psi_0^2\psi_1^3 \\
&- 12h\Gamma^2(\alpha^2+\beta^2)\psi_0^3\psi_1^2\Big], R\Big\rangle - \Big\langle\Big[\Gamma^2\psi_0^3 + (\alpha+i\beta)^2\psi_1^2\psi_0 + 2\Gamma(\alpha+i\beta)\psi_0^2\psi_1 \\
&- 2h\Gamma^4\psi_0^5 - 2h(\alpha^2+\beta^2)(\alpha+i\beta)^2\psi_0\psi_1^4 - 2h\Gamma^3(\alpha-i\beta)\psi_0^4\psi_1 \\
&- 2h\Gamma(\alpha+i\beta)^3\psi_0^2\psi_1^3 - 12h\Gamma^2\alpha(\alpha+i\beta)\psi_0^3\psi_1^2 - 6h\Gamma^3(\alpha+i\beta)\psi_0^4\psi_1 \\
&- 6h\Gamma(\alpha^2+\beta^2)(\alpha+i\beta)\psi_0^2\psi_1^3\Big], \bar{R}\Big\rangle
\end{aligned}$$

$$
\begin{aligned}
&-\left\langle\left[\Gamma\psi_0^2+(\alpha-i\beta)\psi_0\psi_1-3h\Gamma(\alpha-i\beta)^2\psi_0^2\psi_1^2-3h\Gamma^2(\alpha+i\beta)\psi_0^3\psi_1-3h\Gamma^3\psi_0^4\right.\right.\\
&\quad\left.\left.-\,3h(\alpha^2+\beta^2)(\alpha-i\beta)\psi_0\psi_1^3-6h\Gamma^2(\alpha-i\beta)\psi_0^2\psi_1-6h\Gamma(\alpha^2+\beta^2)\psi_0^2\psi_1^2\right],R^2\right\rangle\\
&-\left\langle\left[2\Gamma\psi_0^2+2(\alpha+i\beta)\psi_0\psi_1-6h\Gamma^2(\alpha-i\beta)\psi_0^3\psi_1-6h\Gamma(\alpha+i\beta)^2\psi_0^2\psi_1^2-6h\Gamma^3\psi_0^4\right.\right.\\
&\quad\left.\left.-\,6h(\alpha^2+\beta^2)(\alpha+i\beta)\psi_0\psi_1^3-12h\Gamma^2(\alpha+i\beta)\psi_0^3\psi_1-12h\Gamma(\alpha^2+\beta^2)\psi_0\psi_1^3\right],|R|^2\right\rangle\\
&-\left\langle\left[\psi_0-6h\Gamma^2\psi_0^3-6h(\alpha^2+\beta^2)\psi_0\psi_1^2-12h\Gamma\alpha\psi_0^2\psi_1\right],|R|^2R\right\rangle\\
&+\left\langle\left[h\Gamma^3\psi_0^4+3h\Gamma^2(\alpha+i\beta)\psi_0^3\psi_1+3h\Gamma(\alpha+i\beta)^2\psi_0^2\psi_1^2+h(\alpha+i\beta)^3\psi_0\psi_1^3\right],\bar{R}^2\right\rangle\\
&+\left\langle\left[h\Gamma^2\psi_0^3+h(\alpha-i\beta)^2\psi_0\psi_1^2+2h\Gamma(\alpha-i\beta)\psi_0^2\psi_1\right],R^3\right\rangle\\
&+\left\langle\left[3h\Gamma^2\psi_0^3+3h(\alpha+i\beta)^2\psi_0\psi_1^2+6h\Gamma(\alpha+i\beta)\psi_0^2\psi_1\right],|R|^2\bar{R}\right\rangle\\
&+\left\langle\left[3h\Gamma\psi_0^2+3h(\alpha+i\beta)\psi_0\psi_1\right],|R|^4\right\rangle+\left\langle h\psi_0,|R|^4R\right\rangle\Big),
\end{aligned}
$$

$$
\begin{aligned}
\mathrm{Error}_\alpha(R,\bar{R},\vec{\alpha}) =\mathrm{Im}\Big(&-\left\langle\left[2\Gamma^2\psi_0^2\psi_1+4\Gamma\alpha\psi_0\psi_1^2+2(\alpha^2+\beta^2)\psi_1^3-3h\Gamma^4\psi_0^4\psi_1-3h(\alpha^2+\beta^2)^2\psi_1^5\right.\right.\\
&\quad\left.\left.-\,6h\Gamma^2(\alpha^2+\beta^2)\psi_0^2\psi_1^3-12h\Gamma^3\alpha\psi_0^3\psi_1^2-12h\Gamma(\alpha^3+\alpha\beta^2)\psi_0\psi_1^4\right.\right.\\
&\quad\left.\left.-\,12h\Gamma(\alpha^3+\alpha\beta^2)\psi_0\psi_1^4-12h\Gamma^2(\alpha^2+\beta^2)\psi_0^2\psi_1^3\right],R\right\rangle\\
&-\left\langle\left[\Gamma^2\psi_0^2\psi_1+(\alpha+i\beta)^2\psi_1^3+2\Gamma(\alpha+i\beta)\psi_0\psi_1^2-2h\Gamma^4\psi_0^4\psi_1-2h(\alpha^2+\beta^2)(\alpha+i\beta)^2\psi_1^5\right.\right.\\
&\quad\left.\left.-\,2h\Gamma^3(\alpha-i\beta)\psi_0^3\psi_1^2-2h\Gamma(\alpha+i\beta)^3\psi_0\psi_1^4-12h\Gamma^2\alpha(\alpha+i\beta)\psi_0^2\psi_1^3\right.\right.\\
&\quad\left.\left.-\,6h\Gamma^3(\alpha+i\beta)\psi_0^3\psi_1^2-6h\Gamma(\alpha^2+\beta^2)(\alpha+i\beta)\psi_0\psi_1^4\right],\bar{R}\right\rangle\\
&-\left\langle\left[\Gamma\psi_0\psi_1+(\alpha-i\beta)\psi_1^2-3h\Gamma(\alpha-i\beta)^2\psi_0\psi_1^3-3h\Gamma^2(\alpha+i\beta)\psi_0^2\psi_1^2-3h\Gamma^3\psi_0^3\psi_1\right.\right.\\
&\quad\left.\left.-\,3h(\alpha^2+\beta^2)(\alpha-i\beta)\psi_1^4-6h\Gamma^2(\alpha-i\beta)\psi_0\psi_1^2-6h\Gamma(\alpha^2+\beta^2)\psi_0\psi_1^3\right],R^2\right\rangle\\
&-\left\langle\left[2\Gamma\psi_0\psi_1+2(\alpha+i\beta)\psi_1^2-6h\Gamma^2(\alpha-i\beta)\psi_0^2\psi_1^2-6h\Gamma(\alpha+i\beta)^2\psi_0\psi_1^3-6h\Gamma^3\psi_0^3\psi_1\right.\right.\\
&\quad\left.\left.-\,6h(\alpha^2+\beta^2)(\alpha+i\beta)\psi_1^4-12h\Gamma^2(\alpha+i\beta)\psi_0^2\psi_1^2-12h\Gamma(\alpha^2+\beta^2)\psi_1^4\right],|R|^2\right\rangle\\
&-\left\langle\left[\psi_1-6h\Gamma^2\psi_0^2\psi_1-6h(\alpha^2+\beta^2)\psi_1^3-12h\Gamma\alpha\psi_0\psi_1^2\right],|R|^2R\right\rangle\\
&+\left\langle\left[h\Gamma^3\psi_0^3\psi_1+3h\Gamma^2(\alpha+i\beta)\psi_0^2\psi_1^2+3h\Gamma(\alpha+i\beta)^2\psi_0\psi_1^3+h(\alpha+i\beta)^3\psi_1^4\right],\bar{R}^2\right\rangle\\
&+\left\langle\left[h\Gamma^2\psi_0^2\psi_1+h(\alpha-i\beta)^2\psi_1^3+2h\Gamma(\alpha-i\beta)\psi_0\psi_1^2\right],R^3\right\rangle\\
&+\left\langle\left[3h\Gamma^2\psi_0^2\psi_1+3h(\alpha+i\beta)^2\psi_1^3+6h\Gamma(\alpha+i\beta)\psi_0\psi_1^2\right],|R|^2\bar{R}\right\rangle
\end{aligned}
$$

$$
\begin{aligned}
&+\left\langle\left[3h\Gamma\psi_0\psi_1+3h(\alpha+i\beta)\psi_1^2\right],|R|^4\right\rangle+\left\langle h\psi_1,|R|^4R\right\rangle\Big)\\
&-\beta\Gamma^{-1}\mathrm{Re}\Big(-\Big\langle\Big[2\Gamma^2\psi_0^3+4\Gamma\alpha\psi_0^2\psi_1+2(\alpha^2+\beta^2)\psi_1^2\psi_0-3h\Gamma^4\psi_0^5\\
&\quad-3h(\alpha^2+\beta^2)^2\psi_0\psi_1^4-6h\Gamma^2(\alpha^2+\beta^2)\psi_0^3\psi_1^2-12h\Gamma^3\alpha\psi_0^4\psi_1\\
&\quad-12h\Gamma(\alpha^3+\alpha\beta^2)\psi_0^2\psi_1^3-12h\Gamma^2(\alpha^2+\beta^2)\psi_0^3\psi_1^2\Big],R\Big\rangle\\
&-\Big\langle\Big[\Gamma^2\psi_0^3+(\alpha+i\beta)^2\psi_1^2\psi_0+2\Gamma(\alpha+i\beta)\psi_0^2\psi_1-2h\Gamma^4\psi_0^5\\
&\quad-2h(\alpha^2+\beta^2)(\alpha+i\beta)^2\psi_0\psi_1^4-2h\Gamma^3(\alpha-i\beta)\psi_0^4\psi_1-2h\Gamma(\alpha+i\beta)^3\psi_0^2\psi_1^3\\
&\quad-12h\Gamma^2\alpha(\alpha+i\beta)\psi_0^3\psi_1^2-6h\Gamma^3(\alpha+i\beta)\psi_0^4\psi_1-6h\Gamma(\alpha^2+\beta^2)(\alpha+i\beta)\psi_0^2\psi_1^3\Big],\bar{R}\Big\rangle\\
&-\Big\langle\Big[\Gamma\psi_0^2+(\alpha-i\beta)\psi_0\psi_1-3h\Gamma(\alpha-i\beta)^2\psi_0^2\psi_1^2-3h\Gamma^2(\alpha+i\beta)\psi_0^3\psi_1-3h\Gamma^3\psi_0^4\\
&\quad-3h(\alpha^2+\beta^2)(\alpha-i\beta)\psi_0\psi_1^3-6h\Gamma^2(\alpha-i\beta)\psi_0^2\psi_1-6h\Gamma(\alpha^2+\beta^2)\psi_0^2\psi_1^2\Big],R^2\Big\rangle\\
&-\Big\langle\Big[2\Gamma\psi_0^2+2(\alpha+i\beta)\psi_0\psi_1-6h\Gamma^2(\alpha-i\beta)\psi_0^3\psi_1-6h\Gamma(\alpha+i\beta)^2\psi_0^2\psi_1^2-6h\Gamma^3\psi_0^4\\
&\quad-6h(\alpha^2+\beta^2)(\alpha+i\beta)\psi_0\psi_1^3-12h\Gamma^2(\alpha+i\beta)\psi_0^3\psi_1-12h\Gamma(\alpha^2+\beta^2)\psi_0\psi_1^3\Big],|R|^2\Big\rangle\\
&-\Big\langle\Big[\psi_0-6h\Gamma^2\psi_0^3-6h(\alpha^2+\beta^2)\psi_0\psi_1^2-12h\Gamma\alpha\psi_0^2\psi_1\Big],|R|^2R\Big\rangle\\
&+\Big\langle\Big[h\Gamma^3\psi_0^4+3h\Gamma^2(\alpha+i\beta)\psi_0^3\psi_1+3h\Gamma(\alpha+i\beta)^2\psi_0^2\psi_1^2+h(\alpha+i\beta)^3\psi_0\psi_1^3\Big],\bar{R}^2\Big\rangle\\
&+\Big\langle\Big[h\Gamma^2\psi_0^3+h(\alpha-i\beta)^2\psi_0\psi_1^2+2h\Gamma(\alpha-i\beta)\psi_0^2\psi_1\Big],R^3\Big\rangle\\
&+\Big\langle\Big[3h\Gamma^2\psi_0^3+3h(\alpha+i\beta)^2\psi_0\psi_1^2+6h\Gamma(\alpha+i\beta)\psi_0^2\psi_1\Big],|R|^2\bar{R}\Big\rangle\\
&+\Big\langle\Big[3h\Gamma\psi_0^2+3h(\alpha+i\beta)\psi_0\psi_1\Big],|R|^4\Big\rangle+\langle h\psi_0,|R|^4R\rangle\Big),
\end{aligned}
$$

$$
\begin{aligned}
\mathrm{Error}_\beta(R,\bar{R},\vec{\alpha}) = &-\mathrm{Re}\Big(-\Big\langle\Big[2\Gamma^2\psi_0^2\psi_1+4\Gamma\alpha\psi_0\psi_1^2+2(\alpha^2+\beta^2)\psi_1^3-3h\Gamma^4\psi_0^4\psi_1\\
&\quad-3h(\alpha^2+\beta^2)^2\psi_1^5-6h\Gamma^2(\alpha^2+\beta^2)\psi_0^2\psi_1^3-12h\Gamma^3\alpha\psi_0^3\psi_1^2\\
&\quad-12h\Gamma(\alpha^3+\alpha\beta^2)\psi_0\psi_1^4-12h\Gamma^2(\alpha^2+\beta^2)\psi_0^2\psi_1^3\Big],R\Big\rangle\\
&-\Big\langle\Big[\Gamma^2\psi_0^2\psi_1+(\alpha+i\beta)^2\psi_1^3+2\Gamma(\alpha+i\beta)\psi_0\psi_1^2-2h\Gamma^4\psi_0^4\psi_1\\
&\quad-2h(\alpha^2+\beta^2)(\alpha+i\beta)^2\psi_1^5-2h\Gamma^3(\alpha-i\beta)\psi_0^3\psi_1^2-2h\Gamma(\alpha+i\beta)^3\psi_0\psi_1^4\\
&\quad-12h\Gamma^2\alpha(\alpha+i\beta)\psi_0^2\psi_1^3-6h\Gamma^3(\alpha+i\beta)\psi_0^3\psi_1^2-6h\Gamma(\alpha^2+\beta^2)(\alpha+i\beta)\psi_0\psi_1^4\Big],\bar{R}\Big\rangle\\
&-\Big\langle\Big[\Gamma\psi_0\psi_1+(\alpha-i\beta)\psi_1^2-3h\Gamma(\alpha-i\beta)^2\psi_0\psi_1^3-3h\Gamma^2(\alpha+i\beta)\psi_0^2\psi_1^2-3h\Gamma^3\psi_0^3\psi_1
\end{aligned}
$$

$$
\begin{aligned}
&- 3h(\alpha^2+\beta^2)(\alpha-i\beta)\psi_1^4 - 6h\Gamma^2(\alpha-i\beta)\psi_0\psi_1^2 - 6h\Gamma(\alpha^2+\beta^2)\psi_0\psi_1^3\Big], R^2\Big\rangle \\
&- \Big\langle\Big[2\Gamma\psi_0\psi_1 + 2(\alpha+i\beta)\psi_1^2 - 6h\Gamma^2(\alpha-i\beta)\psi_0^2\psi_1^2 - 6h\Gamma(\alpha+i\beta)^2\psi_0\psi_1^3 - 6h\Gamma^3\psi_0^3\psi_1 \\
&\quad - 6h(\alpha^2+\beta^2)(\alpha+i\beta)\psi_1^4 - 12h\Gamma^2(\alpha+i\beta)\psi_0^2\psi_1^2 - 12h\Gamma(\alpha^2+\beta^2)\psi_1^4\Big], |R|^2\Big\rangle \\
&- \Big\langle\Big[\psi_1 - 6h\Gamma^2\psi_0^2\psi_1 - 6h(\alpha^2+\beta^2)\psi_1^3 - 12h\Gamma\alpha\psi_0\psi_1^2\Big], |R|^2 R\Big\rangle \\
&+ \Big\langle\Big[h\Gamma^3\psi_0^3\psi_1 + 3h\Gamma^2(\alpha+i\beta)\psi_0^2\psi_1^2 + 3h\Gamma(\alpha+i\beta)^2\psi_0\psi_1^3 + h(\alpha+i\beta)^3\psi_1^4\Big], \bar{R}^2\Big\rangle \\
&+ \Big\langle\Big[h\Gamma^2\psi_0^2\psi_1 + h(\alpha-i\beta)^2\psi_1^3 + 2h\Gamma(\alpha-i\beta)\psi_0\psi_1^2\Big], R^3\Big\rangle \\
&+ \Big\langle\Big[3h\Gamma^2\psi_0^2\psi_1 + 3h(\alpha+i\beta)^2\psi_1^3 + 6h\Gamma(\alpha+i\beta)\psi_0\psi_1^2\Big], |R|^2\bar{R}\Big\rangle \\
&+ \Big\langle\Big[3h\Gamma\psi_0\psi_1 + 3h(\alpha+i\beta)\psi_1^2\Big], |R|^4\Big\rangle + \langle h\psi_1, |R|^4 R\rangle\Big) \\
&-\alpha\Gamma^{-1}\mathrm{Re}\Big(-\Big\langle\Big[2\Gamma^2\psi_0^3 + 4\Gamma\alpha\psi_0^2\psi_1 + 2(\alpha^2+\beta^2)\psi_1^2\psi_0 - 3h\Gamma^4\psi_0^5 \\
&\quad - 3h(\alpha^2+\beta^2)^2\psi_0\psi_1^4 - 6h\Gamma^2(\alpha^2+\beta^2)\psi_0^3\psi_1^2 - 12h\Gamma^3\alpha\psi_0^4\psi_1 \\
&\quad - 12h\Gamma(\alpha^3+\alpha\beta^2)\psi_0^2\psi_1^3 - 12h\Gamma^2(\alpha^2+\beta^2)\psi_0^3\psi_1^2\Big], R\Big\rangle \\
&- \Big\langle\Big[\Gamma^2\psi_0^3 + (\alpha+i\beta)^2\psi_1^2\psi_0 + 2\Gamma(\alpha+i\beta)\psi_0^2\psi_1 - 2h\Gamma^4\psi_0^5 \\
&\quad - 2h(\alpha^2+\beta^2)(\alpha+i\beta)^2\psi_0\psi_1^4 - 2h\Gamma^3(\alpha-i\beta)\psi_0^4\psi_1 - 2h\Gamma(\alpha+i\beta)^3\psi_0^2\psi_1^3 \\
&\quad - 12h\Gamma^2\alpha(\alpha+i\beta)\psi_0^3\psi_1^2 - 6h\Gamma^3(\alpha+i\beta)\psi_0^4\psi_1 - 6h\Gamma(\alpha^2+\beta^2)(\alpha+i\beta)\psi_0^2\psi_1^3\Big], \bar{R}\Big\rangle \\
&- \Big\langle\Big[\Gamma\psi_0^2 + (\alpha-i\beta)\psi_0\psi_1 - 3h\Gamma(\alpha-i\beta)^2\psi_0^2\psi_1^2 - 3h\Gamma^2(\alpha+i\beta)\psi_0^3\psi_1 - 3h\Gamma^3\psi_0^4 \\
&\quad - 3h(\alpha^2+\beta^2)(\alpha-i\beta)\psi_0\psi_1^3 - 6h\Gamma^2(\alpha-i\beta)\psi_0^2\psi_1 - 6h\Gamma(\alpha^2+\beta^2)\psi_0^2\psi_1^2\Big], R^2\Big\rangle \\
&- \Big\langle\Big[2\Gamma\psi_0^2 + 2(\alpha+i\beta)\psi_0\psi_1 - 6h\Gamma^2(\alpha-i\beta)\psi_0^3\psi_1 - 6h\Gamma(\alpha+i\beta)^2\psi_0^2\psi_1^2 - 6h\Gamma^3\psi_0^4 \\
&\quad - 6h(\alpha^2+\beta^2)(\alpha+i\beta)\psi_0\psi_1^3 - 12h\Gamma^2(\alpha+i\beta)\psi_0^3\psi_1 - 12h\Gamma(\alpha^2+\beta^2)\psi_0\psi_1^3\Big], |R|^2\Big\rangle \\
&- \Big\langle\Big[\psi_0 - 6h\Gamma^2\psi_0^3 - 6h(\alpha^2+\beta^2)\psi_0\psi_1^2 - 12h\Gamma\alpha\psi_0^2\psi_1\Big], |R|^2 R\Big\rangle \\
&+ \Big\langle\Big[h\Gamma^3\psi_0^4 + 3h\Gamma^2(\alpha+i\beta)\psi_0^3\psi_1 + 3h\Gamma(\alpha+i\beta)^2\psi_0^2\psi_1^2 + h(\alpha+i\beta)^3\psi_0\psi_1^3\Big], \bar{R}^2\Big\rangle \\
&+ \Big\langle\Big[h\Gamma^2\psi_0^3 + h(\alpha-i\beta)^2\psi_0\psi_1^2 + 2h\Gamma(\alpha-i\beta)\psi_0^2\psi_1\Big], R^3\Big\rangle \\
&+ \Big\langle\Big[3h\Gamma^2\psi_0^3 + 3h(\alpha+i\beta)^2\psi_0\psi_1^2 + 6h\Gamma(\alpha+i\beta)\psi_0^2\psi_1\Big], |R|^2\bar{R}\Big\rangle \\
&+ \Big\langle\Big[3h\Gamma\psi_0^2 + 3h(\alpha+i\beta)\psi_0\psi_1\Big], |R|^4\Big\rangle + \langle h\psi_0, |R|^4 R\rangle\Big),
\end{aligned}
$$

and

$$
\begin{aligned}
\mathrm{Error}_{\theta}(R,\bar{R},\vec{\alpha}) = &-\Gamma^{-1}\mathrm{Re}\Big(-\Big\langle\Big[2\Gamma^2\psi_0^3+4\Gamma\alpha\psi_0^2\psi_1+2(\alpha^2+\beta^2)\psi_1^2\psi_0-3h\Gamma^4\psi_0^5\\
&-\ 3h(\alpha^2+\beta^2)^2\psi_0\psi_1^4-6h\Gamma^2(\alpha^2+\beta^2)\psi_0^3\psi_1^2-12h\Gamma^3\alpha\psi_0^4\psi_1\\
&-\ 12h\Gamma(\alpha^3+\alpha\beta^2)\psi_0^2\psi_1^3-12h\Gamma^2(\alpha^2+\beta^2)\psi_0^3\psi_1^2\Big],R\Big\rangle\\
&-\Big\langle\Big[\Gamma^2\psi_0^3+(\alpha+i\beta)^2\psi_1^2\psi_0+2\Gamma(\alpha+i\beta)\psi_0^2\psi_1-2h\Gamma^4\psi_0^5\\
&-\ 2h(\alpha^2+\beta^2)(\alpha+i\beta)^2\psi_0\psi_1^4-2h\Gamma^3(\alpha-i\beta)\psi_0^4\psi_1-2h\Gamma(\alpha+i\beta)^3\psi_0^2\psi_1^3\\
&-\ 12h\Gamma^2\alpha(\alpha+i\beta)\psi_0^3\psi_1^2-6h\Gamma^3(\alpha+i\beta)\psi_0^4\psi_1-6h\Gamma(\alpha^2+\beta^2)(\alpha+i\beta)\psi_0^2\psi_1^3\Big],\bar{R}\Big\rangle\\
&-\Big\langle\Big[\Gamma\psi_0^2+(\alpha-i\beta)\psi_0\psi_1-3h\Gamma(\alpha-i\beta)^2\psi_0^2\psi_1^2-3h\Gamma^2(\alpha+i\beta)\psi_0^3\psi_1-3h\Gamma^3\psi_0^4\\
&-\ 3h(\alpha^2+\beta^2)(\alpha-i\beta)\psi_0\psi_1^3-6h\Gamma^2(\alpha-i\beta)\psi_0^2\psi_1-6h\Gamma(\alpha^2+\beta^2)\psi_0^2\psi_1^2\Big],R^2\Big\rangle\\
&-\Big\langle\Big[2\Gamma\psi_0^2+2(\alpha+i\beta)\psi_0\psi_1-6h\Gamma^2(\alpha-i\beta)\psi_0^3\psi_1-6h\Gamma(\alpha+i\beta)^2\psi_0^2\psi_1^2-6h\Gamma^3\psi_0^4\\
&-\ 6h(\alpha^2+\beta^2)(\alpha+i\beta)\psi_0\psi_1^3-12h\Gamma^2(\alpha+i\beta)\psi_0^3\psi_1-12h\Gamma(\alpha^2+\beta^2)\psi_0\psi_1^3\Big],|R|^2\Big\rangle\\
&-\Big\langle\Big[\psi_0-6h\Gamma^2\psi_0^3-6h(\alpha^2+\beta^2)\psi_0\psi_1^2-12h\Gamma\alpha\psi_0^2\psi_1\Big],|R|^2R\Big\rangle\\
&+\Big\langle\Big[h\Gamma^3\psi_0^4+3h\Gamma^2(\alpha+i\beta)\psi_0^3\psi_1+3h\Gamma(\alpha+i\beta)^2\psi_0^2\psi_1^2+h(\alpha+i\beta)^3\psi_0\psi_1^3\Big],\bar{R}^2\Big\rangle\\
&+\Big\langle\Big[h\Gamma^2\psi_0^3+h(\alpha-i\beta)^2\psi_0\psi_1^2+2h\Gamma(\alpha-i\beta)\psi_0^2\psi_1\Big],R^3\Big\rangle\\
&+\Big\langle\Big[3h\Gamma^2\psi_0^3+3h(\alpha+i\beta)^2\psi_0\psi_1^2+6h\Gamma(\alpha+i\beta)\psi_0^2\psi_1\Big],|R|^2\bar{R}\Big\rangle\\
&+\Big\langle\Big[3h\Gamma\psi_0^2+3h(\alpha+i\beta)\psi_0\psi_1\Big],|R|^4\Big\rangle+\langle h\psi_0,|R|^4R\rangle\Big).
\end{aligned}
$$

Appendix B

Discrete breathers vs. discrete solitons

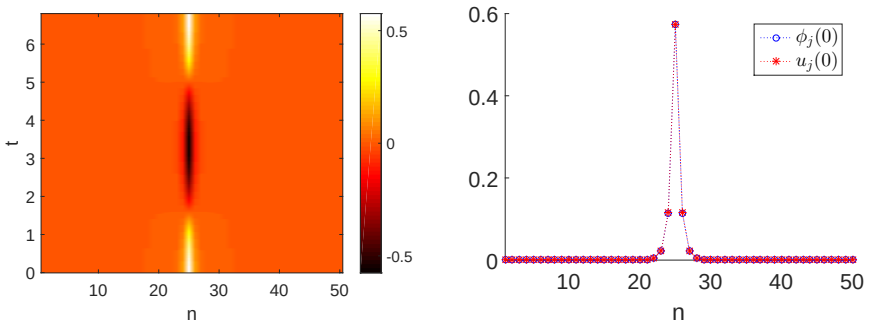

(a) (b)

Figure 1. A breather of (4.1) for $\varepsilon^2 = 0.05$. Panel (a) shows the dynamics of the solution in one period, while panel (b) presents the comparison of the breather and its approximation (4.2) at $t = 0$, with A_j being a discrete soliton of Eq. (4.3).

While discrete solitons of the dNLS (4.3) correspond to spatially localised, but time-independent solutions of the equation and can be computed rather immediately, discrete breathers are spatially localised, but temporally periodic solutions of the dKG equation (4.1).

There are several numerical methods that have been developed to seek for discrete breathers, see the review [36, 37]. Here, we use a Fourier series representation by writing $u_j(t)$ as

$$u_j(t) = \sum_{k=1}^{K} a_{j,k} \cos\left((k-1)\,\Omega t\right) + b_{j,k} \sin\left(k\Omega t\right), \tag{15}$$

where $a_{j,k}$ and $b_{j,k}$ are the Fourier coefficients and $K \gg 1$ is the number of Fourier modes used in our numerics. By substituting the expansion (15) into the dKG equation (4.1), multiplying with each mode, and integrating it over the time-period $2\pi/\Omega$, one will obtain coupled nonlinear algebraic equations for the coefficients $a_{j,k}$ and $b_{j,k}$. Then, we use a Newton's method to solve the equations. Breather solutions will be obtained by choosing a proper initial guess for the coefficients $a_{j,k}$ and $b_{j,k}$.

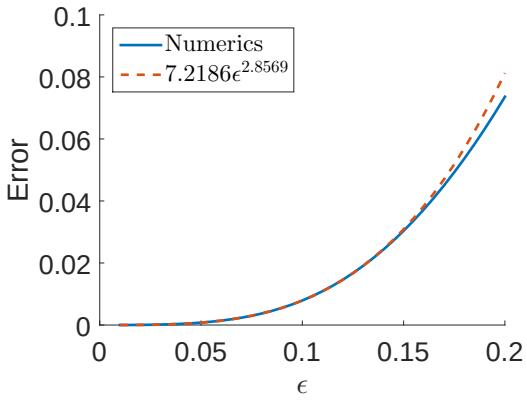

Figure 2. Plot of the maximum difference (20) of the discrete Schrödinger approximation (4.3) for varying ε. The dashed line is the best power fit, indicated in the legend. The inset shows the curves in a log scale.

Once a discrete soliton or a discrete breather is found, it is naturally relevant to study their stability.

Let $\tilde{A}_j = \hat{x}_j + i\hat{y}_j$ be a discrete soliton of the dNLS equation. We determine its linear stability by writing

$$A_j = \tilde{A}_j + \delta(\hat{x}_j + i\hat{y}_j)e^{\lambda\tau}. \tag{16}$$

Substituting (16) into (4.3) and linearising around $\delta = 0$ will yield the eigenvalue problem

$$\lambda \begin{pmatrix} \hat{x}_j \\ \hat{y}_j \end{pmatrix} = \begin{pmatrix} -6\xi x_j y_j - \alpha & \Delta + \Lambda - h - 3\xi\left(x_j^2 + 3y_j^2\right) \\ -\Delta - \Lambda - h + 3\xi\left(3x_j^2 + y_j^2\right) & 6\xi x_j y_j - \alpha \end{pmatrix} \begin{pmatrix} \hat{x}_j \\ \hat{y}_j \end{pmatrix}. \tag{17}$$

In here, the solution $\tilde{A}_j$ is said to be linearly stable when all of the eigenvalues λ have $\mathrm{Re}(\lambda) \leq 0$ and unstable when there is an eigenvalue with $\mathrm{Re}(\lambda) > 0$.

As for discrete breathers of the dKG equation, their linear stability is determined using Floquet theory that can be computed numerically as follows. Let $\tilde{u}_j(t)$ be a breather solution. By defining $u_j(t) = \hat{u}_j(t) + \delta Y_j(t)$, substituting it into Eq. (4.1), and linearising the equation around $\delta = 0$, we obtain the system of linear differential-difference equations

$$\begin{aligned} \dot{Y}_j &= Z_j \\ \dot{Z}_j &= -Y_j - 3\xi \hat{u}_j^2 Y_j + \varepsilon^2 \Delta_2 Y_j - \alpha Z_j + H\cos(2\Omega t) Y_j. \end{aligned} \tag{18}$$

Integrating Eqs. (18) in the numerical domain D, where now $\widetilde{T} = 2\pi/\Omega$, and using the standard basis in $\mathbb{R}^{2N}$, i.e., $\left\{e_1^0, e_2^0, ..., e_{2N}^0\right\}$ as the initial condition at $t = 0$, we will obtain a set of solutions at $t = \widetilde{T}$, which is our monodromy matrix

$$M = \left\{E_1^{\widetilde{T}}, E_2^{\widetilde{T}}, ..., E_{2N}^{\widetilde{T}}\right\} \in \mathbb{R}^{2N\times 2N}. \tag{19}$$

The breather $\tilde{u}_j(t)$ is said to be linearly stable when all the eigenvalues λ_{dKG} of the monodromy matrix M, which are known as Floquet multipliers, lie inside or on the unit circle and unstable when there exists at least one λ_{dKG} lying outside the unit circle. Note that in the presence of damping, the set of continuous multipliers will lie on a circle of radius $e^{\frac{-\alpha\pi}{\Omega}}$, see [67, 68].

In the following, we focus on breathers and discrete solitons for the same parameter values as in Section 4.4, i.e., $\Lambda = -3$, $h = -0.5$, $\hat{\alpha} = 0.1$, and $\xi = -1$. For $\xi = +1$, due to the staggering transformation explained briefly in Section 4.4, discrete breathers of (4.1) with small amplitudes and discrete solitons of (4.3) will have exponentially decaying staggered tails.

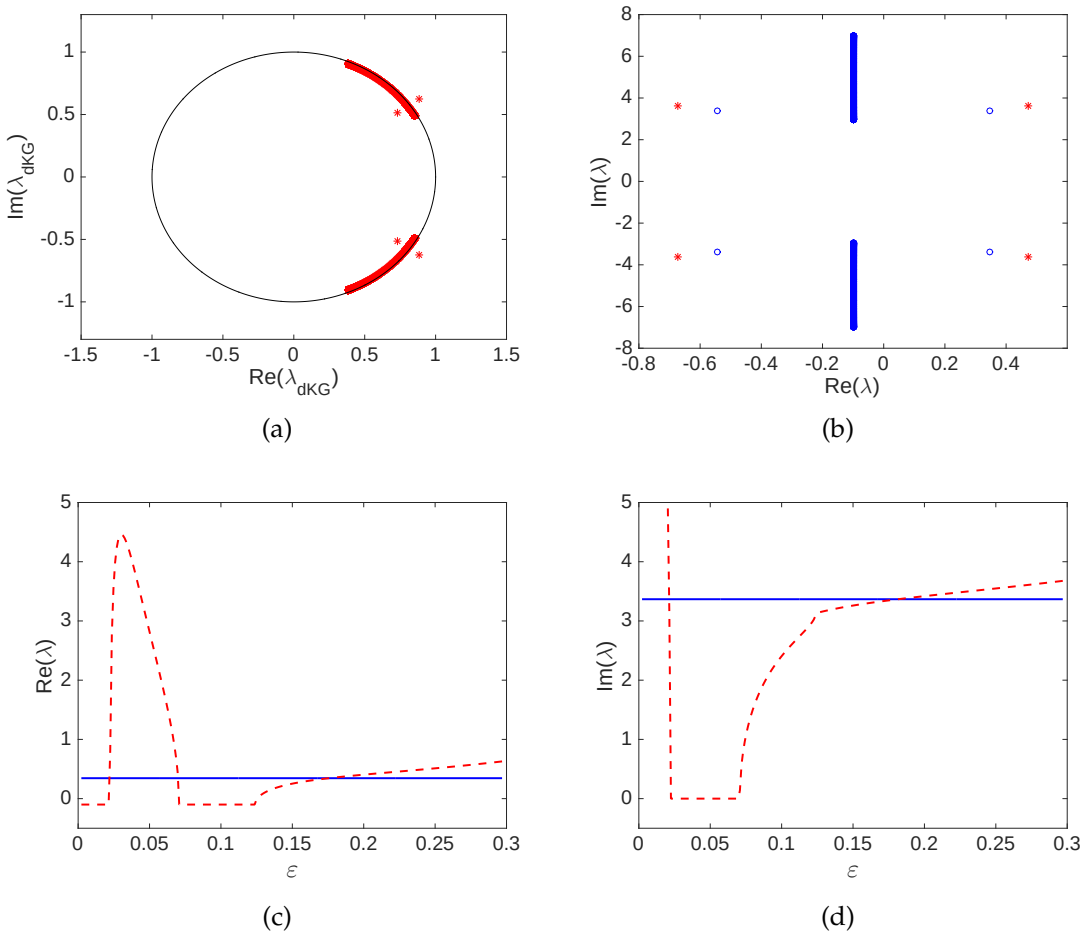

Figure 3. Panel (a) shows Floquet multipliers of the breather in Fig. 1(a), showing the linear instability of the solution. Panel (b) presents the eigenvalues of the corresponding discrete soliton of DNLS equation (4.3). Red stars in the panel are the critical multipliers in panel (a), that have been transformed following the relation (21). Panels (c) and (d) compare the real and imaginary part of the critical eigenvalue of the discrete soliton (blue solid line) and the critical multiplier of the corresponding breather of the dKG equation (red dashed line) for varying ε.

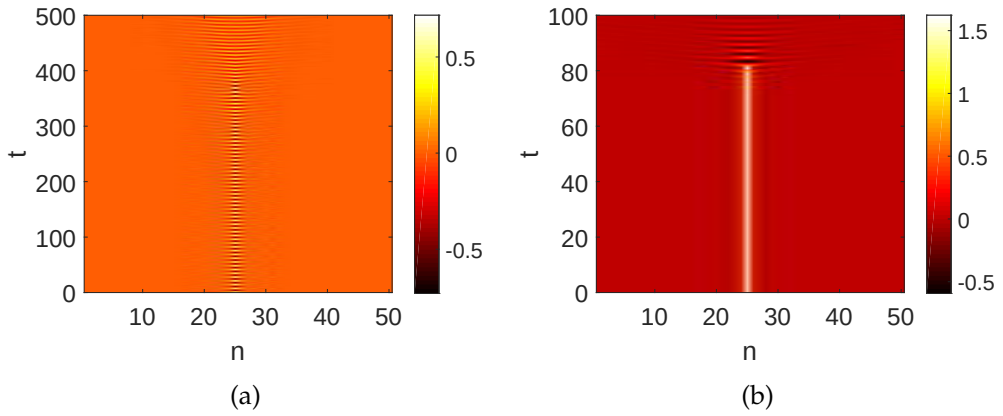

Figure 4. Time dynamics of the unstable breather (a) and discrete soliton (b) shown in Fig. 5.2. Note that the time variable in the second panel has been scaled to the original one.

For our computations, we solve the dKG equation (4.1) for periodic in time solutions using the number of Fourier modes $K = 3$ and the lattice sites $N = 50$. Larger numbers, i.e., $K = 9$ and $N = 400$, have been used as well to make sure that the results are independent of the lattice size and the number of modes.

We present a breather solution and its time dynamics within one period in Fig. 5.2 for $\varepsilon^2 = 0.05$. In Fig. 1(b), we compare the breather in panel (a) with its corresponding approximation (4.2), where A_j is the discrete soliton of Eq. (4.3). One can note that they are in good agreement.

By defining a maximum difference between breathers of (4.1) and their approximations (4.2) using discrete solitons of (4.3) as

$$\mathcal{E} = \sup_{0 \le t \le 2\pi/\Omega} \|y(t)\|_{\ell^2}, \tag{20}$$

we depict the error for varying ε in Fig. 2. We also present in the same panel, the best power fit to the numerical results, which interestingly follows the theoretical prediction of the error in Theorem 4.3.1, i.e., $\sim \varepsilon^3$.

We have computed the corresponding monodromy matrix for the stability of the solution in Fig. 1(a). The Floquet multipliers are plotted in Fig. 3(a). We have

also solved Eq. (17) for the corresponding discrete soliton of the dNLS equation (4.3) and plot the eigenvalues λ in Fig. 3(b), where interestingly we obtain that both solutions experience the same type of instability (i.e., oscillatory instability as the critical multipliers and eigenvalues are both complex valued). For the dNLS solitons, this is in agreement with the results of Refs. [87]. For the dKG breather, the instability is similar to that reported in [25]. Moreover, from the time scales that lead to Eqs. (4.2)–(4.3), we can obtain the relation between Floquet multipliers λ_{dKG} of the dKG monodromy matrix (19) and eigenvalues λ of the dNLS stability matrix (17), i.e.,

$$\lambda_{\mathrm{dKG}} \sim e^{\pi\varepsilon^2\lambda/\Omega}. \tag{21}$$

Using the transformation, we depict in Fig. 3(b) the critical multipliers as red stars, where we learn that the localised solutions do not only have the same type of instability, but their critical eigenvalues have relatively comparable magnitudes.

While in Fig. 2 we plot the error made by the dNLS solitons in approximating the dKG breathers, in Figs. 3(c) and 3(d) we compare their critical eigenvalues and multipliers for varying ε. We obtain that the breathers and solitons do not necessarily share the same type of stability. In fact, there are intervals of coupling constant ε on which the breathers are stable, even though the corresponding dNLS solitons are unstable. This observation nonetheless does not violate the analytical results in Sections 4.2–4.3.

Figures 4(a) and 4(b) show the typical dynamics of the oscillatory instability of the breather and its corresponding discrete soliton approximation. We can observe that in both cases the instability destroys localised solutions, i.e., we also obtain qualitative agreement in the instability dynamics.

Finally, for the sake of completeness, we studied the typical dynamics of dKG breathers when they experience an exponential instability, i.e., the critical Floquet multipliers are real. In Figs. 3(c) and 3(d), they are in a finite interval close to

the uncoupled limit $\varepsilon = 0$ and their absolute magnitudes are near unity. Due to these facts, we could not clearly see any instability in our simulations, even after integrating the dKG equation for quite a long while.